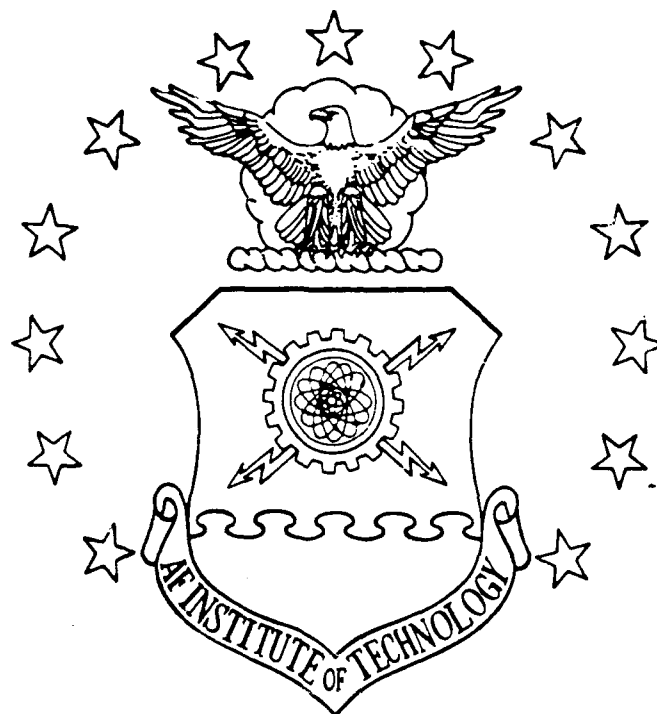


AD-A215 664



DTIC  
ELECTE  
DEC 19 1989  
S B D

DISCRETE PROPORTIONAL PLUS INTEGRAL (PI)  
MULTIVARIABLE CONTROL LAWS FOR THE  
CONTROL RECONFIGURABLE COMBAT  
AIRCRAFT (CRCA)

THESIS

Jamie Lynn Foelker  
Captain, USAF

AFIT/GE/ENG/89-12

DEPARTMENT OF THE AIR FORCE  
AIR UNIVERSITY

**AIR FORCE INSTITUTE OF TECHNOLOGY**

Wright-Patterson Air Force Base, Ohio

DISTRIBUTION STATEMENT A

Approved for public release;  
Distribution Unlimited

89 12 18 094

AFIT/GE/ENG/89-12

DISCRETE PROPORTIONAL PLUS INTEGRAL (PI)  
MULTIVARIABLE CONTROL LAWS FOR THE CONTROL  
RECONFIGURABLE COMBAT AIRCRAFT (CRCA)

THESIS

Presented to the Faculty of the School of Engineering  
of the Air Force Institute of Technology

Air University

In Partial Fulfillment of the  
Requirements for the Degree of  
Master of Science in Electrical Engineering

Jamie Lynn Foelker, B.S.E.E.

Captain, USAF

December, 1989

Approved for public release; distribution unlimited

## *Preface*

The purpose of this thesis is to continue investigation of the applying Porter's high-gain error actuated proportional plus integral (PI) design techniques to the development of control laws for an Advanced Tactical Fighter (ATF) type aircraft, the CRCA. Initial work was accomplished by Capt. Daryl Hammond and the results of applying PI control based upon output feedback were very promising. The results obtained of this effort display very robust tracking and decoupling of outputs with the fixed-gain designs and a much more realistic system bandwidth. More investigation of the adaptive algorithm will be necessary to conclude this study of PI control for the set of inputs and outputs selected on the CRCA.

My personal thanks and gratitude are extended to all who have helped make this thesis effort possible, especially my thesis advisor Dr. John J. D'Azzo and predecessor Capt. Daryl Hammond. Thank you both for the unending support and guidance. The exceptional support and resources made available by the Flight Dynamics Laboratory were also greatly appreciated.

Finally, I would like to thank my family and friends for their kind support and understanding through this long and difficult endeavor.

Jamie Lynn Foelker

Accession For	
NTIS GRA&I	<input checked="checked" type="checkbox"/>
DTIC TAB	<input type="checkbox"/>
Unannounced	<input type="checkbox"/>
Justification	
By _____	
Distribution/	
Availability Codes	
Dist	Avail and/or Special
A-1	

## *Table of Contents*

	Page
Preface . . . . .	i
Table of Contents . . . . .	ii
List of Figures . . . . .	v
List of Tables . . . . .	viii
Abstract . . . . .	x
I. INTRODUCTION . . . . .	1-1
1.1 BACKGROUND . . . . .	1-1
1.2 PROBLEM STATEMENT . . . . .	1-2
1.3 SUMMARY OF CURRENT KNOWLEDGE . . . . .	1-2
1.4 ASSUMPTIONS . . . . .	1-3
1.5 APPROACH . . . . .	1-4
1.6 OVERVIEW . . . . .	1-4
II. DESCRIPTION OF MODELS . . . . .	2-1
2.1 AIRCRAFT DESCRIPTION . . . . .	2-1
2.2 FLIGHT PHASES . . . . .	2-1
2.3 DETERMINATION OF AIRCRAFT MODELS . . . . .	2-3
2.3.1 STATE SPACE MODELS . . . . .	2-3
2.3.2 AUTOREGRESSIVE MOVING AVERAGE (ARMA) MODEL . . . . .	2-8
2.3.3 ACTUATOR MODELS . . . . .	2-9

	Page
III. DESIGN PROCEDURES . . . . .	3-1
3.1 OVERVIEW . . . . .	3-1
3.2 DISCRETE, FIXED-GAIN PI CONTROLLER THEORY . .	3-1
3.3 DESIGN PARAMETERS FOR THE DISCRETE FIXED-GAIN PI CONTROLLER . . . . .	3-9
3.4 DISCRETE STEP RESPONSE PI CONTROLLER THEORY AND DESIGN . . . . .	3-12
3.5 ADAPTIVE STEP RESPONSE PI CONTROLLER . . . . .	3-15
IV. DISCRETE PI CONTROLLER . . . . .	4-1
4.1 TRANSFER FUNCTION ANALYSIS . . . . .	4-1
4.2 TIME RESPONSES . . . . .	4-7
4.3 FREQUENCY ANALYSIS . . . . .	4-25
V. STEP RESPONSE METHOD AND ADAPTIVE RESULTS . . . . .	5-1
5.1 STEP RESPONSE METHOD . . . . .	5-1
5.2 ADAPTIVE CONTROLLER . . . . .	5-12
VI. CONCLUSIONS AND RECOMMENDATIONS . . . . .	6-1
6.1 SUMMARY . . . . .	6-1
6.1.1 DISCRETE PI CONTROLLER . . . . .	6-1
6.1.2 STEP RESPONSE METHOD PI . . . . .	6-1
6.1.3 ADAPTIVE CONTROLLER . . . . .	6-2
6.2 RECOMMENDATIONS FOR FUTURE RESEARCH . . . .	6-2
Appendix A. AIRCRAFT STATE SPACE MODELS . . . . .	A-1
Appendix B. ARMA MODEL GENERATION . . . . .	B-1
B.1 INTRODUCTION . . . . .	B-1
B.2 ARMA MODEL . . . . .	B-1

	Page
B.3 ARMA IMPLEMENTATION . . . . .	B-5
B.3.1 MATRIX <sub>X</sub> ARMA Macro . . . . .	B-7
B.4 AUTO REGRESSIVE MOVING AVERAGE MODELS . . .	B-12
Appendix C.    GAIN MATRICES AND STEP RESPONSE ROOTS . . . .	C-1
Appendix D.    ADAPTIVE ALGORITHM . . . . .	D-1
Bibliography . . . . .	BIB-1
Vita . . . . .	VITA-1

## *List of Figures*

Figure	Page
2.1. Combat Reconfigurable Combat Aircraft (CRCA) . . . . .	2-2
3.1. Discrete PI Controller - Irregular Plant . . . . .	3-3
4.1. Input command for pitch tracking maneuver . . . . .	4-10
4.2. Input command for coordinated turn maneuver . . . . .	4-11
4.3. Input command for sideslip tracking maneuver . . . . .	4-11
4.4. Input command for flat turn maneuver . . . . .	4-12
4.5. Input command for banked turn maneuver . . . . .	4-12
4.6. Discrete Controller pitch rate tracking response in ACM Entry . . . . .	4-13
4.7. Surface deflections for pitch rate tracking in ACM Entry . . . . .	4-14
4.8. Surface rates for pitch rate tracking in ACM Entry . . . . .	4-14
4.9. Discrete Controller coordinated turn response in ACM Entry . . . . .	4-15
4.10. Discrete Controller sideslip tracking response in ACM Entry . . . . .	4-15
4.11. Discrete Controller flat turn response in ACM Entry . . . . .	4-16
4.12. Discrete Controller banked turn response in ACM Entry . . . . .	4-16
4.13. Discrete Controller sideslip tracking response in ACM Exit . . . . .	4-17
4.14. Discrete Controller flat turn response in ACM Exit . . . . .	4-17
4.15. Discrete Controller pitch rate tracking response in TFTA . . . . .	4-18
4.16. Discrete Controller coordinated turn response in TFTA . . . . .	4-18
4.17. Discrete Controller sideslip tracking response in TFTA . . . . .	4-19
4.18. Discrete Controller flat turn response in TFTA . . . . .	4-19
4.19. Discrete Controller banked turn response in TFTA . . . . .	4-20
4.20. Discrete Controller sideslip maneuver response in ACM30TL . . . . .	4-21
4.21. Discrete Controller sideslip maneuver response in ACM50CL . . . . .	4-22

Figure	Page
4.22. Discrete Controller sideslip maneuver response in ACM25RL . . . . .	4-22
4.23. Discrete Controller sideslip maneuver response in TFTA30TL . . . . .	4-23
4.24. Discrete Controller sideslip maneuver response in TFTA50CL . . . . .	4-23
4.25. Discrete Controller sideslip maneuver response in TFTA25RL . . . . .	4-24
4.26. Discrete PI Nichols plot of $\beta/\beta_{cmd}$ in ACM Entry . . . . .	4-27
4.27. Discrete PI open loop Bode plot of $\beta/\beta_{cmd}$ in ACM Entry . . . . .	4-27
4.28. Discrete PI Nichols plot of $\theta/\theta_{cmd}$ in ACM Entry . . . . .	4-28
4.29. Discrete PI open loop Bode plot of $\theta/\theta_{cmd}$ in ACM Entry . . . . .	4-28
4.30. Discrete PI Nichols plot of $\beta/\beta_{cmd}$ in TFTA . . . . .	4-29
4.31. Discrete PI open loop Bode plot of $\beta/\beta_{cmd}$ in TFTA . . . . .	4-29
4.32. Discrete PI Nichols plot of $\theta/\theta_{cmd}$ in TFTA . . . . .	4-30
4.33. Discrete PI open loop Bode plot of $\theta/\theta_{cmd}$ in TFTA . . . . .	4-30
4.34. Discrete PI closed loop Bode plot of $\beta/\beta_{cmd}$ in ACM Entry . . . . .	4-31
4.35. Discrete PI closed loop Bode plot of $\theta/\theta_{cmd}$ in ACM Entry . . . . .	4-31
4.36. Discrete PI closed loop Bode plot of $\beta/\beta_{cmd}$ in TFTA . . . . .	4-32
4.37. Discrete PI closed loop Bode plot of $\theta/\theta_{cmd}$ in TFTA . . . . .	4-32
5.1. Step response method pitch rate tracking response in ACM Entry . . .	5-3
5.2. Step response method coordinated turn response in ACM Entry . . . .	5-3
5.3. Step response method sideslip tracking response in ACM Entry . . . . .	5-4
5.4. Step response method flat turn response in ACM Entry . . . . .	5-4
5.5. Step response method banked turn response in ACM Entry . . . . .	5-5
5.6. Step response method pitch sideslip tracking response in ACM Exit . .	5-5
5.7. Step response method flat turn response in ACM Exit . . . . .	5-6
5.8. Step response method pitch rate tracking response in TFTA . . . . .	5-6
5.9. Step response method coordinated turn response in TFTA . . . . .	5-7
5.10. Step response method sideslip tracking response in TFTA . . . . .	5-7
5.11. Step response method flat turn response in TFTA . . . . .	5-8



Figure	Page
5.12. Step response method banked turn response in TFTA . . . . .	5-8
5.13. Step response method sideslip tracking response in ACM30TL . . . . .	5-9
5.14. Step response method sideslip tracking response in ACM50CL . . . . .	5-9
5.15. Step response method sideslip tracking response in ACM25RL . . . . .	5-10
5.16. Step response method sideslip tracking response in TFTA30TL . . . . .	5-10
5.17. Step response method sideslip tracking response in TFTA50CL . . . . .	5-11
5.18. Step response method sideslip tracking response in TFTA25RL . . . . .	5-11
5.19. Adaptive pitch rate tracking response in ACM Entry . . . . .	5-13
5.20. Adaptive coordinated turn response in ACM Entry . . . . .	5-14
5.21. Adaptive sideslip tracking response in ACM Entry . . . . .	5-14
5.22. Adaptive flat turn response in ACM Entry . . . . .	5-15
5.23. Adaptive banked turn response in ACM Entry . . . . .	5-15
5.24. Adaptive pitch rate tracking response in TFTA . . . . .	5-16
5.25. Adaptive coordinated turn response in TFTA . . . . .	5-16
5.26. Adaptive sideslip tracking response in TFTA . . . . .	5-17
5.27. Adaptive flat turn response in TFTA . . . . .	5-17
5.28. Adaptive banked turn response in TFTA . . . . .	5-18
5.29. Adaptive sideslip tracking response in ACM30TEL with $\lambda=.90$ and failure at $t=0$ . . . . .	5-19
5.30. Adaptive flat turn response in ACM30TEL with $\lambda=.90$ and failure at $t=0$	5-20
5.31. Adaptive sideslip tracking response in ACM30TEL with $\lambda=.90$ and failure at $t=2$ . . . . .	5-20
5.32. Adaptive flat turn response in ACM30TEL with $\lambda=.90$ and failure at $t=2$	5-21

# *List of Tables*

Table	Page
2.1. Flight Conditions . . . . .	2-3
2.2. Aircraft State Space Matrices for ACM Entry . . . . .	2-4
2.3. Open Loop Eigenvalues of 8x8 CRCA Models . . . . .	2-6
2.4. Open Loop Transmission Zeros of 8x8 CRCA Models . . . . .	2-6
2.5. Equivalent Aircraft 8x8 Matrices For ACM Entry . . . . .	2-7
2.6. Control Surface Position and Rate Limits . . . . .	2-10
4.1. $r_{cmd}$ - 45° Bank Angle . . . . .	4-2
4.2. Steady State Control Inputs - Pitch Rate Tracking . . . . .	4-4
4.3. Steady State Control Inputs - 45° Coordinated Turn . . . . .	4-5
4.4. Steady State Control Inputs - Sideslip Tracking . . . . .	4-5
4.5. Steady State Control Inputs - Flat Turn . . . . .	4-6
4.6. Steady State Control Inputs - 45° Banked Turn . . . . .	4-6
4.7. Steady State Control Inputs - 15° Banked Turn . . . . .	4-7
4.8. Control Surface Position and Rate Limits . . . . .	4-7
4.9. Stability Analysis Using discrete PI design parameters . . . . .	4-9
4.10. Bandwidth of discrete PI design . . . . .	4-26
4.11. $w'$ plane roots for ACM Entry and TFTA . . . . .	4-26
4.12. Gain and Phase Margins - Discrete PI Design . . . . .	4-33
5.1. Stability Analysis Using step response design parameters . . . . .	5-2
A.1. ACM Entry Matrices - No Failures . . . . .	A-2
A.2. ACM Entry Matrices - 30% Loss Of Effectiveness Left Trailing Edge . .	A-3
A.3. ACM Entry Matrices - 50% Loss Of Effectiveness Left Canard . . . . .	A-4
A.4. ACM Entry Matrices - 25% Loss Of Effectiveness Rudder . . . . .	A-5

Table	Page
A.5. ACM Exit Matrices - No Failures . . . . .	A-6
A.6. TF/TA Matrices - No Failures . . . . .	A-7
A.7. TF/TA Matrices - 30% Loss of Effectiveness Left Trailing Edge . . . . .	A-8
A.8. TF/TA Matrices - 50% Loss of Effectiveness Left Canard . . . . .	A-9
A.9. TF/TA Matrices - 25% Loss of Effectiveness Rudder . . . . .	A-10
B.1. ACM Entry ARMA Model - No Failures . . . . .	B-12
B.2. ACM Entry ARMA Model - 30% Loss of Effectiveness Left Trailing Edge . . . . .	B-13
B.3. ACM Entry ARMA Model - 50% Loss of Effectiveness Left Canard . . . . .	B-14
B.4. ACM Entry ARMA Model - 25% Loss of Effectiveness Rudder . . . . .	B-15
B.5. ACM Exit ARMA Model - No Failures . . . . .	B-16
B.6. TF/TA ARMA Model - No Failures . . . . .	B-17
B.7. TF/TA ARMA Model - 30% Loss of Effectiveness Left Trailing Edge . . . . .	B-18
B.8. TF/TA ARMA Model - 50% Loss of Effectiveness Left Canard . . . . .	B-19
B.9. TF/TA ARMA Model - 25% Loss of Effectiveness Rudder . . . . .	B-20
C.1. Discrete PI Controller Gain Matrices - ACMENTRY . . . . .	C-2
C.2. Discrete PI Controller Gain Matrices - ACMEXIT . . . . .	C-2
C.3. Discrete PI Controller Gain Matrices - TF/TA . . . . .	C-3
C.4. Step Response PI Controller Gain Matrices - ACM Entry . . . . .	C-3
C.5. Step Response PI Controller Gain Matrices - ACM Exit . . . . .	C-4
C.6. Step Response PI Controller Gain Matrices - TF/TA . . . . .	C-4
C.7. $w$ plane roots for ACM Entry and TFTA for the step response method . . . . .	C-5

*Abstract*

Multivariable control laws developed by Dr. Brian Porter of the University of Salford, England are used to successfully perform maneuvering tracking tasks with the NASA/Grumman Control Reconfigurable Combat Aircraft (CRCA). Porter's method is used to design discrete Proportional plus Integral (PI) control laws. Output and selected state rate feedback are used. The results in three no failure flight conditions show robust tracking control of the CRCA for five selected maneuvers. Single failures are introduced to test the ability of the fixed-gain designs to successfully control the aircraft and perform the maneuvers. The time responses show that discrete PI control law can make the CRCA successfully perform all five maneuvers for two of the three control surface failures investigated in two of the three point designs. The step response PI control law results in stable control for only one of three failure situations. For high gains, the system transfer function becomes asymptotically diagonal (the outputs are decoupled). Based on this property, the frequency analysis is obtained for the discrete PI design using each output with respect to its associated input. Phase margins in excess of  $45^\circ$ , gain margins of greater than 6dB, and bandwidths in the range of 5-10 rad/sec are the result. The adaptive controller displays a larger than expected roll angle output in two of the maneuvers as compared to the step response PI results. An adaptive algorithm using a recursive least squares estimation is run with failure introduction occurring at one of two times in the simulation. The adaptive results also display decoupling of the outputs in the steady state.

# DISCRETE PROPORTIONAL PLUS INTEGRAL (PI) MULTIVARIABLE CONTROL LAWS FOR THE CONTROL RECONFIGURABLE COMBAT AIRCRAFT (CRCA)

## *I. INTRODUCTION*

### *1.1 BACKGROUND*

Modern aircraft designs present the control engineer with great challenges. The demands for increased maneuverability can be met only at the expense of aerodynamic stability. As aircraft become highly maneuverable there are some mission flight conditions which a human alone cannot control, and an on-board computer must be used for basic stability. These control systems are termed fly-by-wire since there are no mechanical connections between the pilot and control surfaces; only electrical signals from the flight control computer. In addition to the role of stabilizing the aircraft, the flight control system must also provide the plane with the ability to make the outputs follow input commands. The control laws developed are the mathematical equations which compute the required inputs to the aircraft or plant.

Modern techniques using multivariable control have a distinct advantage over their conventional counterparts in that only one control system need be developed for the aircraft to be able to perform specific tracking tasks where more than one set of inputs and outputs are commanded. Separate loop designs are necessary in order to make each output track a specific input when single input single output (SISO) designs are used. This can make the design of a multiple input multiple output (MIMO) system extremely involved and tedious.

Another issue which must be addressed is that of whether the designed fixed-gain flight control system is robust enough to provide adequate control when the aircraft suffers a control surface loss or malfunction. This problem is one of substantial concern to the military. The first most important area of concern is that of returning the flight crews

and aircraft to safety after combat damage has been sustained. Another concern is that of accomplishing the mission. The aircraft must remain stable and retain at least limited mission capabilities.

## 1.2 PROBLEM STATEMENT

Design techniques developed by Professor Brian Porter of the University of Salford, England allow for the development of a single, fixed gain control algorithm which uses output feedback to make the plant of interest perform tracking tasks with little to no coupling of the outputs.

The goal of this thesis is to use Porter's multivariable design techniques to assess the effects of single failure conditions on control algorithms designed for a healthy aircraft performing five specified maneuvers in three different points on its flight envelope. The most desirable result of this thesis would be that one set of design parameters for the fixed-gain designs would yield adequate stability and control of the aircraft in all three flight conditions as well as provide satisfactory performance when a single failure condition is introduced. Responses obtained from single failure modes, however, prove that a fixed set of design parameters is an optimistic goal. Thus, the introduction of adaptive control is deemed necessary.

This thesis effort is a follow-on to the work accomplished by Capt. Daryl Hammond in *MULTIVARIABLE CONTROL LAW DESIGN FOR THE CONTROL RECONFIGURABLE COMBAT AIRCRAFT (CRCA)*, 1988 (4). Hammond's results were the first obtained using Porter's control techniques on the CRCA and served as a baseline for performance comparisons. The number of maneuvers performed will be increased from Hammond's two to five and an additional failure condition will be simulated.

## 1.3 SUMMARY OF CURRENT KNOWLEDGE

Hammond used two of Porter's design methods to develop Proportional plus Integral (PI) and Proportional plus Integral plus Derivative (PID) control algorithms. Hammond used four different techniques to design PI controllers:

1. continuous controller based on known plant parameters,
2. discrete controller based on known plant parameters,
3. discrete step response controller based on unknown plant parameters, and
4. adaptive version of step response controller to take plant variations into consideration.

His research concluded with an investigation of the discrete PID controller both with and without the actuator dynamics.

Hammond found that the fixed, high gain PI controller based on knowledge of the aircraft parameters displayed robust performance in normal aircraft flight conditions and that a fixed set of design parameters provided satisfactory performance in 70% of the flight configurations tested. He also found that the discrete PI controller outperformed its continuous counterpart. However, the discrete step response PI controller could not adequately control the left flaperon failure, so adaptive control was applied. The adaptive controller's performance was exceptional in the simulation tested. The PID controller performed very well in simulations where the CRCA's actuator dynamics were not included.

#### 1.4 ASSUMPTIONS

The following assumptions made in Hammond's thesis will be used in this effort, and their effects on the thesis scope will be noted.

1. The linearized equations of motion are used in a point design (initial velocity and altitude are assumed fixed at a trim condition) and only small variations are allowed about the trim point.
2. The outputs used are assumed to be measurable and readily accessible.
3. The aircraft is treated as a rigid body so that bending modes do not appear in the linearized equations of motion.
4. Fuel consumption is considered minimal over the short simulation durations, so mass is treated as a constant.

5. The earth's surface is used as the inertial reference frame which can again be attributed to short simulations and aircraft sensors that are not sensitive enough to detect the earth's rotation (4:1-6).
6. The atmosphere is assumed fixed to the earth's surface and wind effects are not considered.

## 1.5 APPROACH

This thesis effort focuses on the two methods of designing discrete non-adaptive PI controllers and also investigates an adaptive approach where applicable. Hammond's previous work is used as a baseline and the new research has been built from his existing computer programs. These computer programs are expanded to perform the additional flight operations.

The CRCA is chosen as the research vehicle primarily because there is a great deal of aerodynamic data available for single and multiple control surface losses and failures. *This data is an invaluable aid in assessing the robustness of the individual PI designs.*

Hammond's design parameters are used initially and then necessary changes made to them to satisfactorily control all outputs. An additional goal of trying to obtain "reasonable" controller gains is added. Frequency analysis will be performed to ensure that the phase and gain margins specified by MIL-F-9490C are met and a realistic bandwidth is obtained.

The research will be performed on the powerful software package MATRIX<sub>X</sub>. All necessary modifications have been made to the computer programs in order to run the simulations on Version 7.0. The System Build feature of MATRIX<sub>X</sub> (6) allows for straightforward multivariable design and analysis.

## 1.6 OVERVIEW

The remainder of this thesis is organized according to the following schedule. The aircraft models, actuators, and ARMA representation are discussed in Chapter 2. The theory behind the different control law design methods are presented in Chapter 3. The



The results obtained from the discrete PI controller can be found in Chapter 4, and the step response and adaptive results are contained in Chapter 5. Chapter 6 contains a summary of the results obtained and includes recommendations for future work using Porter's methods on the CRCA flight control system.

## II. DESCRIPTION OF MODELS

### 2.1 AIRCRAFT DESCRIPTION

The Control Reconfigurable Combat Aircraft (CRCA) is a NASA/Grumman Advanced Tactical Fighter (ATF) type design. The CRCA was designed for high performance with relaxed static instability of 12% at low airspeeds (12:3-1). The plane is not slated for production, but it is being used to assess combat damage survivability. The CRCA, shown in Figure 2.1, has nine separate control surfaces consisting of two canards, a rudder, and two flaperons and an elevator on the trailing edge of each wing. The three surfaces on the trailing edge of each wing are commanded together in this thesis effort in order to preserve the laminar airflow over the wings. The canards have 30° of positive dihedral (upward cant from the horizontal) and are "all-flying", meaning that the longitudinal and lateral-directional equations of motion for the aircraft are coupled.

### 2.2 FLIGHT PHASES

The aerodynamic data on the CRCA is available for four design points and the four design points, or flight conditions are representative of the aircraft's performance range. Descriptions of the four flight phases was obtained from Appendix C of Reference (12) and Hammond's Chapter 2.

The first flight condition is **Air Combat Maneuvering (ACM) Entry**. This flight phase is representative of aircraft conditions normally encountered at the initiation of an air-to-air engagement or weapons delivery. Altitude can vary from 10,000 to 30,000 feet with velocities just under Mach 1.

The next flight phase is **Terrain-Following/Terrain-Avoidance (TFTA)**. This is a low altitude, high velocity flight condition commonly used to avoid enemy radar detection. Velocities are as high as those used in ACM Entry, but with altitudes as low as 200 feet above local ground level. The dynamic pressure,  $\bar{q}$ , is very high for this condition and rapid changes in pitch angle can be expected.

The third point design is **ACM Exit**. This condition is very difficult to control since the aircraft has low airspeed with a high angle of attack ( $\sim 30^\circ$ ), steep bank angle ( $\sim 70^\circ$ ),

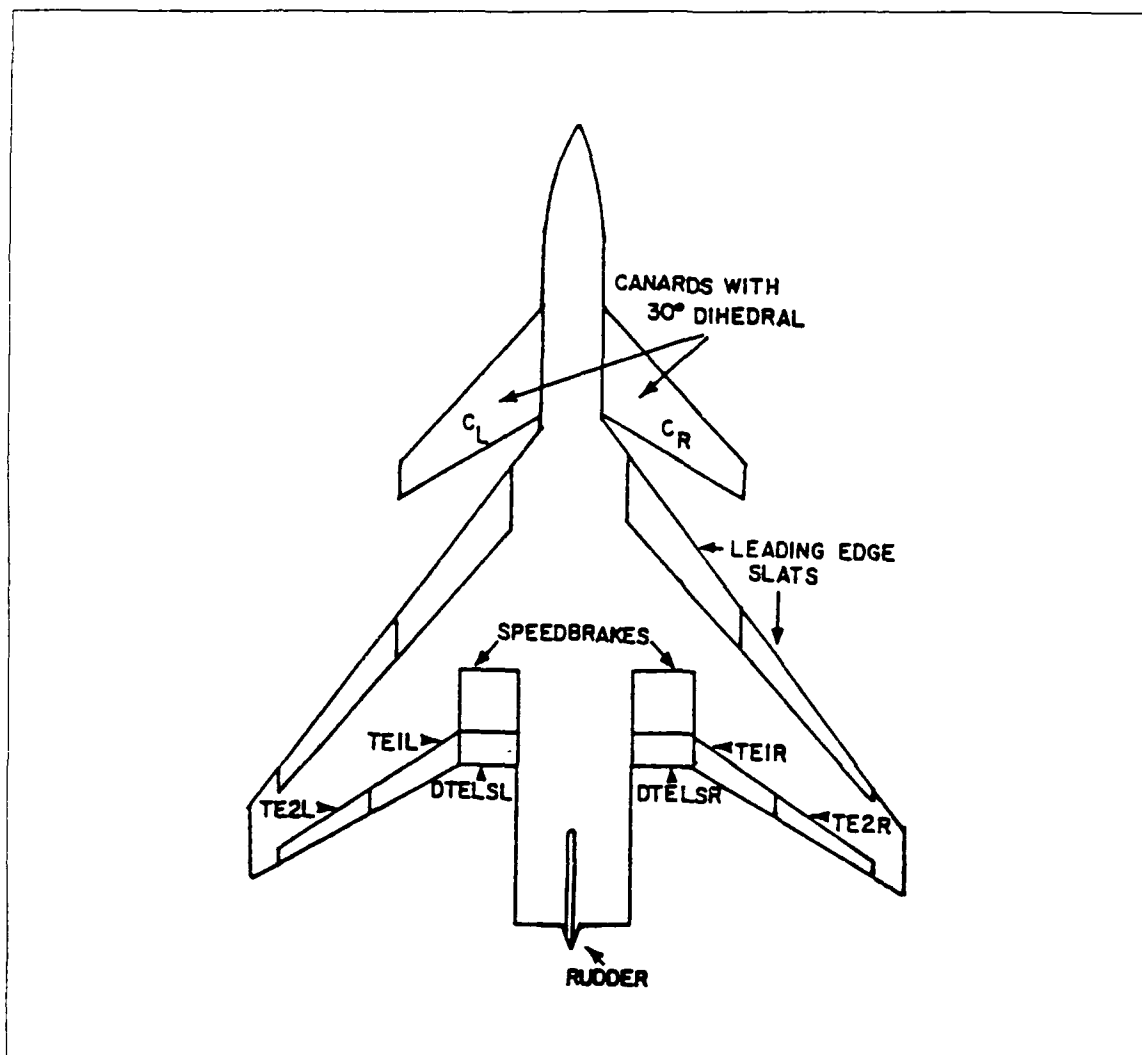


Figure 2.1. Combat Reconfigurable Combat Aircraft (CRCA) (4)

and a high load factor ( $\sim 3g$ ). The aircraft has been pushed very close to its limits by the end of the air-to-air encounter.

The fourth flight phase is **Short Take-Off and Landing (STOL)**. This condition has the lowest airspeed of all four and is the most critical flight phase. The landing requirements are a maximum landing distance of 1500 feet and a crosswind of 30 knots. This data was unfortunately not available in time to be incorporated in this thesis effort.

Table 2.1 (4:2-3) summarizes the characteristics of the CRCA's flight phases. The point designs accomplished in this thesis are valid since the maneuvers performed do not stray significantly from the design points.

Table 2.1. Flight Conditions

MISSION SEGMENT	ALTITUDE, FT	MACH NO.	LOAD FACTOR
ACM ENTRY	30,000	0.9	1g
TF/TA	SEA LEVEL	0.9	1g
ACM EXIT	10,000	0.275	3g
STOL	1200	0.185	1g

## 2.3 DETERMINATION OF AIRCRAFT MODELS

**2.3.1 STATE SPACE MODELS** Linearized state space models of the CRCA have been obtained utilizing computer programs at the Flight Dynamics Laboratory at Wright Patterson Air Force Base (4, 7). All aircraft models used in this thesis are those obtained from Hammond, with the exception of the 25% rudder failure case models which are extracted from Capt. Kurt Neumann's thesis computer files (7).

The result of using the CRCA's nonlinear equations of motion and control and stability derivatives is a linearized model containing nine states and nine inputs, as shown in Table 2.2 (4:2-9) for the ACM Entry flight condition.

Table 2.2. Aircraft State Space Matrices for ACM Entry

$$A = \begin{bmatrix} -.0119 & -.0186 & -31.2350 & -32.1804 & .0000 & .0000 & .0000 & .0000 & .0000 \\ -.0324 & -1.0634 & 894.4548 & -1.0634 & .0000 & .0000 & .0000 & .0000 & .0000 \\ -.0002 & .0069 & -.6015 & .0000 & .0000 & .0000 & .0000 & .0000 & .0000 \\ .0000 & .0000 & 1.0000 & .0000 & .0000 & .0000 & .0000 & .0000 & .0000 \\ .0000 & .0000 & .0000 & .0000 & .0000 & .0000 & .0000 & 1.0000 & .0000 \\ .0000 & .0000 & .0000 & .0000 & .0000 & .0000 & .0000 & 1.0000 & .0349 \\ .0060 & .0000 & .0000 & .0000 & .0000 & .0360 & -.0929 & .0349 & -.9994 \\ .0000 & .0000 & .0000 & .0000 & .0000 & .0000 & -27.8066 & -2.0376 & .4913 \\ .0000 & .0000 & .0000 & .0000 & .0000 & .0000 & 2.4582 & -.0241 & -.4377 \end{bmatrix}$$

$$B = \begin{bmatrix} .0411 & .0411 & .1322 & .0866 & .1322 & .0866 & .1018 & .1018 & .0000 \\ -.3163 & -.3163 & -.9597 & -.6194 & -.9597 & -.6194 & -1.0183 & -1.0183 & .0000 \\ .1014 & .1014 & -.0284 & -.0215 & -.0284 & -.0215 & -.0200 & -.0200 & .0000 \\ .0003 & -.0003 & -.0002 & -.0001 & .0002 & .0001 & -.0001 & .0001 & .0006 \\ .0000 & .0000 & .0000 & .0000 & .0000 & .0000 & .0000 & .0000 & .0000 \\ .0000 & .0000 & .0000 & .0000 & .0000 & .0000 & .0000 & .0000 & .0000 \\ .0000 & .0000 & .0000 & .0000 & .0000 & .0000 & .0000 & .0000 & .0010 \\ .0762 & -.0762 & .2219 & .2011 & -.2219 & -.2011 & .1109 & -.1109 & .1144 \\ .0486 & -.0486 & .0029 & .0021 & -.0029 & -.0021 & .0021 & -.0021 & -.0544 \end{bmatrix}$$

$$x = \begin{bmatrix} u & w & q & \theta & \psi & \phi & \beta & p & r \end{bmatrix}^T \quad (2.1)$$

$$u = \begin{bmatrix} \delta_{cl} & \delta_{cr} & \delta_{tel1} & \delta_{te2l} & \delta_{te1r} & \delta_{te2r} & \delta_{dtelsl} & \delta_{dtelsr} & \delta_{rud} \end{bmatrix}^T \quad (2.2)$$

The eight states As mentioned previously, the three trailing edge control surfaces on each wing are commanded together. This effectively reduces the number of control surfaces from nine to the following five;

$$\begin{aligned}\delta_{cl} &= \text{left canard} \\ \delta_{cr} &= \text{right canard} \\ \delta_{tel} &= \text{left trailing edge flaperon} \\ \delta_{ter} &= \text{right trailing edge flaperon} \\ \delta_{rud} &= \text{rudder}\end{aligned}$$

The columns of the corresponding left and right trailing edge surfaces of the **B** matrix are summed to form a reduced input **B** matrix. Now that there are only five inputs, only five outputs can be controlled using output feedback. The five chosen outputs are

$$\begin{aligned}v &= \text{forward velocity} \\ \beta &= \text{sideslip angle} \\ \theta &= \text{pitch angle} \\ \phi &= \text{bank angle} \\ r &= \text{yaw rate}\end{aligned}$$

The 9x9 **A** matrix does not have full rank since the state  $\psi$  is redundant. Therefore, the fifth row and column are removed and **A** is reduced to an eight state model. Also, Hammond found that the remaining eight states had to be reordered so that Autoregressive Moving Average (ARMA) models could be generated more directly. Table 2.5 (4:2-10) contains the resulting ACM Entry model of the CRCA used in this and Hammond's thesis. The order of inputs and states remains the same for the rest of the flight conditions used

where the eight remaining states are

$u$  = velocity in aircraft X axis

$w$  = velocity in aircraft Z axis

$q$  = pitch rate

$\theta$  = pitch angle

$\psi$  = yaw angle

$\phi$  = roll angle

$\beta$  = sideslip angle

$p$  = roll rate

$r$  = yaw rate

The aircraft open loop eigenvalues for the three point designs used are listed in Table 2.3 and the transmission zeros in Table 2.4.

Table 2.3. Open Loop Eigenvalues of 8x8 CRCA Models

ACMENTRY	ACMEXIT	TFTA
$-0.0078 \pm j0.0495$	$0.0220 \pm j0.0363$	0.0236
-0.0562	-0.2139	-0.0457
1.6669	-0.3059	-0.0583
$-0.2482 \pm j1.8323$	0.4718	$-0.7559 \pm j2.9853$
-2.0156	-1.7162	$-2.4418 \pm j4.4400$
-3.3281	$-0.6572 \pm j1.7084$	-5.4284

Table 2.4. Open Loop Transmission Zeros of 8x8 CRCA Models

ACMENTRY	ACMEXIT	TFTA
-1.6844	-0.0902	-2.8974

Table 2.5. Equivalent Aircraft 8x8 Matrices For ACM Entry

$$A = \begin{bmatrix} .0000 & .0000 & .0000 & .0000 & 1.0000 & .0000 & .0000 & .0000 \\ .0000 & .0000 & .0000 & .0000 & .0000 & .0000 & 1.0000 & .0350 \\ -32.1804 & .0000 & -.0119 & -.0186 & -31.2350 & .0000 & .0000 & .0000 \\ -1.0634 & .0000 & -.0324 & -1.0634 & 894.4548 & .0000 & .0000 & .0000 \\ .0000 & .0000 & .0000 & .0069 & -.6015 & .0000 & .0000 & .0000 \\ .0000 & .0360 & .0000 & .0000 & .0000 & -.0929 & .0349 & -.0994 \\ .0000 & .0000 & .0000 & .0000 & .0000 & -27.8066 & -2.0376 & .1913 \\ .0000 & .0000 & .0000 & .0000 & .0000 & 2.4582 & -.0211 & -.1377 \end{bmatrix}$$

$$B = \begin{bmatrix} .0000 & .0000 & .0000 & .0000 & .0000 \\ .0000 & .0000 & .0000 & .0000 & .0000 \\ .0411 & .0411 & .3206 & .3206 & .0000 \\ -.3163 & -.3163 & -2.5974 & -2.5974 & .0000 \\ .1014 & .1014 & -.0699 & -.0699 & .0000 \\ .0003 & -.0003 & -.0004 & .0004 & .0006 \\ .0762 & -.0762 & .5339 & -.5339 & .1144 \\ .0486 & -.0486 & .0071 & -.0071 & -.0544 \end{bmatrix}$$

$$x = \begin{bmatrix} \theta & \phi & u & w & q & \beta & p & r \end{bmatrix}^T \quad (2.3)$$

$$u = \begin{bmatrix} \delta_{cl} & \delta_{cr} & \delta_{tel} & \delta_{ter} & \delta_{rud} \end{bmatrix}^T \quad (2.4)$$

The output matrix is

$$C = \begin{bmatrix} 0 & 0 & 1 & .0349 & 0 & 0 & 0 & 0 \\ 0 & 0 & 0 & 0 & 0 & 1 & 0 & 0 \\ 1 & 0 & 0 & 0 & 0 & 0 & 0 & 0 \\ 0 & 1 & 0 & 0 & 0 & 0 & 0 & 0 \\ 0 & 0 & 0 & 0 & 0 & 0 & 0 & 1 \end{bmatrix}$$



Simulations will be performed in the three flight phases **ACMENTRY**, **ACMEXIT**, and **TFTA** and the following single failure cases are investigated in the ACM Entry and TFTA flight modes:

1. 30% loss of left trailing edge (combination of three surfaces)
2. 50% loss of left canard
3. 25% loss of rudder

No failures are investigated in ACM Exit since the flight condition is very difficult to control with the healthy plant. Appendix A contains the reduced order(8x8) state-space models for all flight conditions and for the single failures used in this thesis.

*2.3.2 AUTOREGRESSIVE MOVING AVERAGE (ARMA) MODEL* Bokor and Keviczky's (1) technique is used to transform a plant model from state space form

$$\begin{aligned}\dot{x} &= Ax + Bu \\ y &= Cx\end{aligned}$$

to an ARMA representation where

$$y(kT) + A_1 y(k-1)T + \dots + A_N y(k-N)T = B_1 u(k-1)T + \dots + B_N u(k-N)T \quad (2.5)$$

and the matrices  $A_1$  through  $A_N$  and  $B_1$  through  $B_N$  are the ARMA coefficients. This equation is used by Porter and Fripp (9, 8) with no noise source considered. The reduced order ARMA model is determined using the ratio of the number of states  $n$  to the number of inputs  $m$ ,  $N \approx n/m$ . For the eight state, five input model used in this thesis, two  $A_i$  and  $B_i$  ARMA coefficients are sufficient to form the output Equation 2.5

Equation 2.5 can also be expressed as

$$y(kT) = \theta^T(kT)\phi(kT) = \bar{\theta}^T(kT)\bar{\phi}^T(kT) \quad (2.6)$$

where, for ease of simulation,

$$\bar{\theta}(kT) = \begin{bmatrix} A_1 \\ \vdots \\ A_N \\ B_1 \\ \vdots \\ B_N \end{bmatrix} \quad \bar{\phi}(kT) = \begin{bmatrix} -y(k-1)T \\ \vdots \\ -y(k-N)T \\ u(k-1)T \\ \vdots \\ u(k-N)T \end{bmatrix}$$

Each coefficient of  $\bar{\theta}(kT)$  is a column vector containing the  $l^2$  terms of that ARMA coefficient. Thus, the elements in the rows of  $A_1$  are transposed and placed in one column that contains the  $l^2$  values. Then the elements of  $A_2$  occupy the next  $l^2$  positions. Similarly, the elements of  $B_1$  and  $B_2$  each occupy  $l^2$  positions in  $\bar{\theta}(kT)$ .

Each term of  $\bar{\phi}(kT)$  is an  $l^2 \times m$  block diagonal sub matrix. The past outputs  $y(k-i)T$ , with  $1 \leq i \leq N$ , for each of the  $m$  inputs appear as diagonal blocks. The inputs  $u(k-i)T$ , with  $1 \leq i \leq N$ , appear in diagonal subblocks, each of size  $m \times 1$ , with only  $u_i$  appearing in each subblock. See the example matrices on the next page.

The reduced order model for the CRCA uses

$$\bar{\theta}(kT)^T = [A_1^T \ A_2^T \ B_1^T \ B_2^T]^T \in R^{1 \times 100} \quad (2.7)$$

$$\bar{\phi}(kT)^T = [-y^T(k-1)T \ -y^T(k-2)T \ u^T(k-1)T \ u^T(k-2)T]^T \in R^{5 \times 100} \quad (2.8)$$

The program used to generate the ARMA coefficients for each flight condition along with the coefficients for each flight condition is listed in Appendix B. The ARMA representation of the system is used to run the adaptive algorithm of references (8, 13).

For example, with  $n = 2$  with 2 inputs and outputs:

$$\bar{\theta} = \begin{bmatrix} A_1(1,1) \\ A_1(1,2) \\ A_1(2,1) \\ A_1(2,2) \\ A_2(1,1) \\ A_2(1,2) \\ A_2(2,1) \\ A_2(2,2) \\ B_1(1,1) \\ B_1(1,2) \\ B_1(2,1) \\ B_1(2,2) \\ B_2(1,1) \\ B_2(1,2) \\ B_2(2,1) \\ B_2(2,2) \end{bmatrix} \quad \bar{\phi} = \begin{bmatrix} -y_1(k-1) & 0 \\ -y_2(k-1) & 0 \\ 0 & -y_1(k-1) \\ 0 & -y_2(k-1) \\ -y_1(k-2) & 0 \\ -y_2(k-2) & 0 \\ 0 & -y_1(k-2) \\ 0 & -y_2(k-2) \\ u_1(k-1) & 0 \\ u_2(k-1) & 0 \\ 0 & u_1(k-1) \\ 0 & u_2(k-1) \\ u_1(k-2) & 0 \\ u_2(k-2) & 0 \\ 0 & u_1(k-2) \\ 0 & u_2(k-2) \end{bmatrix}$$

**2.3.3 ACTUATOR MODELS** The CRCA has no mechanical connections between the pilot and the control surfaces and is thus termed a fly-by-wire control system. In order to add validity to the designs accomplished, actuator dynamics must be taken into consideration. In addition to actuator dynamics, the physical limitations of maximum deflections and deflection rates must also be incorporated into the actuator model. Table 2.6 lists the limitations for the three different control surfaces.

Hammond worked primarily with the first order actuator model

$$\delta_{control}(s) = \frac{20}{(s + 20)} \delta_{cmd} \quad (2.9)$$

Table 2.6. Control Surface Position and Rate Limits

Surface	Position Limit (deg)		Rate Limit (deg/sec)
Canards	+60	-30	$\pm 100$
Trailing Edges	+30	-30	$\pm 100$
Rudder	+20	-20	$\pm 100$

A second order approximation of the actuator model is used exclusively throughout this thesis effort.

$$\delta_{control}(s) = \frac{5113}{(s + 53 \pm j48)} \delta_{cmd} \quad (2.10)$$

A description of the CRCA is described by a set of linear differential equations and an eight state model. The aircraft models are linearized about 3 flight conditions, TF/TA, ACM Entry, and ACM Exit and include second order actuator dynamics. The autoregressive moving average (ARMA) representation of aircraft is also presented. The PI control law development is presented in Chapter 3.

### III. DESIGN PROCEDURES

#### 3.1 OVERVIEW

The PI controller design techniques developed by Porter are implemented using output feedback. Using output feedback is often more advantageous than using state feedback if all of the states are not readily available and estimates would have to be used (3:660). Using Porter's method, tracking can be achieved with little to no coupling occurring between outputs. The use of high gain in the forward loop results in an asymptotic transfer function for the closed loop system composed of fast and slow modes. "The slow modes are asymptotically uncontrollable or unobservable, and thus the output response is dominated by the fast modes." (3:661)

#### 3.2 DISCRETE, FIXED-GAIN PI CONTROLLER THEORY

The plant must satisfy four necessary criteria before any of Porter's design techniques can be used:

1. The plant must be completely controllable.
2. The plant must be completely observable.
3.  $\text{rank} \begin{bmatrix} B & A \\ D & C \end{bmatrix} = n + l$
4. Transmission zeros can be computed from

$$\begin{vmatrix} sI - A & B \\ -C & D \end{vmatrix} = 0$$

for the completely controllable and completely observable plant. No transmission zeros can be located at the origin, or the plant is functionally uncontrollable. The number of transmission zeros for the plant where  $l = m$  is  $n - m - d$ , where  $d$  is the rank deficiency of **CB** (3:668).

The continuous aircraft, or plant, may be represented by equations of the form

$$\begin{bmatrix} \dot{x}_1(t) \\ \dot{x}_2(t) \end{bmatrix} = \begin{bmatrix} A_{11} & A_{12} \\ A_{21} & A_{22} \end{bmatrix} \begin{bmatrix} x_1(t) \\ x_2(t) \end{bmatrix} + \begin{bmatrix} 0 \\ B_2 \end{bmatrix} u(t) \quad (3.1)$$

$$y(t) = \begin{bmatrix} C_1 & C_2 \end{bmatrix} \begin{bmatrix} x_1(t) \\ x_2(t) \end{bmatrix} \quad (3.2)$$

where the dimensions are

$$x_1 : (n - m) \times 1$$

$$x_2 : m \times 1$$

$$A_{11} : (n - m) \times (n - m)$$

$$A_{22} : m \times 1$$

$$B_2 : m \times m \text{ and has rank } m$$

$$C_2 : m \times m \text{ and has rank } m$$

Notice that the **B** matrix in Table 2.5 and the **B** matrices for the rest of the CRCA's flight conditions are not of the required form in Equation 3.1. A transformation could be performed to express the CRCA state space matrices in the form of Equation 3.1. However, this step has been proven to be unnecessary (3:668-669), and the design can be performed for any form of the state equations.

The rank of the matrix product **CB** (the first Markov parameter) must be checked. For a plant that has  $\text{rank}(\mathbf{CB})=m$ , the plant is termed "regular" and only requires output feedback. For a plant like the CRCA where  $\text{rank}(\mathbf{CB}) < m$ , the plant has a rank deficient first Markov parameter and rate feedback of the state vector  $\dot{x}_1$  must augment the output feedback. Figure 3.1 illustrates the control law used for irregular plants.

The feedback signal with rate feedback incorporated is now

$$w = y + M\dot{x}_1$$

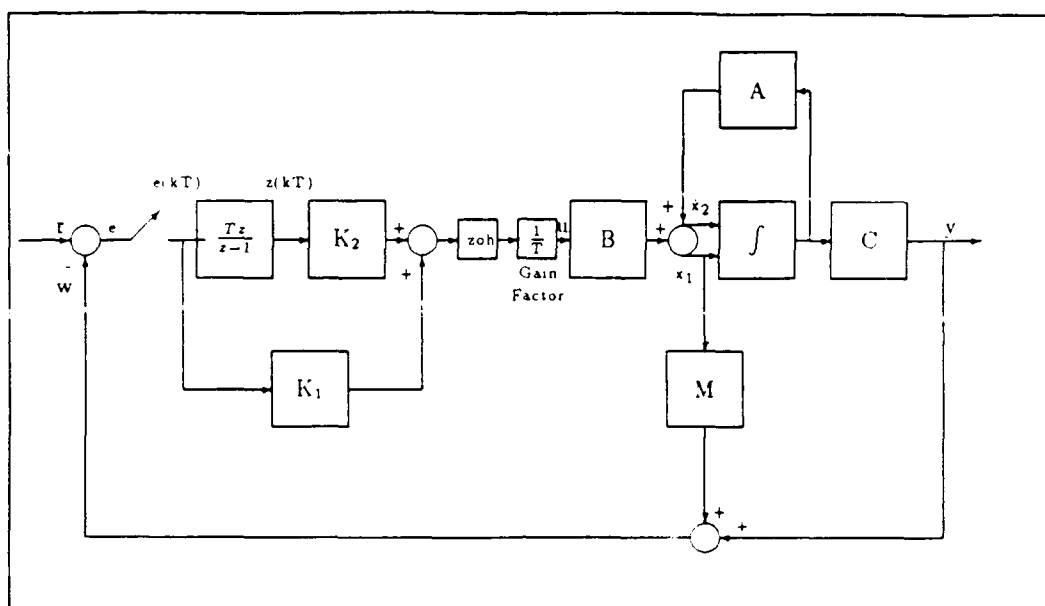


Figure 3.1. Discrete PI Controller - Irregular Plant  
(4)

From Equations 3.1 and 3.2 it can be shown that

$$\begin{aligned}
 w &= \begin{bmatrix} C_1 & C_2 \end{bmatrix} \begin{bmatrix} x_1 \\ x_2 \end{bmatrix} + M \begin{bmatrix} A_{11} & A_{12} \end{bmatrix} \begin{bmatrix} x_1 \\ x_2 \end{bmatrix} \\
 &= \begin{bmatrix} F_1 & F_2 \end{bmatrix} \begin{bmatrix} x_1 \\ x_2 \end{bmatrix}
 \end{aligned} \tag{3.3}$$

From Figure 3.1 it can be seen that

$$e = r - w$$

where  $r$  = commanded input signal.

Expressing the state equation in the discrete time domain yields the difference equation

$$x(k+1)T = \Phi(T)x(kT) + \Psi(T)u(kT) \tag{3.4}$$

where

$$\Phi(T) = e^{AT} = \begin{bmatrix} \phi_{11}(T) & \phi_{12}(T) \\ \phi_{21}(T) & \phi_{22}(T) \end{bmatrix} \quad (3.5)$$

and

$$\Psi(T) = \int_0^T e^{A\tau} d\tau \begin{bmatrix} 0 \\ B_2 \end{bmatrix} = \begin{bmatrix} \psi_1(T) \\ \psi_2(T) \end{bmatrix} \quad (3.6)$$

and the difference equation representing the integral of the error is

$$\begin{aligned} z(k+1)T &= z(kT) + Te(kT) \\ &= z(kT) + T[r(kT) - w(kT)] \\ &= z(kT) + Tr(kT) - TF_1x_1(kT) - TF_2x_2(kT) \end{aligned} \quad (3.7)$$

The composite difference equation for the open loop of Figure 3.1 is

$$\begin{aligned} \begin{bmatrix} z(k+1)T \\ x_1(k+1)T \\ x_2(k+1)T \end{bmatrix} &= \begin{bmatrix} I_l & -TF_1 & -TF_2 \\ 0 & \phi_{11} & \phi_{12} \\ 0 & \phi_{21} & \phi_{22} \end{bmatrix} \begin{bmatrix} z(kT) \\ x_1(kT) \\ x_2(kT) \end{bmatrix} + \begin{bmatrix} 0 \\ \psi_1 \\ \psi_2 \end{bmatrix} u(kT) \\ &+ \begin{bmatrix} TI_l \\ 0 \\ 0 \end{bmatrix} r(kT) \end{aligned} \quad (3.8)$$

$$y = \begin{bmatrix} 0 & C_1 & C_2 \end{bmatrix} \begin{bmatrix} z(kT) \\ x_1(kT) \\ x_2(kT) \end{bmatrix} \quad (3.9)$$

where the control law is

$$\begin{aligned} u(kT) &= \frac{1}{T}[K_1e(kT) + K_2z(kT)] \\ &= \frac{1}{T}[K_1r(kT) - K_1F_1x_1(kT) - K_1F_2x_2(kT) + K_2z(kT)] \end{aligned}$$



The closed loop equation for the system can now be written as

$$\begin{bmatrix} z(k+1)T \\ x_1(k+1)T \\ x_2(k+1)T \end{bmatrix} = \begin{bmatrix} I_l & -TF_1 & -TF_2 \\ \frac{1}{T}\psi_1 K_2 & \phi_{11} - \frac{1}{T}\psi_1 K_1 F_1 & \phi_{12} - \frac{1}{T}\psi_1 K_1 F_2 \\ \frac{1}{T}\psi_2 K_2 & \phi_{21} - \frac{1}{T}\psi_2 K_1 F_1 & \phi_{22} - \frac{1}{T}\psi_2 K_1 F_2 \end{bmatrix} \begin{bmatrix} z(kT) \\ x_1(kT) \\ x_2(kT) \end{bmatrix} + \begin{bmatrix} TI_l \\ \frac{1}{T}\psi_1 K_1 \\ \frac{1}{T}\psi_2 K_1 \end{bmatrix} r(kT) \quad (3.10)$$

No changes appear in Equation 3.9, the system output.

The form of Equation 3.10 that is in Porter's paper (2) is obtained by making the substitutions

$$\Phi(T) = e^{AT} = I + AT + \frac{A^2 T^2}{2!} + \dots \quad (3.11)$$

$$\lim_{T \rightarrow 0} e^{AT} = I + AT + 0(\text{H.O.T.})$$

$$\lim_{T \rightarrow 0} \frac{1}{T} [e^{AT} - I] = A + 0(\text{H.O.T.})$$

$$\begin{bmatrix} \phi_{11} & \phi_{12} \\ \phi_{12} & \phi_{22} \end{bmatrix} = \begin{bmatrix} A_{11}T + I_{n-l} & A_{12}T \\ A_{21}T & A_{22}T + I_l \end{bmatrix} \quad (3.12)$$

$$\lim_{T \rightarrow 0} \frac{1}{T} \Psi(T) = \frac{1}{T} \int_0^T [I] d\tau \begin{bmatrix} 0 \\ B_2 \end{bmatrix} = \frac{1}{T}(T) \begin{bmatrix} 0 \\ B_2 \end{bmatrix} = \begin{bmatrix} 0 \\ B_2 \end{bmatrix} = \begin{bmatrix} \frac{1}{T}\psi_1(T) \\ \frac{1}{T}\psi_2(T) \end{bmatrix}$$

Equation 3.10 can now be written as

$$\begin{bmatrix} z(k+1)T \\ x_1(k+1)T \\ x_2(k+1)T \end{bmatrix} = \begin{bmatrix} I_l & -TF_1 & -TF_2 \\ 0 & A_{11}T + I_{n-l} & A_{12}T \\ B_2K_2 & A_{21}T - B_2K_1F_1 & A_{22}T + I_l - B_2K_1F_2 \end{bmatrix} \begin{bmatrix} z(kT) \\ x_1(kT) \\ x_2(kT) \end{bmatrix} + \begin{bmatrix} TI_l \\ 0 \\ B_2K_1 \end{bmatrix} r(kT) \quad (3.13)$$

The output equation has not changed from Equation 3.9.

Singular perturbation methods, where  $\epsilon = \frac{1}{T} \rightarrow \infty$  are the perturbation variable, is used to block diagonalize the closed loop system of Equation 3.13 and to determine the *fast* and *slow* modes of the system (3, 2).

Equation 3.13 must first be represented by the form

$$\begin{bmatrix} \bar{x}_1(k+1)T \\ \bar{x}_2(k+1)T \end{bmatrix} = \begin{bmatrix} \bar{A}_1 & \bar{A}_2 \\ \bar{A}_3 & \bar{A}_4 \end{bmatrix} \bar{x}(kT) + \begin{bmatrix} \bar{B}_1 \\ \bar{B}_2 \end{bmatrix} r(kT) = \bar{A}\bar{x}(kT) + \bar{B}r(kT) \quad (3.14)$$

$$y(kT) = \begin{bmatrix} \bar{C}_1 & \bar{C}_2 \end{bmatrix} \bar{x}(kT) \quad (3.15)$$

where

$$\bar{x}_1(kT) = \begin{bmatrix} z(kT) \\ x_1(kT) \end{bmatrix}$$

and the matrix dimensions are

$$\bar{A}_1 : (n-m) \times (n-m)$$

$$\bar{A}_4 : m \times m$$

$$\bar{B}_2 : m \times m \text{ and has rank } m$$

A transformation matrix,  $T$ , can be used to transform Equation 3.14 into block diagonal form (3)

$$\begin{bmatrix} x_s(k+1)T \\ x_f(k+1)T \end{bmatrix} = \begin{bmatrix} A_s & 0 \\ 0 & A_f \end{bmatrix} \begin{bmatrix} x_s(kT) \\ x_f(kT) \end{bmatrix} + \begin{bmatrix} B_s \\ B_f \end{bmatrix} r(kT) \quad (3.16)$$

$$y(kT) = \begin{bmatrix} C_s & C_f \end{bmatrix} \begin{bmatrix} x_s(kT) \\ x_f(kT) \end{bmatrix} \quad (3.17)$$

D'Azzo explains the steps to block diagonalize Equation 3.14 (3:663-667). Comparing D'Azzo's results to those that Porter obtained for the discrete plant (2:1210),

$$A_s = I + TA_0 \quad A_0 = \begin{bmatrix} -K_1^{-1}K_2 & 0 \\ A_{12}F_2^{-1}K_1^{-1}K_2 & A_{11} - A_{12}F_2^{-1}F_1 \end{bmatrix}$$

$$A_f = I + A_4 \quad A_4 = -B_2K_1F_2$$

$$B_s = TB_0 \quad B_0 = \begin{bmatrix} 0 \\ A_{12}F_2^{-1} \end{bmatrix}$$

$$B_f = B_2K_1$$

$$C_s = C_0 \quad C_0 = \begin{bmatrix} C_2F_2^{-1}K_1^{-1}K_2 & C_1 - C_2F_2^{-1}F_1 \end{bmatrix}$$

$$C_f = C_2$$

The overall transfer function for the closed loop system is

$$\begin{aligned}
 \Gamma(\lambda) &= \begin{bmatrix} C_s & C_f \end{bmatrix} \begin{bmatrix} \lambda I - A_s & 0 \\ 0 & \lambda I - A_f \end{bmatrix}^{-1} \begin{bmatrix} B_s \\ B_f \end{bmatrix} \\
 &= C_s(\lambda I - A_s)^{-1} B_s + C_f(\lambda I - A_f)^{-1} B_f \\
 &= \Gamma_s(\lambda) + \Gamma_f(\lambda)
 \end{aligned} \tag{3.18}$$

There are three sets of eigenvalues for the asymptotic transfer function, two *slow* and one *fast*. The first set of *slow* eigenvalues is

$$\mathcal{Z}_1 = \left\{ \left| \lambda I_l - I_l + T K_1^{-1} K_2 \right| = 0 \right\}$$

This set of poles is asymptotically uncontrollable because of the zero element in  $B_s$ .

The second set of *slow* eigenvalues is both controllable and observable. This set contains the transmission zeros of the plant augmented with the minor loop rate feedback through the measurement matrix,  $M$ .

$$\mathcal{Z}_2 = \left\{ \left| \lambda I_{n-l} - I_{n-l} - T A_1 + T A_{12} F_2^{-1} F_1 \right| = 0 \right\}$$

The set of *fast* eigenvalues are also controllable and observable. Note that eigenvalues obtained from  $A_4 = B_2 K_1 F_2$  and  $F_2 B_2 K_1$  (which is used below) are identical.

$$\mathcal{Z}_3 = \{ |\lambda I_l - I_l + F_2 B_2 K_1| = 0 \}$$

All three sets of poles must lie in the open left half  $s$  plane or open unit circle in the  $z$  plane. The output consists of the *fast* modes containing the poles  $\mathcal{Z}_3$  and a set of *slow* modes containing the poles  $\mathcal{Z}_2$ .

### 3.3 DESIGN PARAMETERS FOR THE DISCRETE FIXED-GAIN PI CONTROLLER

In order to achieve a diagonal transfer function,  $\Gamma(\lambda)$  for an irregular plant, the measurement matrix,  $M$  in Figure 3.1 must be chosen carefully.  $M$  should be formed with as few non-zero elements as possible so that

$$F_2 = C_2 + MA_{12} \quad (3.19)$$

has full rank  $m$  and  $C_2 F_2^{-1}$  is diagonal.

The following steps outline the procedure to determine the form of the measurement matrix (3, 4):

1. Form the matrix

$$B^* = \begin{bmatrix} c_1^T A_{11}^{d_1} A_{12} \\ \vdots \\ c_m^T A_{11}^{d_m} A_{12} \end{bmatrix} \quad (3.20)$$

where  $m$  is the number of control inputs,  $c_i^T$  is the  $i$ th row of  $C_1$  and

$$d_i = \min [j : c_i^T A_{11}^j A_{12} \neq 0, j = 0, 1, \dots, n-1] \quad (3.21)$$

Equation 3.21 specifies that  $d_i$  is the smallest value of  $j$  for which  $c_i^T A_{11}^j A_{12} \neq 0$ . The permissible values of  $j$  are  $0, 1, \dots, n-1$ . If all the values of  $j$  result in  $c_i^T A_{11}^j A_{12} = 0$ , then use  $d_i = n-1$ , where  $n = \text{dimension of } A_{11}$ .

2. Form  $F_2 = C_2 + MA_{12}$  using a general form of the matrix  $M = [m_{ij}]$ . The elements  $m_{ij}$  appearing in  $F_2$  are permitted nonzero values only if  $B^*$  has a non-zero element in a corresponding position. All other elements of  $M$  are set equal to zero.
3. Form  $C_2 F_2^{-1}$  and set off-diagonal terms to zero if possible to ensure a diagonal matrix.
4. Ensure that  $F_2$  has rank  $m$ .

For the CRCA, Equation 3.20 is formed using the parameters from ACM Entry.

$$C_1 = \begin{bmatrix} 0 & 0 & 1 \\ 0 & 0 & 0 \\ 1 & 0 & 0 \\ 0 & 1 & 0 \\ 0 & 0 & 0 \end{bmatrix}$$

$$C_2 = \begin{bmatrix} .0349 & 0 & 0 & 0 & 0 \\ 0 & 0 & 1 & 0 & 0 \\ 0 & 0 & 0 & 0 & 0 \\ 0 & 0 & 0 & 0 & 0 \\ 0 & 0 & 0 & 0 & 1 \end{bmatrix}$$

$$A_{11} = \begin{bmatrix} 0 & 0 & 0 \\ 0 & 0 & 0 \\ -32.1804 & 0 & -.0119 \end{bmatrix}$$

$$A_{12} = \begin{bmatrix} 0 & 1 & 0 & 0 & 0 \\ 0 & 0 & 0 & 1 & 0.035 \\ -.0186 & -31.235 & 0 & 0 & 0 \end{bmatrix}$$

It can be verified that the form of  $M$  does not change for the different flight conditions by noting the same location of non-zero elements in  $A_{11}$ ,  $A_{12}$ ,  $C_1$ , and  $C_2$  terms of Appendix A.

Equation 3.20 yields the values  $d_1 = d_2 = d_3 = d_4 = d_5 = 0$ . Then  $B^*$  is formed.

$$B^* = \begin{bmatrix} -.0186 & -31.235 & 0 & 0 & 0 \\ 0 & 0 & 0 & 0 & 0 \\ 0 & 1 & 0 & 0 & 0 \\ 0 & 0 & 0 & 1 & 0.0349 \\ 0 & 0 & 0 & 0 & 0 \end{bmatrix} \quad (3.22)$$

The matrix  $C_2$  in Equation 3.19 has a dimension  $5 \times 5$ . Since the dimension of  $A_{12}$  is  $3 \times 5$ , the necessary dimension of  $M$  is  $5 \times 3$ . Using  $M$  of the form

$$M = \begin{bmatrix} m_{11} & m_{12} & m_{13} \\ m_{21} & m_{22} & m_{23} \\ m_{31} & m_{32} & m_{33} \\ m_{41} & m_{42} & m_{43} \\ m_{51} & m_{52} & m_{53} \end{bmatrix} \quad (3.23)$$

the matrix  $F_2$  of Equation 3.19 is

$$F_2 = \begin{bmatrix} .0349 - .0186m_{13} & m_{11} - 31.235m_{13} & 0 & m_{12} & .035m_{12} \\ -.0186m_{23} & m_{21} - 31.235m_{23} & 1 & m_{22} & .035m_{22} \\ -.0186m_{33} & m_{31} - 31.235m_{33} & 0 & m_{32} & .035m_{32} \\ -.0186m_{43} & m_{41} - 31.235m_{43} & 0 & m_{42} & .035m_{42} \\ -.0186m_{53} & m_{51} - 31.235m_{53} & 0 & m_{52} & 1 + .035m_{52} \end{bmatrix} \quad (3.24)$$

The assignable elements of  $F_2$  are permitted non-zero values only if  $B^*$  has a nonzero element in the same position. Thus, it is required that  $m_{23} = m_{33} = m_{43} = m_{53} = m_{21} = m_{41} = m_{51} = m_{12} = m_{22} = m_{32} = m_{52} = 0$ . This leaves an  $F_2$  matrix of the form

$$F_2 = \begin{bmatrix} .0349 - .0186m_{13} & m_{11} - 31.235m_{13} & 0 & 0 & 0 \\ 0 & 0 & 1 & 0 & 0 \\ 0 & m_{31} & 0 & 0 & 0 \\ 0 & 0 & 0 & m_{42} & .035m_{42} \\ 0 & 0 & 0 & 0 & 1 \end{bmatrix} \quad (3.25)$$

The matrix  $C_2 F_2^{-1}$  must be diagonal, therefore the third element in the first row of Equation 3.26,  $m_{11} = 31.235m_{13}$ . It is also apparent from the first and third terms of the first row that setting  $m_{13} = 0$  ensures that the matrix product is diagonal and insensitive to variation of the measurement matrix values. With non-zero values of  $m_{31}$  and  $m_{42}$ , rank of  $F_2$  is  $m$ . Since the measurement matrix implemented in the computer simulations has only two non-zero elements  $m_{31}$  and  $m_{42}$ , a reduced  $5 \times 2$   $M$  matrix is used since the third column of  $M$  contains only zeros.

$$C_2 F_2^{-1} = \begin{bmatrix} \frac{.0349}{.0349 - .0186m_{13}} & 0 & \frac{.0349(m_{11} - 31.235m_{13})}{-(.0349 - .0186m_{13})m_{31}} & 0 & 0 \\ 0 & 1 & 0 & 0 & 0 \\ 0 & 0 & 0 & 0 & 0 \\ 0 & 0 & 0 & 0 & 0 \\ 0 & 0 & 0 & 0 & 1 \end{bmatrix} \quad (3.26)$$

The proportional path gain matrix,  $K_1$  in Figure 3.1 is selected to make the fast transfer function,  $\Gamma_f(\lambda)$  of Equation 3.18 diagonal. Therefore,

$$F_2 B_2 K_1 = \Sigma \quad (3.27)$$

where  $\Sigma$  is a diagonal matrix of elements  $\sigma_i$ . So

$$K_1 = (F_2 B_2)^{-1} \Sigma \quad (3.28)$$

and

$$K_2 = -\lambda_0 K_1 \quad (3.29)$$

$\lambda_0$  is the ratio of integral to proportional control.

This form of  $M$  and the appropriate choice of  $K_1$  only ensure that the fast transfer function,  $\Gamma_f(\lambda)$  of Equation 3.18 is diagonal. All of the terms of  $\Gamma_s(\lambda)$  must also be diagonal to ensure an overall diagonal transfer function  $\Gamma(\lambda)$ .

The elements of the  $\Sigma$  matrix are selected by a trial and error process. When a diagonal  $\Gamma(\lambda)$  has been achieved, each element of the  $\Sigma$  matrix,  $\sigma_i$  fine tunes the  $i$ th input's affect on the  $i$ th output.

### 3.4 DISCRETE STEP RESPONSE PI CONTROLLER THEORY AND DESIGN

Porter has developed a technique that can be used to design a control system for a plant when the mathematical equations are not known (10, 8). The method has been developed for a regular and asymptotically stable plants (where all open loop eigenvalues are in the open unit circle of the  $z$  plane) where the steady state transfer function,  $G(0)$ , has rank  $m$  (no transmission zeros at the origin) and  $F^*$ , the plant decoupling matrix, has full rank  $m$ .

$$F^* = \begin{bmatrix} c_1^T A^{d_1} B \\ \vdots \\ c_m^T A^{d_m} B \end{bmatrix} \quad (3.30)$$



$m$  is the number of control inputs,  $c_i^T$  is the  $i$ th row of  $C$  and

$$d_i = \min [j : c_i^T A^j B \neq 0, j = 0, 1, \dots, n-1] \quad (3.31)$$

An effort has been made in Hammond's thesis to extend this design to the case of an irregular and unstable plant. The extension of the step response method is continued in this thesis effort.

The discretized plant Equations 3.4, 3.7 are repeated and Equation 3.3 is used to form

$$\begin{aligned} x(k+1)T &= \Phi x(kT) + \Psi u(kT) \\ z(k+1)T &= z(kT) + T e(kT) \\ &= z(kT) + T r(kT) - T w(kT) \\ &= x(kT) + T r(kT) - T F x(kT) \end{aligned}$$

The control law is

$$u(kT) = T [K_1 e(kT) + K_2 z(kT)] \quad (3.32)$$

Note that Figure 3.1 is applicable, if the gain factor is changed to  $T$  for this design. The closed loop equation can now be expressed as

$$\begin{aligned} x(k+1)T &= (\Phi - T\Psi K_1 F)x(kT) + T\Psi K_2 z(kT) + T\Psi K_1 r(kT) \\ z(k+1)T &= -TFx(kT) + z(kT) + Tr(kT) \end{aligned}$$

The block diagonalization depicted in Equations 3.16 and 3.17 is performed and the following two sets of eigenvalues result. The *slow* set is determined from

$$\mathcal{Z}_1 = \{|\lambda I_n - I_n + T A| = 0\}$$

and the *fast* set is

$$\mathcal{Z}_2 = \{|\lambda I_l - I_l + T^2 A^{-1} B K_2| = 0\}$$

The step response method is designed around two plant responses,  $H(T)$  and  $G(0) = H(\infty)$ . The response with a step input at the first sampling time,  $T$ , is

$$H(T) = CA^{-1}(e^{AT} - I_n)B$$

Referencing Equation 3.11,  $H(T)$  can be approximated as  $T \rightarrow 0$  by

$$H(T) = CA^{-1}ATB = TCB \quad (3.33)$$

$$G(s) = C(sI_n - A)^{-1}B$$

and as  $s \rightarrow 0$ ,

$$G(0) = -CA^{-1}B \quad (3.34)$$

The proportional and integral path gain matrices are given as (10, 9, 8)

$$K_1 = H(T)^{-1}\Sigma \quad (3.35)$$

and

$$K_2 = G(0)^{-1}\Gamma\Pi \quad (3.36)$$

where  $\Sigma$  is a diagonal matrix as defined in Equation 3.27 and  $\Gamma\Pi$  is another diagonal matrix of arbitrary values which are determined by trial and error through computer simulations.

Using the  $A$ ,  $B$ , and  $C$  matrices for the representative flight condition of Table 2.5, the resulting  $F^*$  and  $G(0)$  matrices have full rank of  $m = 5$ .

If the plant equations are known in advance, the approximations of Equations 3.33 and 3.34 can be used. Otherwise, off line, open loop tests could be performed on the plant to determine  $H(T)$  and  $G(0)$  for a known input.

The aircraft equations

$$\dot{x} = Ax + Bu$$

and

$$y = Cx$$

can be expressed in terms of ARMA coefficients. The algorithm developed by Velez (11) was used to generate the ARMA coefficients for the model.

$$y(kT) + A_1 y(k-1)T + \dots + A_N y(k-N)T = B_1 u(k-1)T + \dots + B_N u(k-N)T \quad (3.37)$$

It can be seen from the equation above that

$$H(T) = B_1$$

and since,  $y(0)=0$ ,

$$G(0) = (I + A_1 + \dots + A_N)^{-1}(B_1 + \dots + B_N)$$

### 3.5 ADAPTIVE STEP RESPONSE PI CONTROLLER

There are many parameter adaptive algorithms from which the designer can choose. Hammond chose to use a least squares method since "It is conceptually simple and exhibits statistical properties that are as good as those of maximum likelihood method for most practical situations." (4:3-12)

The parameter that is to be estimated is the ARMA coefficient representation of the plant, or the vector  $\theta$ . The ARMA model representation of Equation 3.37 is used and the ARMA output Equations 2.6., 2.7. and 2.8 are repeated here.

$$y(kT) = \theta^T(kT)\phi(kT)$$

where for the reduced second order ARMA model of the CRCA,

$$\begin{aligned} \theta^T(kT) &= [A_1^T \ A_2^T \ B_1^T \ B_2^T]^T \\ \phi(kT)^T &= [-y^T(k-1)T \ -y^T(k-2)T \ u^T(k-1)T \ u^T(k-2)T]^T \end{aligned}$$

Hammond used the following equations to implement the least squares estimate of  $\theta$  (4:3-13).

$$\theta(k+1) = \theta(k) + P(k)x(k+1)\gamma(k+1)[y(k+1) - x^T(k+1)\theta(k)] \quad (3.38)$$

$$P(k+1) = P(k) - P(k)x(k+1)\gamma(k+1)x^T(k+1)P(k) \quad (3.39)$$

$$\gamma(k+1) = \frac{1}{[\alpha_t + x^T(k+1)P(k)x(k+1)]} \quad (3.40)$$

where  $x(k+1)$  is Hammond's notation in the adaptive algorithm for  $\phi(k+1)$ ,  $P(k)$  is the covariance matrix, and  $\alpha_t$  is a weighting factor = 1 for this effort.

Calculation of  $P(k+1)$  in Equation 3.39 can be changed by the introduction of a forgetting factor,  $\lambda$  (Hammond used  $\gamma$  as the forgetting factor, but that notation is confusing since there is another term  $\gamma(k+1)$  used in the Equations 3.38 and 3.39).

$$P(k+1) = \frac{1}{\lambda} [P(k) - P(k)x(k+1)\gamma(k+1)x^T(k+1)P(k)] \quad (3.41)$$

and  $\gamma(k+1)$  of Equation 3.40 now becomes

$$\gamma(k+1) = \frac{1}{[\lambda\alpha_t + x^T(k+1)P(k)x(k+1)]} \quad (3.42)$$

When the forgetting factor is incorporated in simulations, Equations 3.38, 3.41, and 3.42 are used to update the changing ARMA coefficients.

This chapter details the mathematical development of Porter's discrete PI control laws; discrete PI, step response, and parameter adaptive based upon an ARMA model. Procedures are outlined for determination of the controller gain matrices  $K_1$  and  $K_2$  based upon known plant matrices or step responses. The chapter concludes with a presentation of the recursive least squares parameter estimation algorithm to be used. Chapter 4 contains the results from the discrete PI controller.

## IV. DISCRETE PI CONTROLLER

### 4.1 TRANSFER FUNCTION ANALYSIS

In addition to the plant meeting the conditions listed in Section 3.2, the steady state control surface deflections necessary to perform each maneuver in every flight condition (including failures) must be examined. If the amount of control surface deflection required in steady state is larger than the position limits listed in Table 2.6, then the maneuver cannot be performed for that particular flight condition. The control surface rate and position limits cannot be exceeded at any time in the simulations or the responses will become nonlinear when limit circuits are encountered. The steady state surface deflections determined for each combination of maneuvers will be used as a guide to determine the feasibility of maneuver performance.

The output relationship shown below is used to determine the steady state surface deflections (inputs) required to perform each maneuver.

$$y(s) = G(s)u(s)$$

Applying the final value theorem, where  $u_{ss}$  is the magnitude of the step input and  $y_{ss}$  is the magnitude of the desired system output,

$$u_{ss} = G(0)^{-1}y_{ss} \quad (4.1)$$

where  $G(0)$  is defined in Equation 3.34, which is repeated below, and  $y_{ss} = r(t)$  for a tracking system.

$$G(0) = -CA^{-1}B$$

The five maneuvers and their associated input commands are

1. pitch rate tracking -  $q=2^\circ/\text{sec}$  for 3 sec and zero thereafter. The pitch rate command is generated by ramping  $\theta$  to  $6^\circ$  over 3 seconds.

2. coordinated turn - 45° roll angle ( $\phi$ ) and yaw rate ( $r$ ) determined from Equation 4.2 (4.4-7).

$$r \left( \frac{deg}{sec} \right) = \frac{g}{V} \sin(\phi) 57.3 \frac{deg}{rad} \quad (4.2)$$

where,

$g$  = the gravitational constant (32.174 ft/sec<sup>2</sup>)

$V$  = the forward velocity of the aircraft

$\phi$  = the desired bank angle

3. sideslip tracking - 2° of sideslip angle ( $\beta$ )  
 4. flat turn - 1°/sec yaw rate ( $r$ ) with zero roll angle ( $\phi$ )  
 5. banked turn - only roll angle ( $\phi$ ) commanded

Table 4.1 gives the corresponding yaw rate ( $r$ ) for each of the flight conditions considered in this thesis when the bank angle ( $\phi$ ) is equal to 45 degrees.

Table 4.1.  $r_{cmd}$  - 45° Bank Angle

Flight Condition	Velocity ft/sec	Gravity ft/sec <sup>2</sup>	Yaw Rate deg/sec
ACM Entry	895.0	32.17	1.457
ACM Exit	263.0	32.17	4.956
TF/TA	1004.9	32.17	1.297

The output vectors for each maneuver,  $y_{ss}$ , consist of the following five outputs and the units are expressed in ft/sec for the velocity, radians for the angles, and rad/sec for the yaw rate,

$v$  = forward velocity

$\beta$  = sideslip angle

$\theta$  = pitch angle

$\phi$  = bank angle

$r$  = yaw rate

and the input vector,  $u_{ss}$ , consists of the five control surface inputs, where the units are expressed in degrees.

$$\begin{aligned}\delta_{cl} &= \text{left canard} \\ \delta_{cr} &= \text{right canard} \\ \delta_{tel} &= \text{left trailing edge} \\ \delta_{ter} &= \text{right trailing edge} \\ \delta_{rud} &= \text{rudder}\end{aligned}$$

The steady state output vector for a 45° coordinated turn in ACM Entry is:

$$y_{ss} = \begin{bmatrix} 0.0000 \text{ ft/sec} \\ 0.0000 \text{ rad} \\ 0.1047 \text{ rad} \\ 0.0000 \text{ rad} \\ 0.0000 \text{ rad/sec} \end{bmatrix} \quad (4.3)$$

and from Equation 4.1, the steady state surface deflections are:

$$u_{ss} = \begin{bmatrix} -1.4411 \text{ deg} \\ 1.4411 \text{ deg} \\ 0.4767 \text{ deg} \\ -0.4767 \text{ deg} \\ -2.6545 \text{ deg} \end{bmatrix} \quad (4.4)$$

The necessary surface deflections to perform each maneuver in all flight conditions considered are listed in Tables 4.2, 4.3, 4.4, 4.5, 4.6, and 4.7. The  $G(0)$  for 25% loss of rudder in **ACM Entry** is not invertible.

Table 4.2. Steady State Control Inputs - Pitch Rate Tracking

Flight Condition	$\delta_{cl}$ (deg)	$\delta_{cr}$ (deg)	$\delta_{tel}$ (deg)	$\delta_{ter}$ (deg)	$\delta_{rud}$ (deg)
ACMENTRY	1.2100	1.2100	1.3836	1.3836	0.0000
ACM30TL	2.6967	2.7687	5.4502	3.1944	0.0000
ACM50CL	-16.3074	-3.6573	-4.6384	-6.0154	-3.6573
ACM25RL	N/A	N/A	N/A	N/A	N/A
ACMEXIT	-16.4536	-14.4260	-31.9885	-28.6533	-3.0725
TFTA	1.0384	1.1469	1.6532	1.5927	-0.0945
TFTA30TL	0.8025	0.7998	2.0189	1.1727	-0.0013
TFTA50CL	2.2060	1.1090	1.8015	1.7633	0.0060
TFTA25RL	-2.1867	3.2095	1.0801	1.3309	5.3962

where,

**ACMENTRY** = ACM Entry (nominal flight condition)

**ACM30TL** = 30% loss of effectiveness of the left trailing edge - ACM Entry

**ACM50CL** = 50% loss of effectiveness of the left canard - ACM Entry

**ACM25RL** = 25% loss of effectiveness of the rudder - ACM Entry

**ACMEXIT** = ACM Exit flight condition

**TFTA** = TF/TA flight condition

**TFTA30TL** = 30% loss of effectiveness of the left trailing edge - TF/TA

**TFTA50CL** = 50% loss of effectiveness of the left canard - TF/TA

**TFTA25RL** = 25% loss of effectiveness of the rudder - TF/TA



Table 4.3. Steady State Control Inputs - 45° Coordinated Turn

Flight Condition	$\delta_{cl}$ (deg)	$\delta_{cr}$ (deg)	$\delta_{tel}$ (deg)	$\delta_{ter}$ (deg)	$\delta_{rud}$ (deg)
ACMENTRY	-1.4411	1.4411	0.4767	-0.4767	-2.6545
ACM30TL	-1.6473	1.5466	0.7891	-0.5858	-2.8283
ACM50CL	0.8474	1.6176	1.1141	0.7271	-1.2235
ACM25RL	N/A	N/A	N/A	N/A	N/A
ACMEXIT	46.8304	42.2510	100.3224	90.4552	7.7426
TFTA	-0.3664	0.3664	0.2181	-0.2181	-0.7977
TFTA30TL	-0.4190	0.3684	0.3435	-0.2782	-0.8498
TFTA50CL	-0.9488	0.1031	-0.1306	-0.4729	-0.6676
TFTA25RL	-1.9385	1.9385	0.2696	-0.2696	1.3886

Table 4.4. Steady State Control Inputs - Sideslip Tracking

Flight Condition	$\delta_{cl}$ (deg)	$\delta_{cr}$ (deg)	$\delta_{tel}$ (deg)	$\delta_{ter}$ (deg)	$\delta_{rud}$ (deg)
ACMENTRY	1.4671	-1.4671	0.2431	-0.2431	4.2623
ACM30TL	0.8361	-0.9397	0.8124	-0.6032	-3.4561
ACM50CL	-0.3633	-0.6934	0.1201	-0.9094	2.1692
ACM25RL	N/A	N/A	N/A	N/A	N/A
ACMEXIT	0.9444	-0.8711	1.6158	-1.4159	1.2350
TFTA	1.0973	-1.0973	0.2444	-0.2444	3.5678
TFTA30TL	0.9310	-0.9946	0.4317	-0.3497	3.3312
TFTA50CL	2.9287	-0.3182	1.3314	0.5312	3.0699
TFTA25RL	3.5708	-3.5708	0.2099	-0.2099	0.8878

Table 4.5. Steady State Control Inputs - Flat Turn

Flight Condition	$\delta_{cl}$ (deg)	$\delta_{cr}$ (deg)	$\delta_{tel}$ (deg)	$\delta_{ter}$ (deg)	$\delta_{rud}$ (deg)
ACMENTRY	9.3284	-9.3284	-3.0266	3.0266	15.7374
ACM30TL	11.0335	-10.3688	-5.2088	3.8672	17.4679
ACM50CL	-5.6600	-10.8046	-7.3813	-4.9166	6.6545
ACM25RL	N/A	N/A	N/A	N/A	N/A
ACMEXIT	7.4212	-6.8452	-5.1607	6.7319	15.2521
TFTA	2.9565	-2.9565	-1.6359	1.6359	5.0267
TFTA30TL	3.4114	-3.0262	-2.6129	2.1166	5.5084
TFTA50CL	7.7362	-0.8407	1.1951	3.7252	4.0173
TFTA25RL	13.2925	-13.2925	-1.8054	1.8054	-9.1315

Table 4.6. Steady State Control Inputs - 45° Banked Turn

Flight Condition	$\delta_{cl}$ (deg)	$\delta_{cr}$ (deg)	$\delta_{tel}$ (deg)	$\delta_{ter}$ (deg)	$\delta_{rud}$ (deg)
ACMENTRY	-15.0300	15.0300	4.8857	-4.8857	-25.5798
ACM30TL	-17.7202	16.6512	8.3768	-6.2193	-28.2744
ACM50CL	9.0926	17.3571	11.8667	7.8892	-10.9173
ACM25RL	N/A	N/A	N/A	N/A	N/A
ACMEXIT	36.0196	52.2227	107.8402	80.6486	-14.4756
TFTA	-4.2022	4.2022	2.3406	-2.3406	-7.3194
TFTA30TL	-4.8451	4.2947	3.7335	-3.0243	-7.9965
TFTA50CL	-10.9859	1.1938	-1.6811	-5.3060	-5.8797
TFTA25RL	-19.1844	19.1844	2.6120	-2.6120	13.2360

Table 4.7. Steady State Control Inputs - 15° Banked Turn

Flight Condition	$\delta_{cl}$ (deg)	$\delta_{cr}$ (deg)	$\delta_{tel}$ (deg)	$\delta_{ter}$ (deg)	$\delta_{rud}$ (deg)
ACMENTRY	-10.0181	10.0181	3.2565	-3.2565	-17.0499
ACM30TL	-11.8112	11.0987	5.5835	-4.1454	-18.8460
ACM50CL	6.0605	11.5692	7.9096	5.2585	-7.2738
ACM25RL	N/A	N/A	N/A	N/A	N/A
ACMEXIT	24.0085	34.8085	71.8797	53.7554	-9.6486
TFTA	-2.8009	2.8009	1.5601	-1.5601	-4.8787
TFTA30TL	-3.2294	2.8626	2.4885	-2.0158	-5.3300
TFTA50CL	-7.3225	0.7957	-1.1205	-3.5367	-3.9190
TFTA25RL	-12.7871	12.7871	1.7410	-1.7410	8.8223

Comparison between the necessary steady state control surface deflections to perform the maneuvers listed in Tables 4.2, through 4.7 with the control surface limitations listed in Table 4.8 determine which maneuvers can possibly be performed in each flight condition.

Table 4.8. Control Surface Position and Rate Limits

Surface	Position Limit (deg)		Rate Limit (deg/sec)
Canards	+60	-30	$\pm 100$
Trailing Edges	+30	-30	$\pm 100$
Rudder	+20	-20	$\pm 100$

Comparison between Tables 4.2 - 4.7 and Table 4.8 yields the fact that only the sideslip tracking and flat turn maneuvers can be performed in **ACM Exit**. The magnitude of the banked turn must be reduced to 15° in **ACM Entry**, and the results for the 25% rudder loss conditions are questionable.

#### 4.2 TIME RESPONSES

The time responses obtained include the two maneuvers investigated by Hammond, pitch rate tracking and the coordinated turn, plus an additional three maneuvers listed in Section 4.1. All maneuvers are investigated in all failure conditions possible, including the new case of 25% rudder loss. A single set of design parameters,  $\sigma_i$ ,  $m_{31}$ ,  $m_{42}$ , and  $\lambda_0$

from Equations 3.28, 3.23, and 3.29 are used for all tested flight conditions. An attempt is made to obtain a universal set of gains that will stabilize the aircraft in all combinations of maneuvers and failure situations. The values of the design parameters are chosen to optimize the time responses and to try to keep all individual controller gain values below 20. The gain values are minimized in order to reduce the magnification of noise signals.

The command inputs used are ramped step inputs since it is physically unrealizable for a pilot to generate a pure step input. The following approximation has been used (4:5-14)

$$\text{ramp time} = \frac{\text{position limit}}{\text{rate limit}} = \frac{60^\circ}{100^\circ/\text{sec}}$$

where the largest allowable surface deflection for the canard is used. A ramp time of 0.5 sec is used for all inputs to simplify the MATRIX<sub>X</sub> simulations. In addition to the ramping, Hammond also inserted a prefilter to remove high frequency spikes. The prefilter is selected to limit the bandwidth to under 10 rad/sec which does not adversely affecting the speed of system response.

$$\text{Prefilter} = \frac{10}{s + 10}$$

All of the time responses collected for the discrete PI design used the following values of  $\sigma_1$ ,  $m_{31}$ ,  $m_{42}$ , and  $\lambda_0$  in Equations 3.28 and 3.29:

$\sigma_1 = 0.2$	$m_{31} = 0.1$
$\sigma_2 = 0.05$	$m_{42} = 0.1$
$\sigma_3 = 0.5$	$\lambda_0 = 0.3$
$\sigma_4 = 0.3$	
$\sigma_5 = 0.5$	

Appendix C contains the  $K_1$  and  $K_2$  matrices for each flight condition and Table 4.9 shows the stability of results for all flight conditions using the design parameters listed above. The time responses have been generated using the input commands shown in Figures 4.1 through 4.5. The magnitudes of the input commands (displayed in degrees) are shown for **ACM Entry**. The yaw rate differs on the coordinated turn input for **TFTA**

(see Table 4.1), and the banked turn can be performed at 45° in **TFTA**.

Table 4.9. Stability Analysis Using discrete PI design parameters

Flight Condition	Stable With Universal Gain	Requires Gain Change
ACMENTRY	X	
ACM30TL	X (1)	
ACM50CL		X
ACM25RL		X
ACMEXIT	X	
TFTA	X	
TFTA30TL	X	
TFTA50CL	X	
TFTA25RL		X

(1) = The flat turn maneuver is not stable for the universal gain.

The four responses in Figures 4.1 through 4.5 are defined as follows

—  $\beta$  ...  $\theta$   
 --  $\phi$  --  $r$

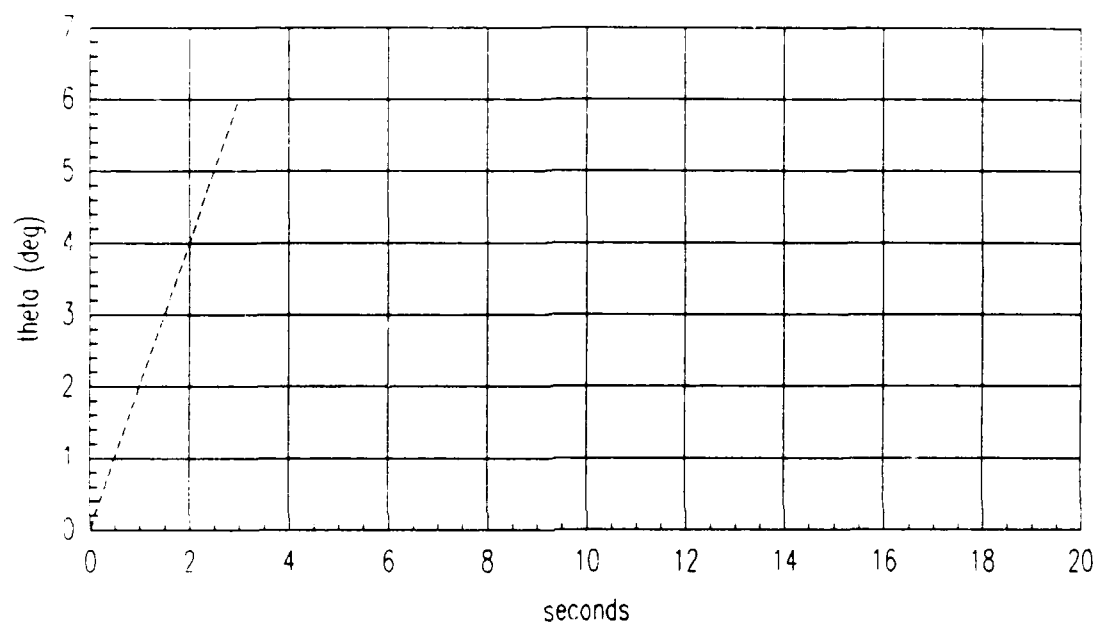


Figure 4.1. Input command for pitch tracking maneuver

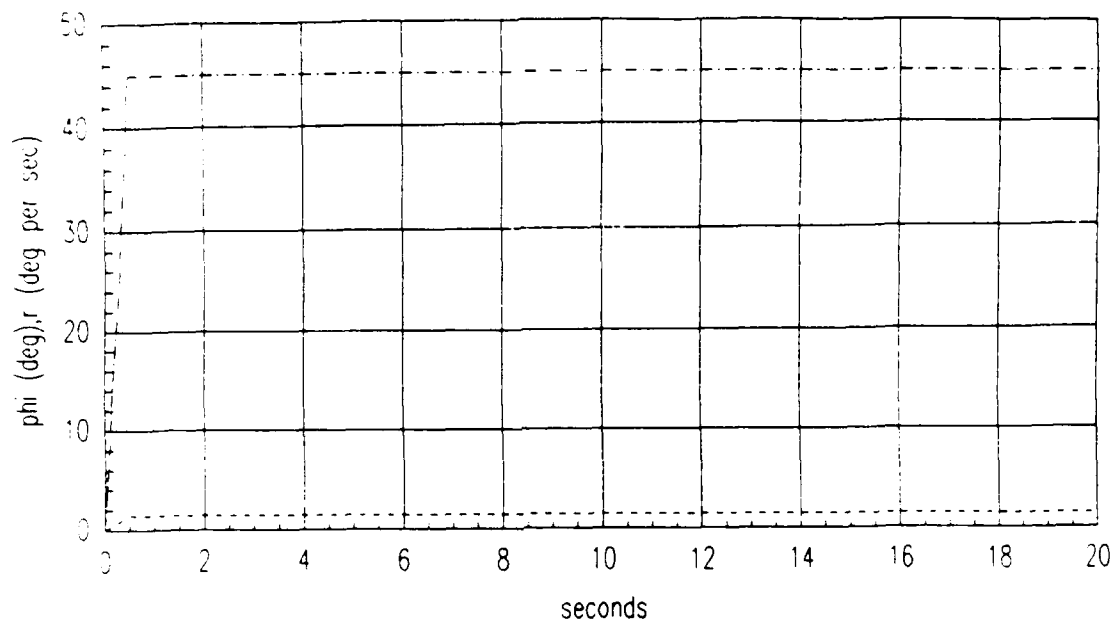


Figure 4.2. Input command for coordinated turn maneuver

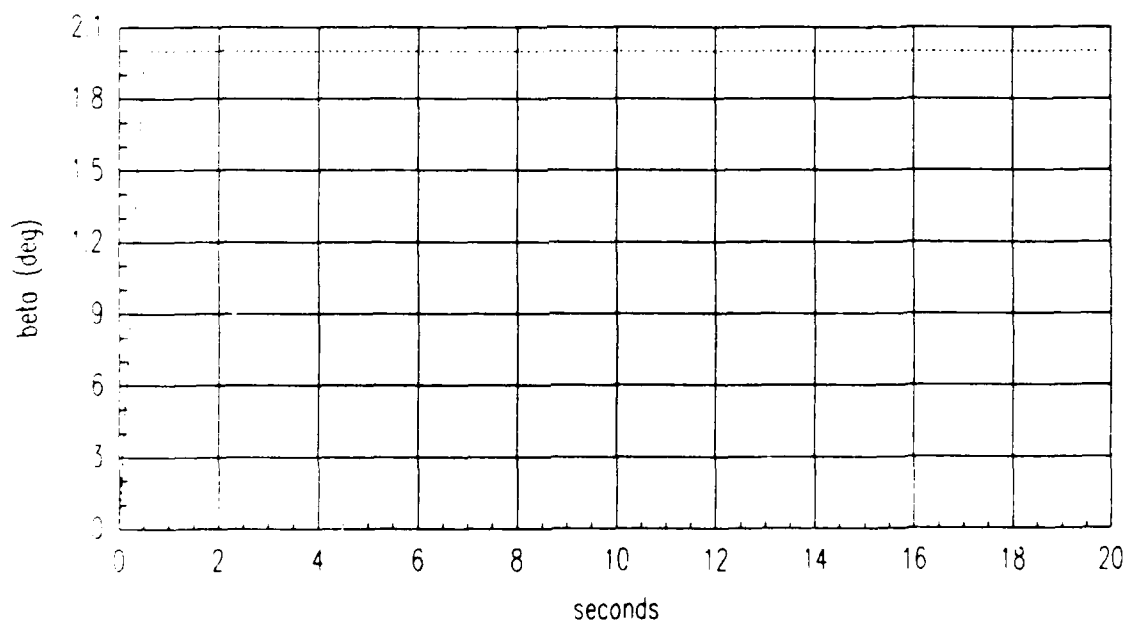


Figure 4.3. Input command for sideslip tracking maneuver

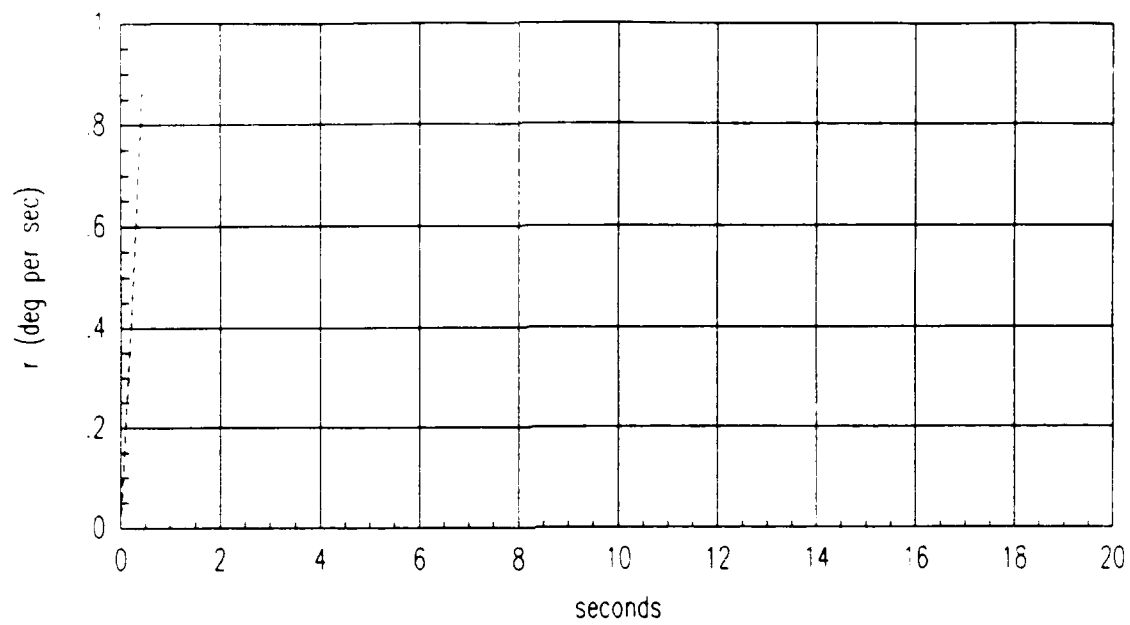


Figure 4.4. Input command for flat turn maneuver

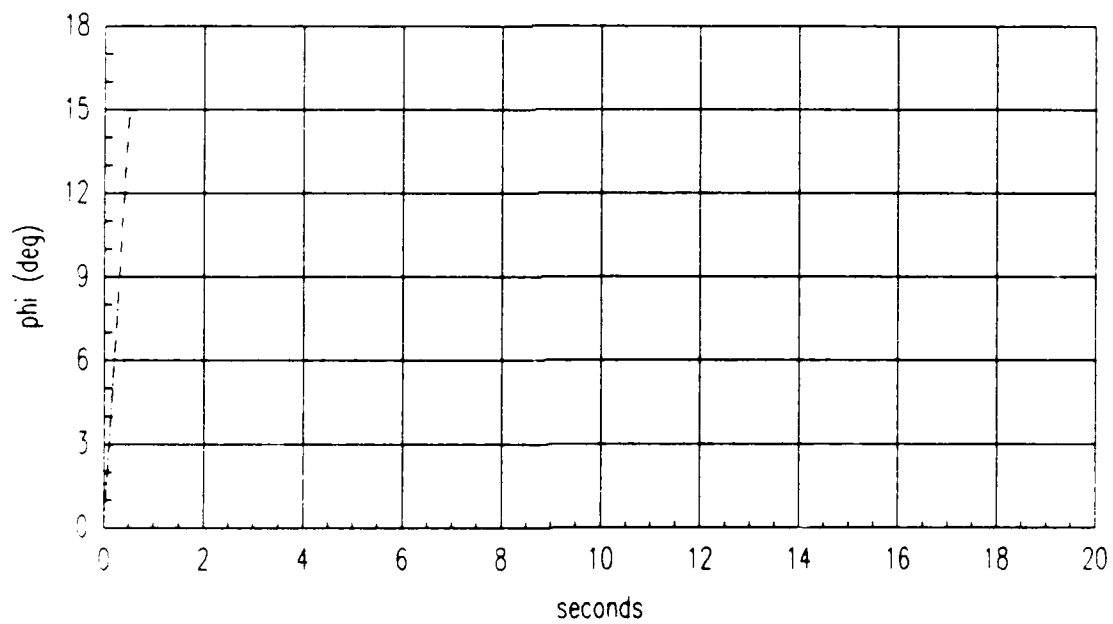


Figure 4.5. Input command for banked turn maneuver



The resulting time responses for simulations in **ACM Entry**, **ACM Exit**, and **TFTA** follow and sample surface deflections and rates are included only for the first maneuver, pitch rate tracking. Limiting devices are included in the simulation to keep the surface deflections and rates within the limits defined in Table 4.8. Once the surface deflection and rate limits are exceeded, the limiting devices are saturated and the simulation becomes nonlinear and this normally drives the time responses unstable.

The four responses on each of the next plots are again defined as follows

—  $\beta$  ...  $\theta$   
 --  $\phi$  - -  $r$

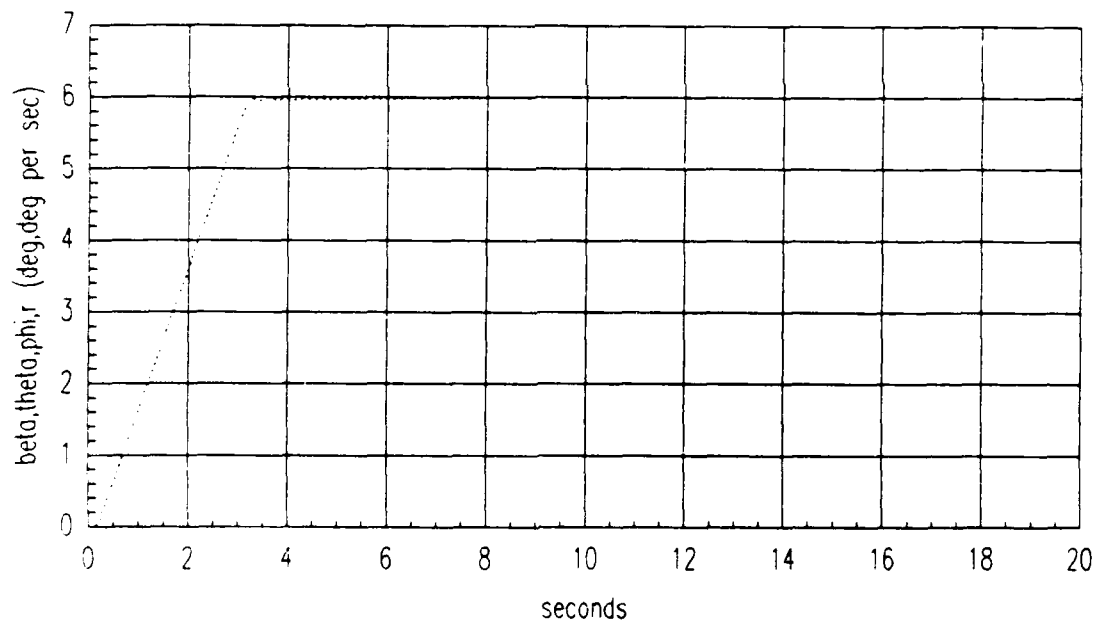


Figure 4.6. Discrete Controller pitch rate tracking response in ACM Entry

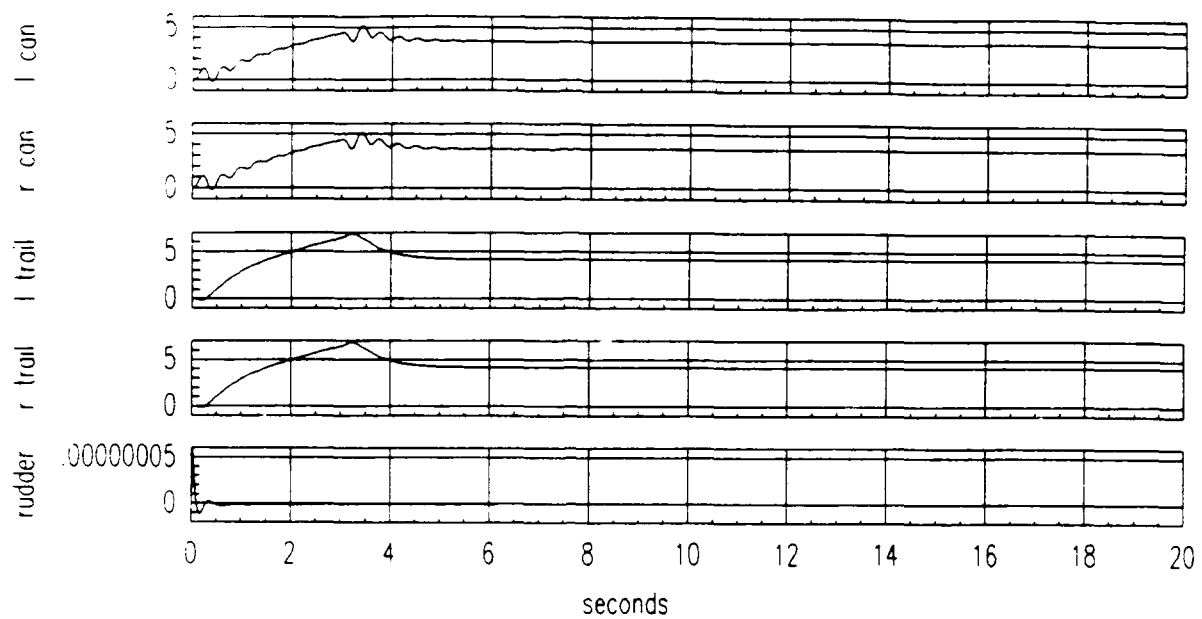


Figure 4.7. Surface deflections for pitch rate tracking in ACM Entry

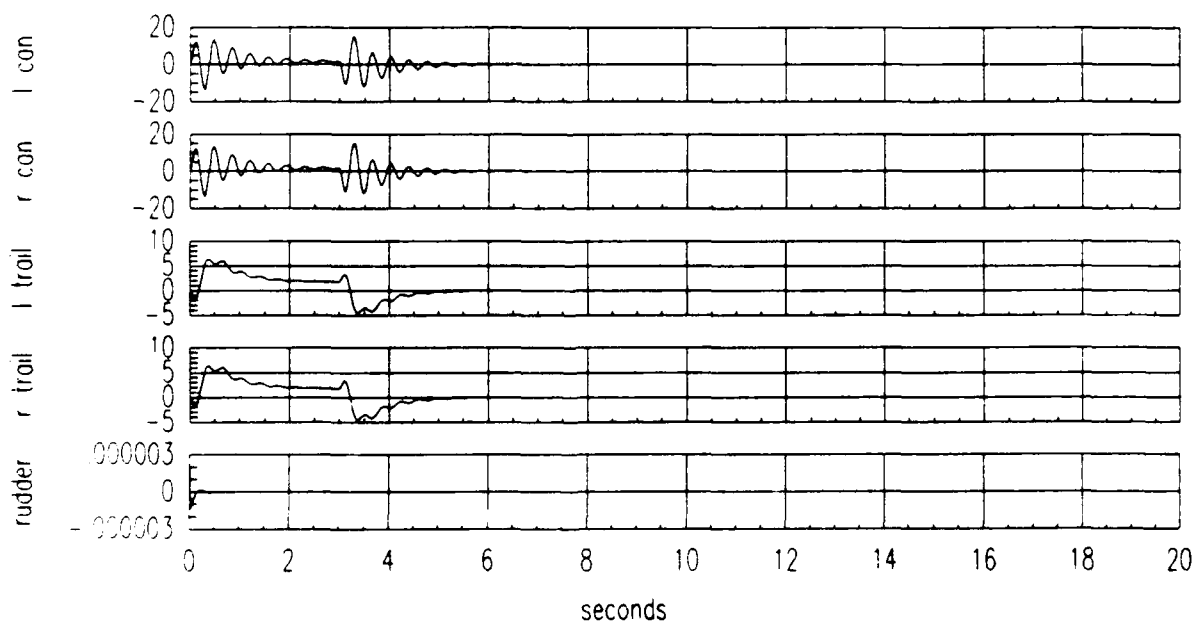


Figure 4.8. Surface rates for pitch rate tracking in ACM Entry

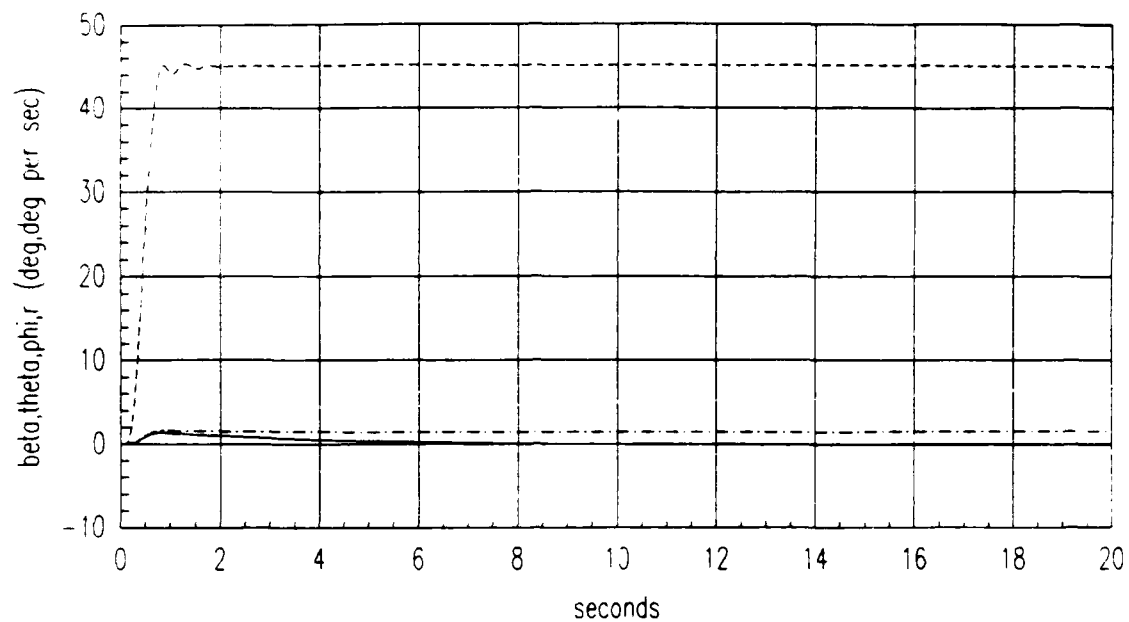


Figure 4.9. Discrete Controller coordinated turn response in ACM Entry

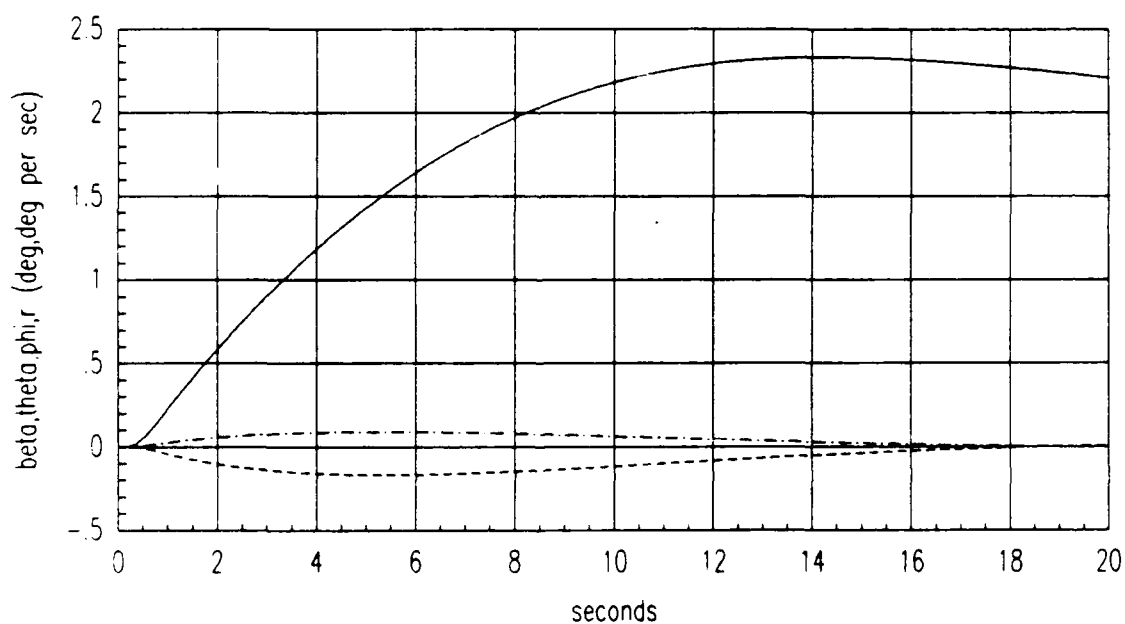


Figure 4.10. Discrete Controller sideslip tracking response in ACM Entry

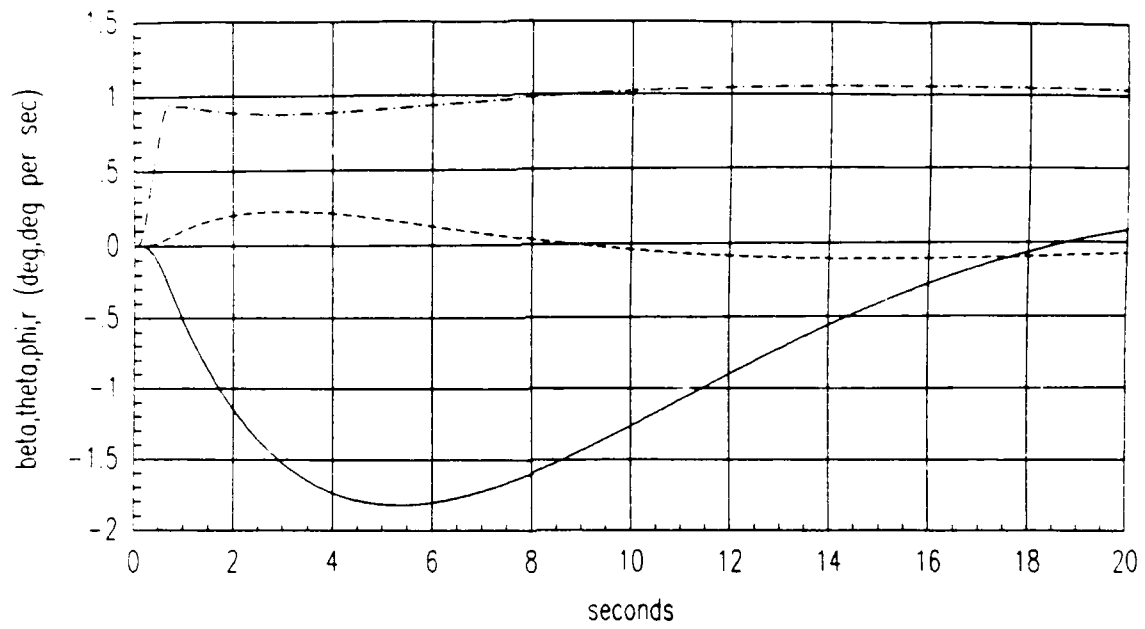


Figure 4.11. Discrete Controller flat turn response in ACM Entry

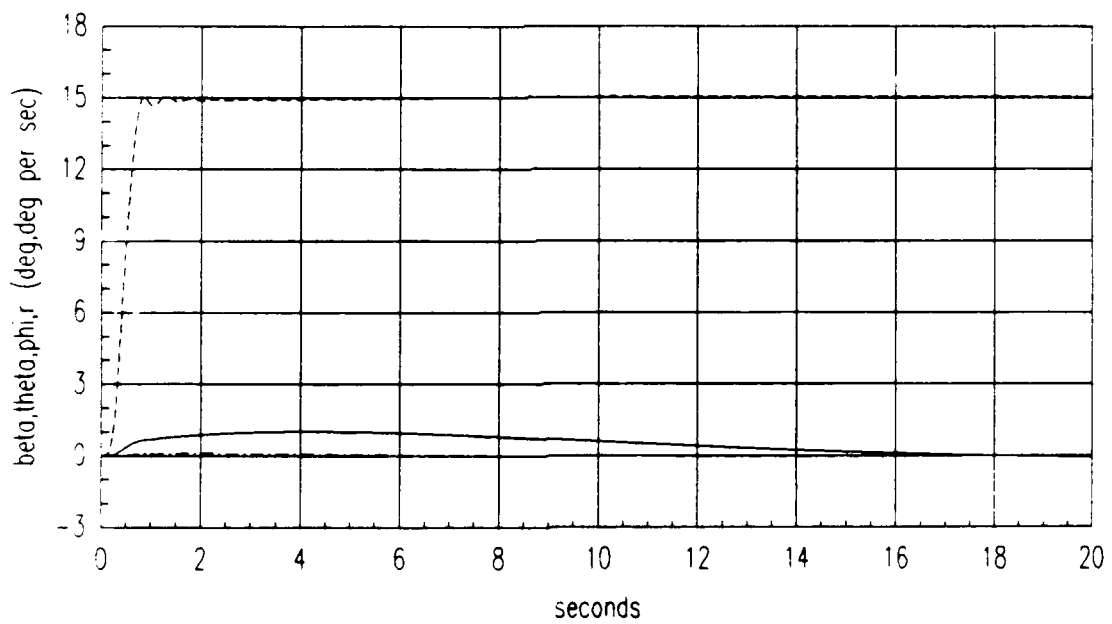


Figure 4.12. Discrete Controller banked turn response in ACM Entry

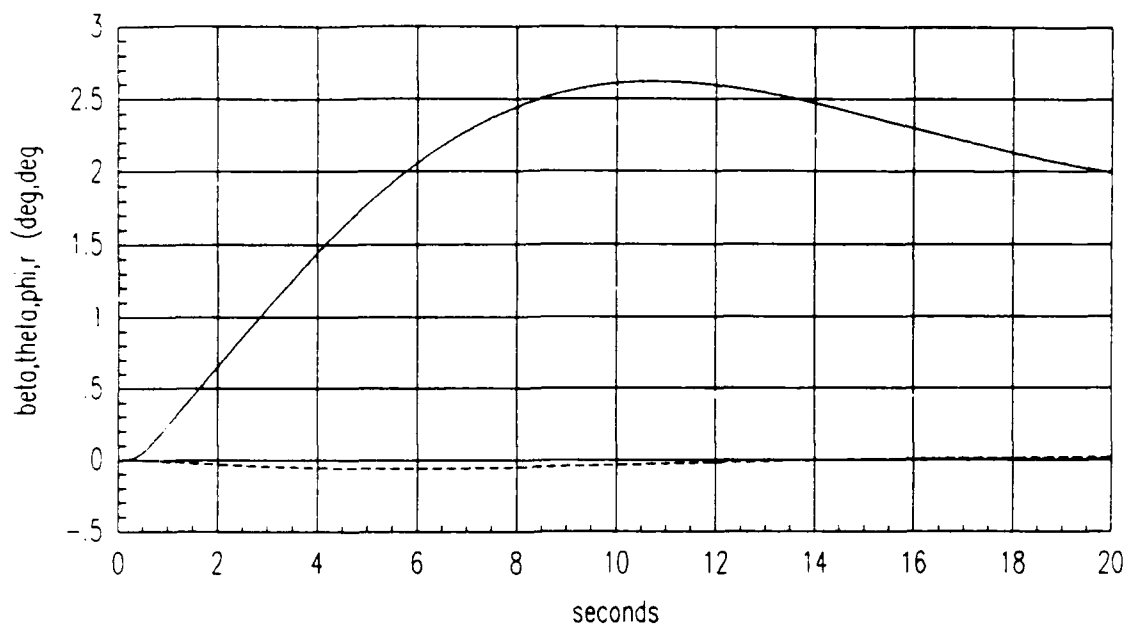


Figure 4.13. Discrete Controller sideslip tracking response in ACM Exit

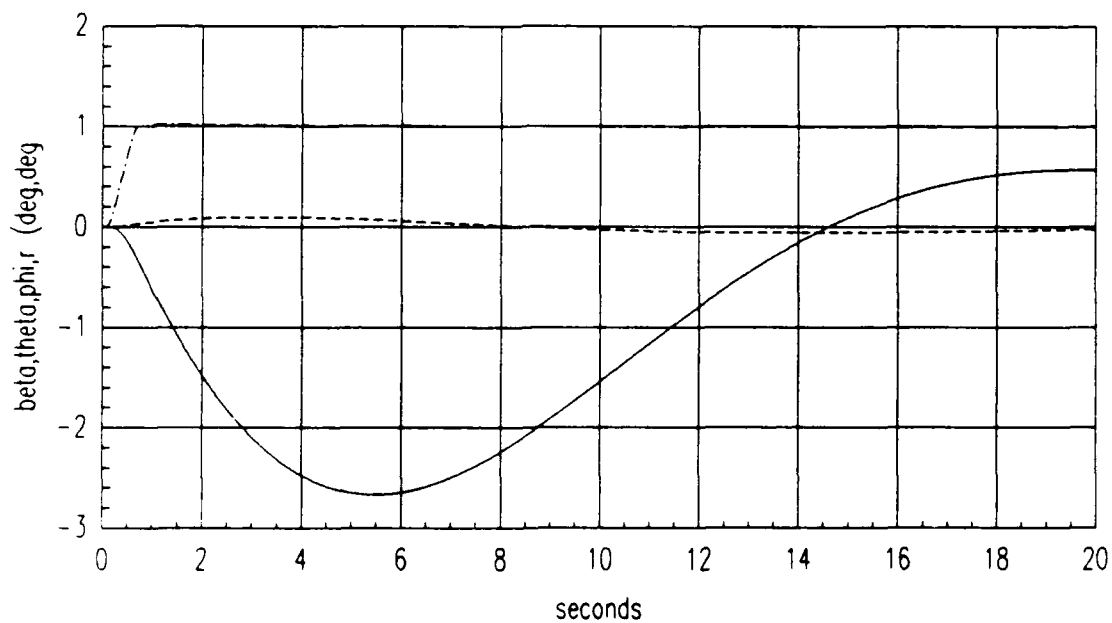


Figure 4.14. Discrete Controller flat turn response in ACM Exit

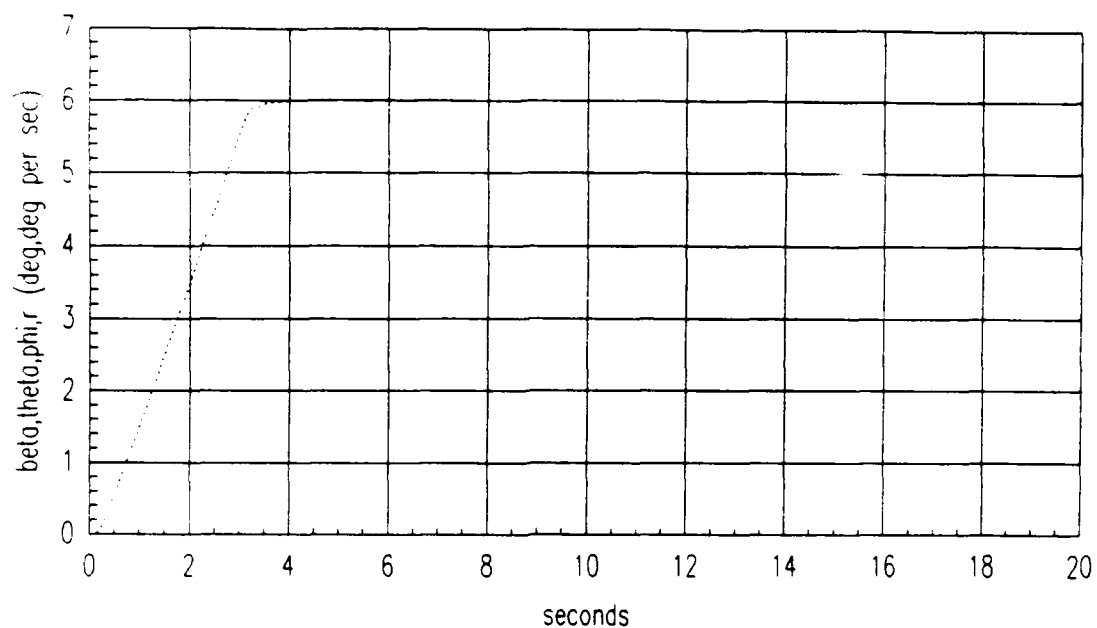


Figure 4.15. Discrete Controller pitch rate tracking response in TFTA

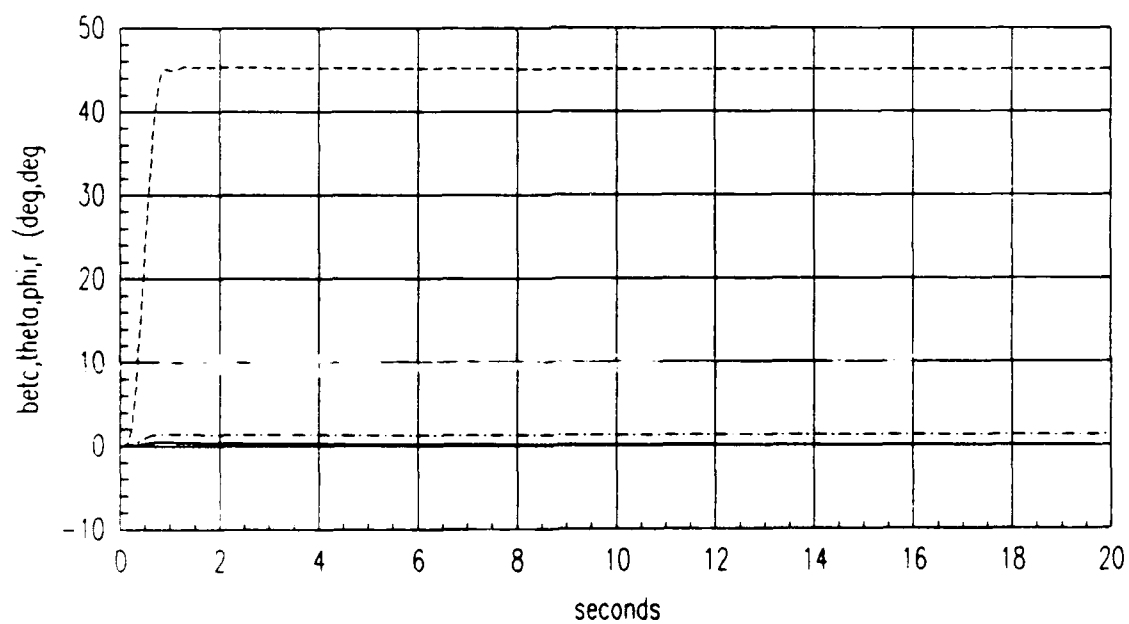


Figure 4.16. Discrete Controller coordinated turn response in TFTA

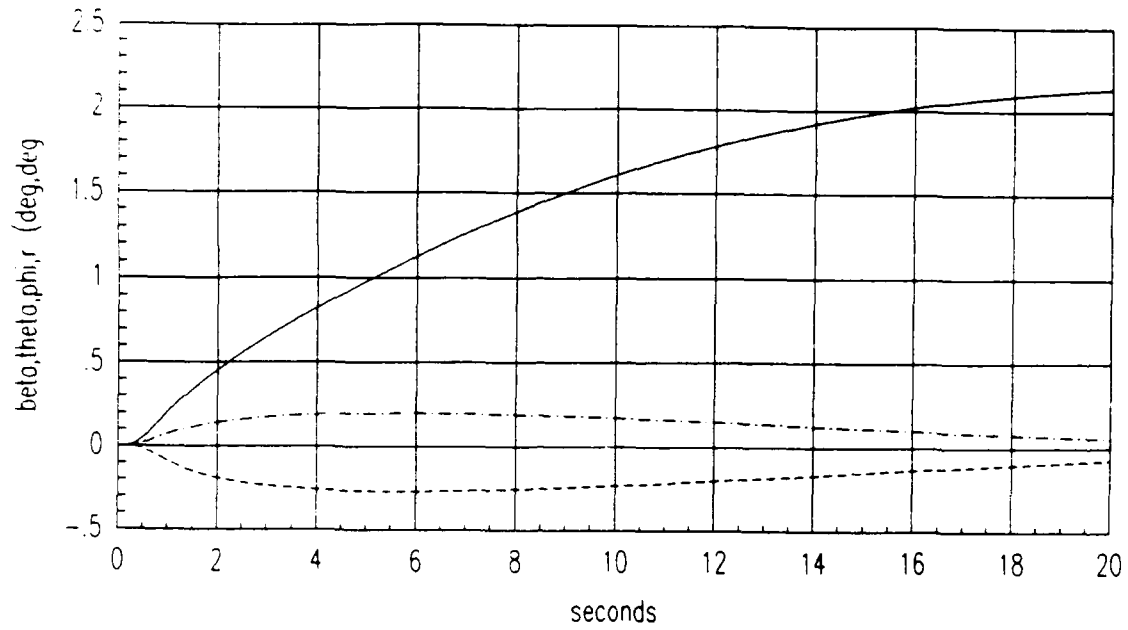


Figure 4.17. Discrete Controller sideslip tracking response in TFTA

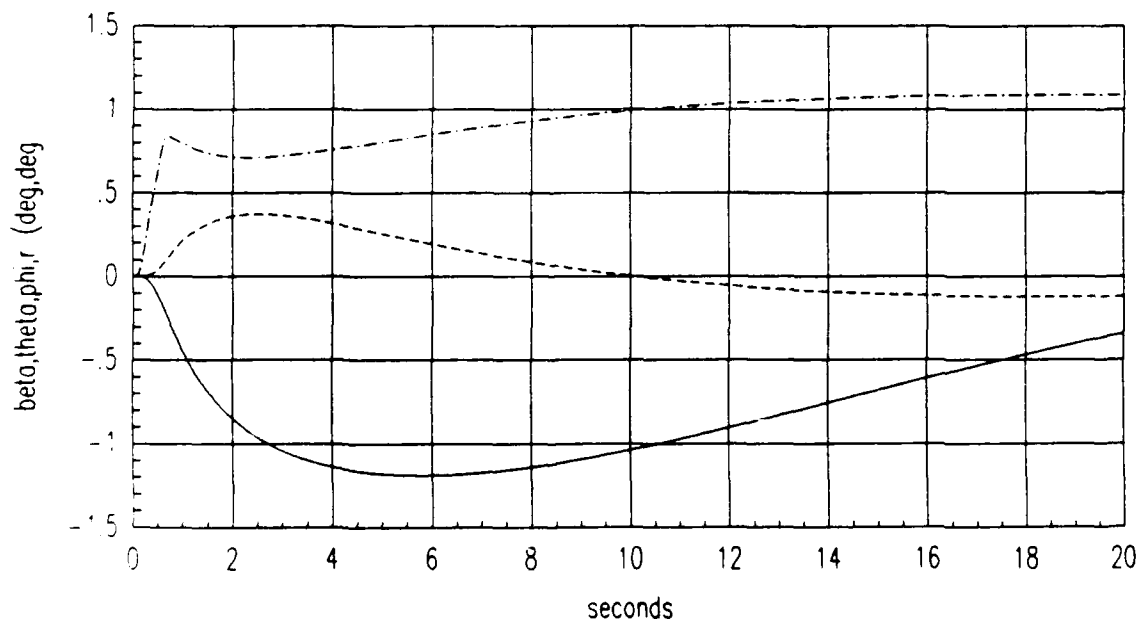


Figure 4.18. Discrete Controller flat turn response in TFTA

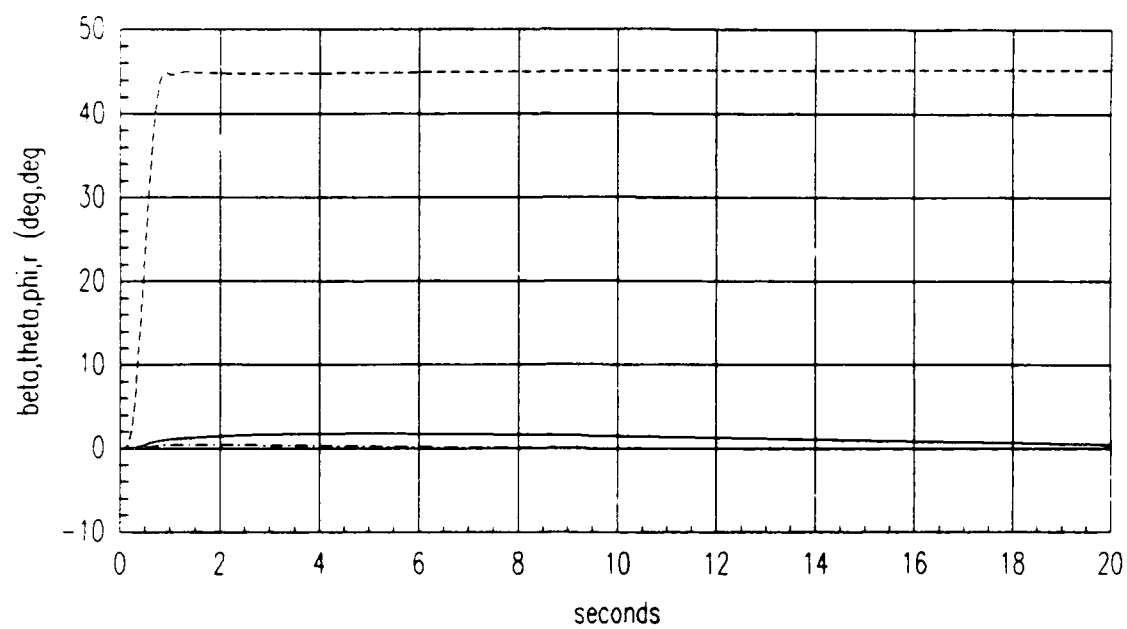


Figure 4.19. Discrete Controller banked turn response in TFTA



Time responses for a selected maneuver, sideslip tracking, are shown for all of the failure conditions in **ACM Entry** and **TFTA**. The simulations were performed using the fixed  $K_1$  and  $K_2$  values calculated for the non-failed **ACM Entry** and **TFTA** flight conditions (see Appendix C). From Figures 4.22 and 4.25, it can be seen that the sideslip tracking task cannot be accomplished for the 25% rudder loss in **ACM Entry** or **TFTA**.

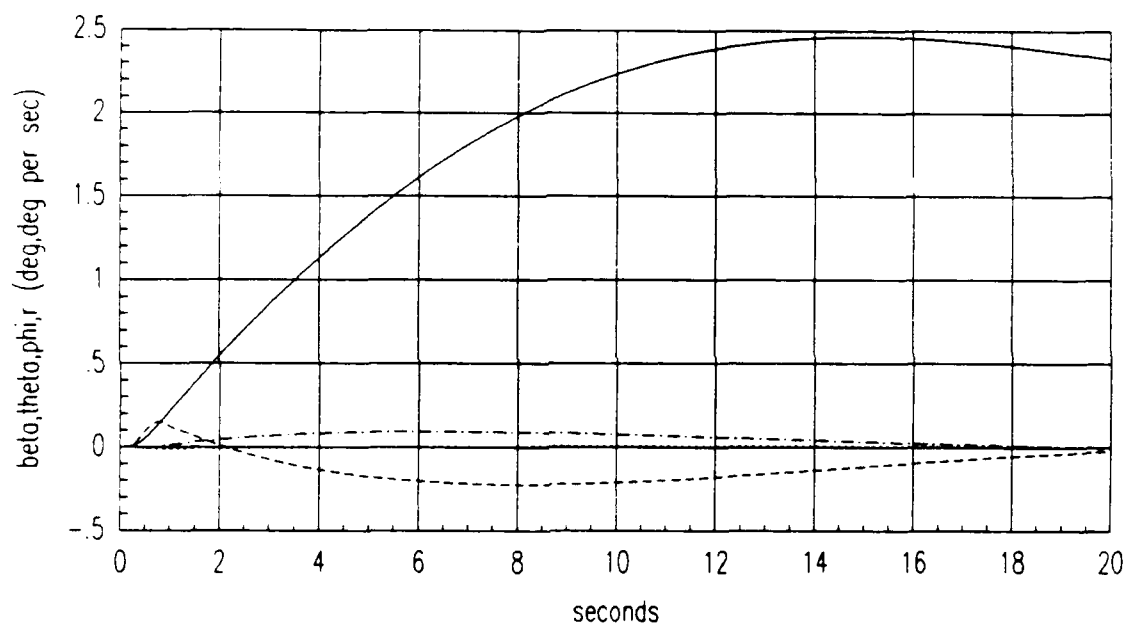


Figure 4.20. Discrete Controller sideslip maneuver response in ACM30TL

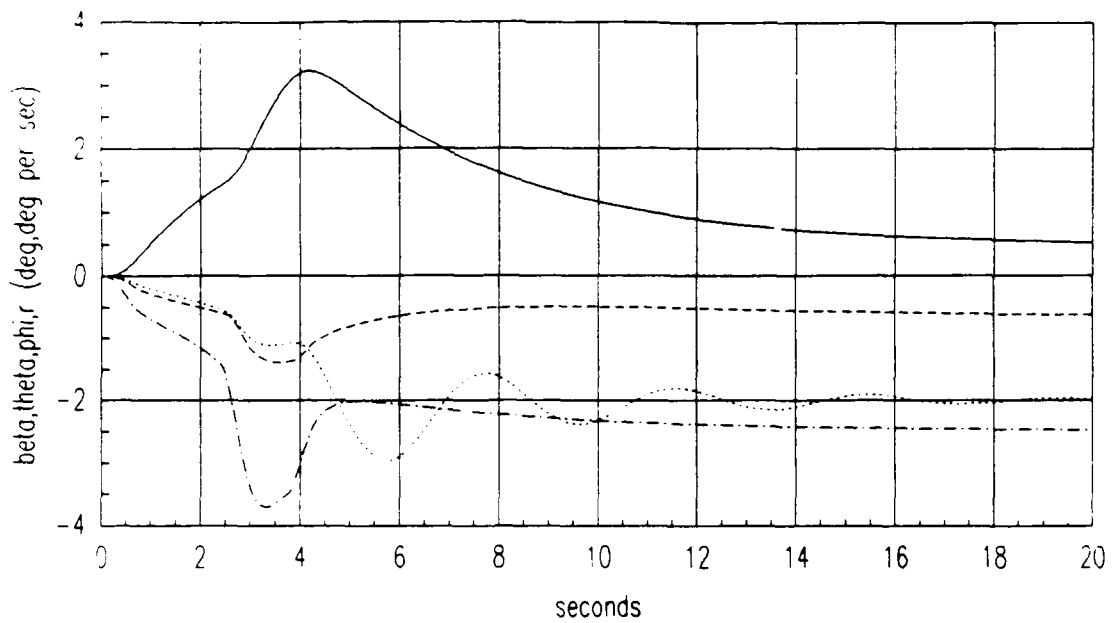


Figure 4.21. Discrete Controller sideslip maneuver response in ACM50CL

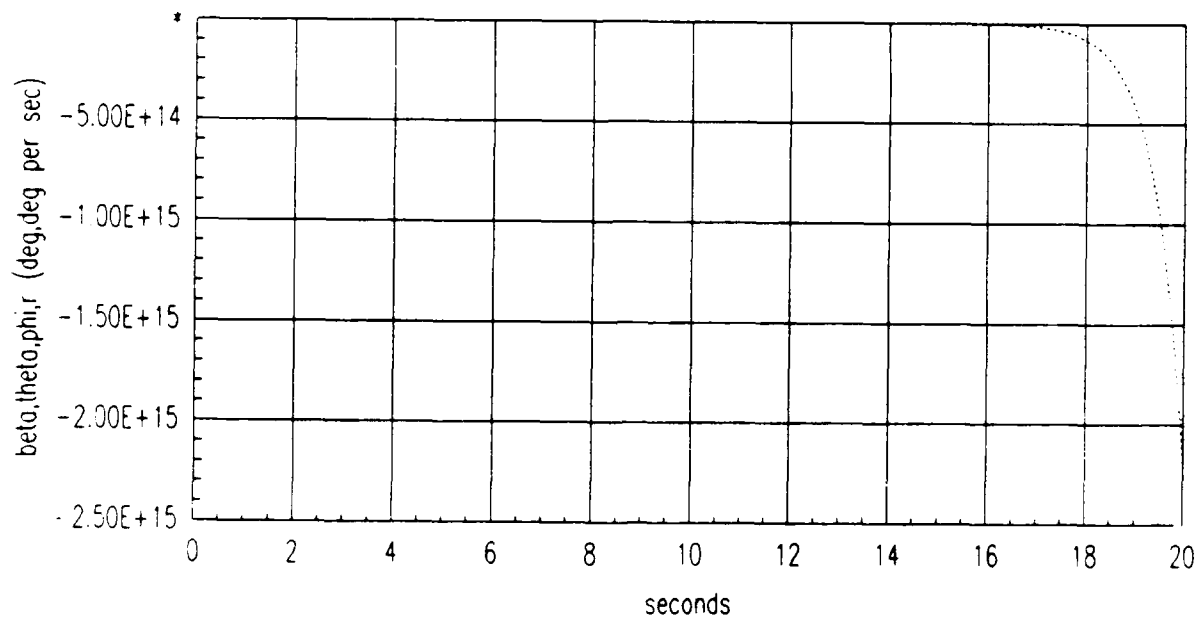


Figure 4.22. Discrete Controller sideslip maneuver response in ACM25RL

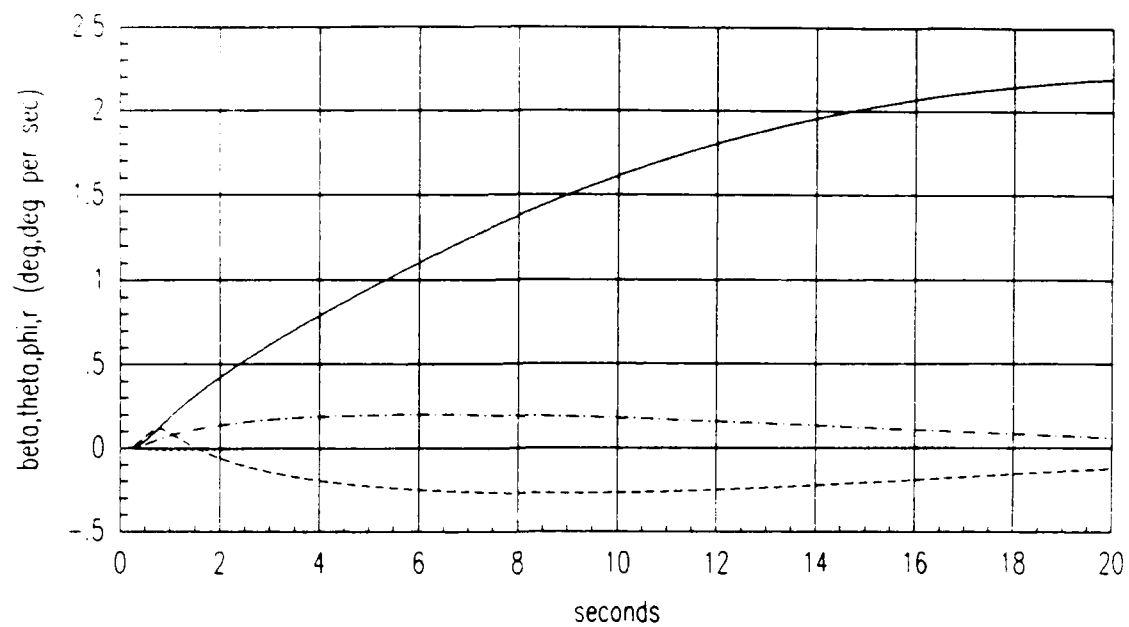


Figure 4.23. Discrete Controller sideslip maneuver response in TFTA30FL

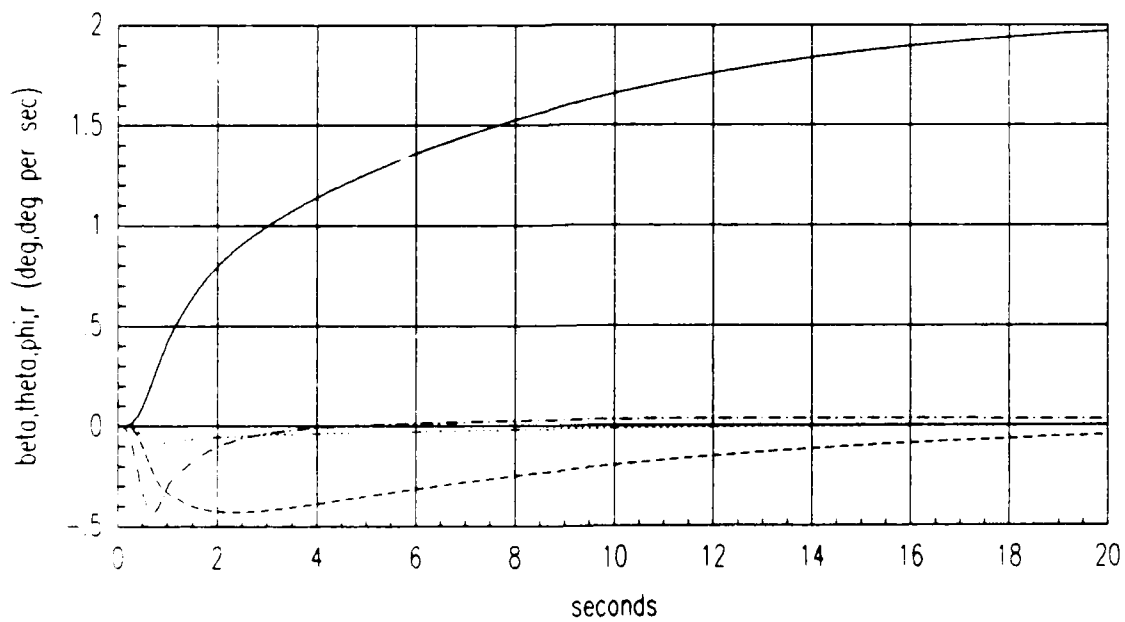


Figure 4.24. Discrete Controller sideslip maneuver response in TFTA50CL

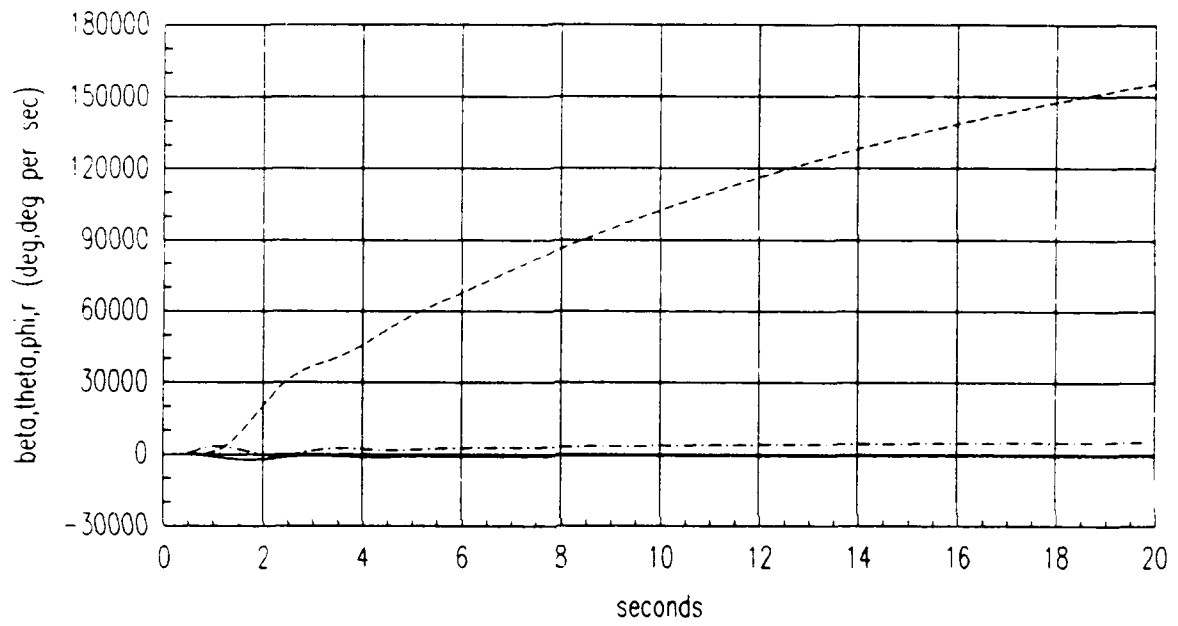


Figure 4.25. Discrete Controller sideslip maneuver response in TFTA25RL

### 4.3 FREQUENCY ANALYSIS

Conventional frequency analysis of a MIMO system is difficult, but is made easier when the outputs are relatively decoupled, as is the case with this design method. Since the outputs are decoupled, only the diagonal transfer function pairs are considered, i.e.,  $\beta/\beta_{cmd}$ . "For statically unstable aircraft, the military specification MIL -F -9490D, specifies the gain margin to be  $\pm 6.0$  dB and the phase margin to be  $\pm 45$  degrees. For these types of aircraft the system may have a low and high frequency gain margin. At the low frequency crossover frequency of -180 degrees the gain margin should be smaller than -6.0 dB. At the high frequency crossover of -180 degrees the gain margin should be greater than +6.0 dB (4:4-17)." The Nichols plots of  $\theta/\theta_{cmd}$  in Figures 4.28 and 4.32, illustrate the high and low gain margin characteristics of the unstable CRCA.

The aircraft/controller model simulated in MATRIX<sub>X</sub> is a hybrid model consisting of a continuous plant with a discrete controller. In order to conduct a frequency analysis, an equivalent discrete model of the overall system must be generated. This is accomplished by treating the controller as a continuous unit and then transforming the "continuous system" to the  $w'$  plane via a Hofmann transformation. The Hofmann transformation used in this thesis was obtained from Hammond's computer files (4:4-29).

$$\begin{aligned} F(w') &= \left[ I - \frac{1}{3} \left( \frac{A(s)T}{2} \right)^2 + \frac{2}{15} \left( \frac{A(s)T}{2} \right)^4 - \frac{17}{315} \left( \frac{A(s)T}{2} \right)^6 \right] A(s) \\ G(w') &= \left\{ \left[ I - \frac{1}{3} \left( \frac{A(s)T}{2} \right)^2 + \frac{2}{15} \left( \frac{A(s)T}{2} \right)^4 - \frac{17}{315} \left( \frac{A(s)T}{2} \right)^6 \right] B(s) \right\} \left[ I - \frac{F(w')T}{2} \right] \\ H(w') &= C(s) \\ D(w') &= -\frac{C(s)T}{2} \left\{ \left[ I - \frac{1}{3} \left( \frac{A(s)T}{2} \right)^2 + \frac{2}{15} \left( \frac{A(s)T}{2} \right)^4 - \frac{17}{315} \left( \frac{A(s)T}{2} \right)^6 \right] B(s) \right\} \end{aligned}$$

According to Houpis and Lamont (5), quantities in the  $w'$  plane can be handled like continuous quantities and the  $z$  plane roots can be found from the following equation.

$$z = \frac{Tw' + 2}{-Tw' + 2} \quad (4.5)$$

Selected Nichols and Bode diagrams are included for both the healthy **ACM Entry** and **TFTA** flight conditions. Figures 4.26 through 4.33 show the open loop frequency characteristics of the discrete PI controller design. The closed loop Bode plots show the bandwidth of the system with the control law incorporated for the two selected outputs, in Figures 4.34 through 4.37. The bandwidth characteristics of the healthy aircraft design are included in Table 4.10 and the  $w'$  plane roots are listed in Table 4.11.

Table 4.10. Bandwidth of discrete PI design

output	ACM Entry	TFTA
$v$	7.22	6.89
$\beta$	0.30	0.17
$\theta$	9.77	7.22
$\phi$	10.23	7.74
$r$	9.54	8.90

Table 4.11.  $w'$  plane roots for ACM Entry and TFTA

ACM ENTRY	TFTA
-0.1119 $\pm j$ 0.1536	-0.2266 $\pm j$ 0.1380
-0.2960	-0.3017
-0.3014	-0.3020
-0.3055	-0.3074
-0.4947	-0.7228
-2.0425	-3.6890
-8.2710	-9.9482 (5)
-9.9482 (5)	-11.0842 $\pm j$ 5.1379
-7.4002 $\pm j$ 10.4555	-13.1893
-14.7533 $\pm j$ 13.2824	13.1976
-38.8237	-29.2678 $\pm j$ 35.2494
-40.7383 $\pm j$ 25.8551	-16.4291 $\pm j$ 54.7333
-36.6469 $\pm j$ 33.5002	-57.4723
-50.2105 $\pm j$ 29.3661	-51.5347 $\pm j$ 30.4394
-52.7656 $\pm j$ 30.7213	-61.4256
-58.1497 $\pm j$ 31.3455	-57.9341 $\pm j$ 31.3275
	-14.8236 $\pm j$ 74.5446

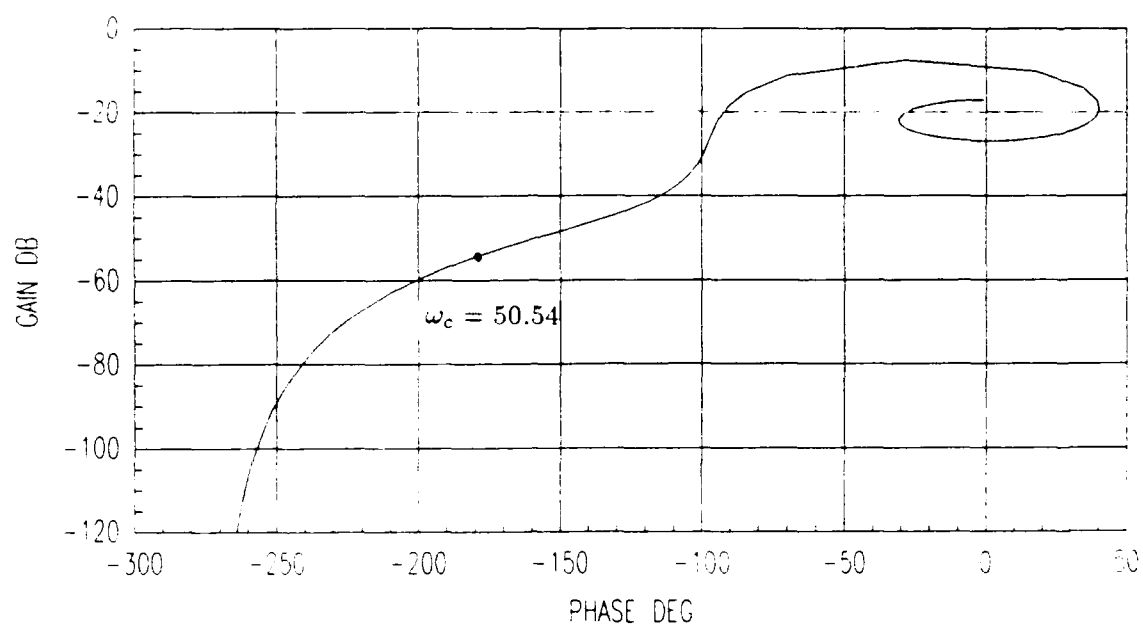


Figure 4.26. Discrete PI Nichols plot of  $\beta/\beta_{cml}$  in ACM Entry

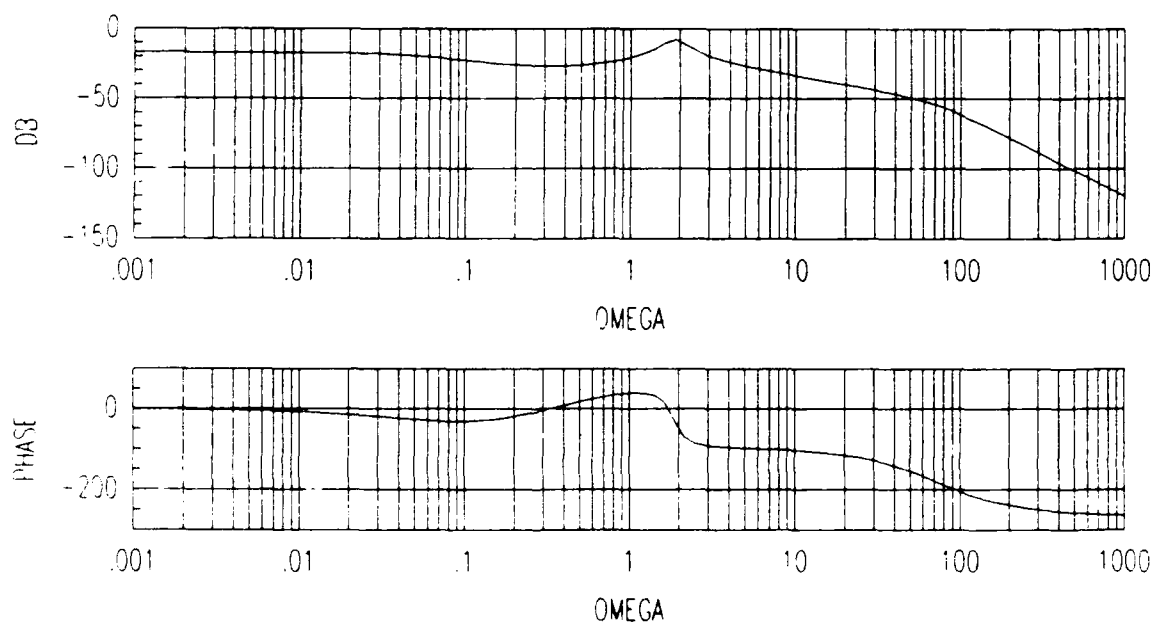


Figure 4.27. Discrete PI open loop Bode plot of  $\beta/\beta_{cml}$  in ACM Entry

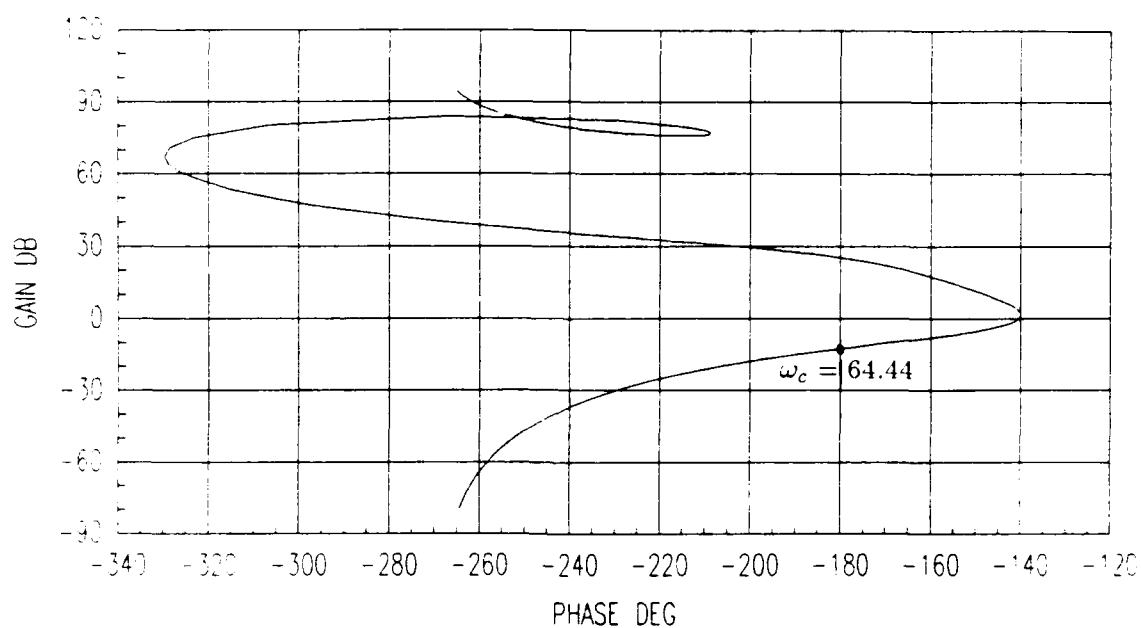


Figure 4.28. Discrete PI Nichols plot of  $\theta/\theta_{cmd}$  in ACM Entry

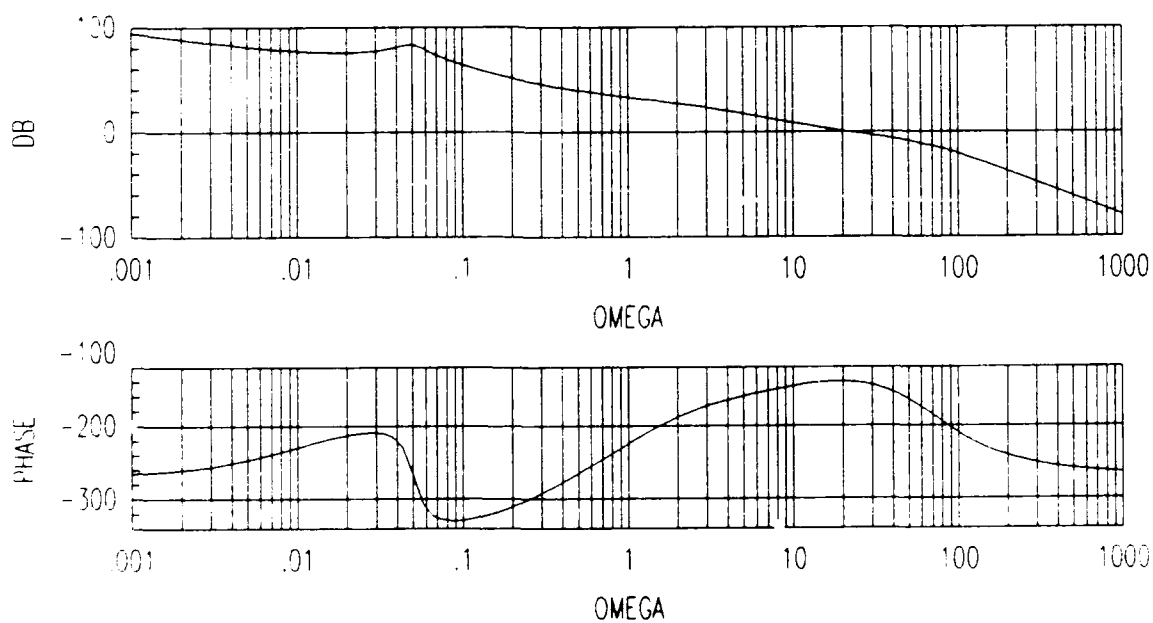


Figure 4.29. Discrete PI open loop Bode plot of  $\theta/\theta_{cmd}$  in ACM Entry



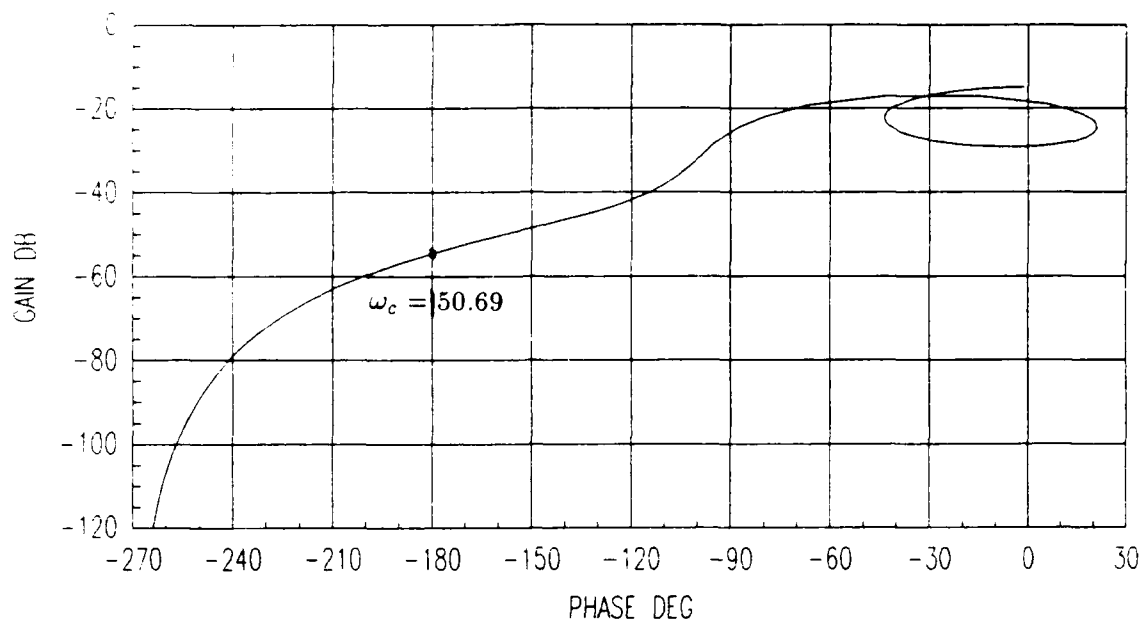


Figure 4.30. Discrete PI Nichols plot of  $\beta/\beta_{cnd}$  in TFTA

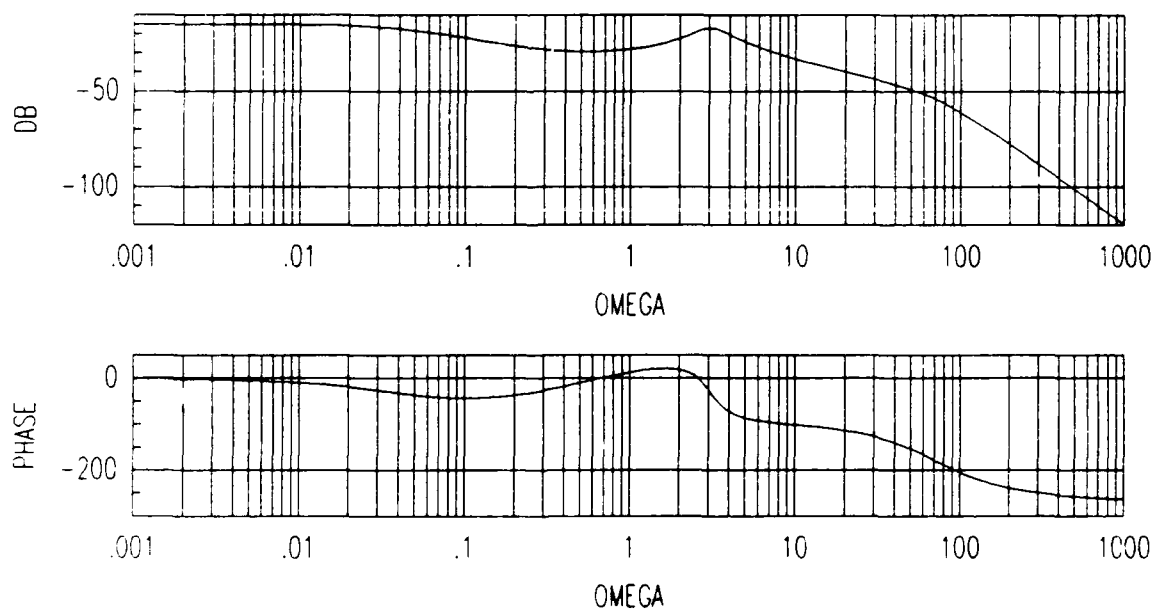


Figure 4.31. Discrete PI open loop Bode plot of  $\beta/\beta_{cnd}$  in TFTA

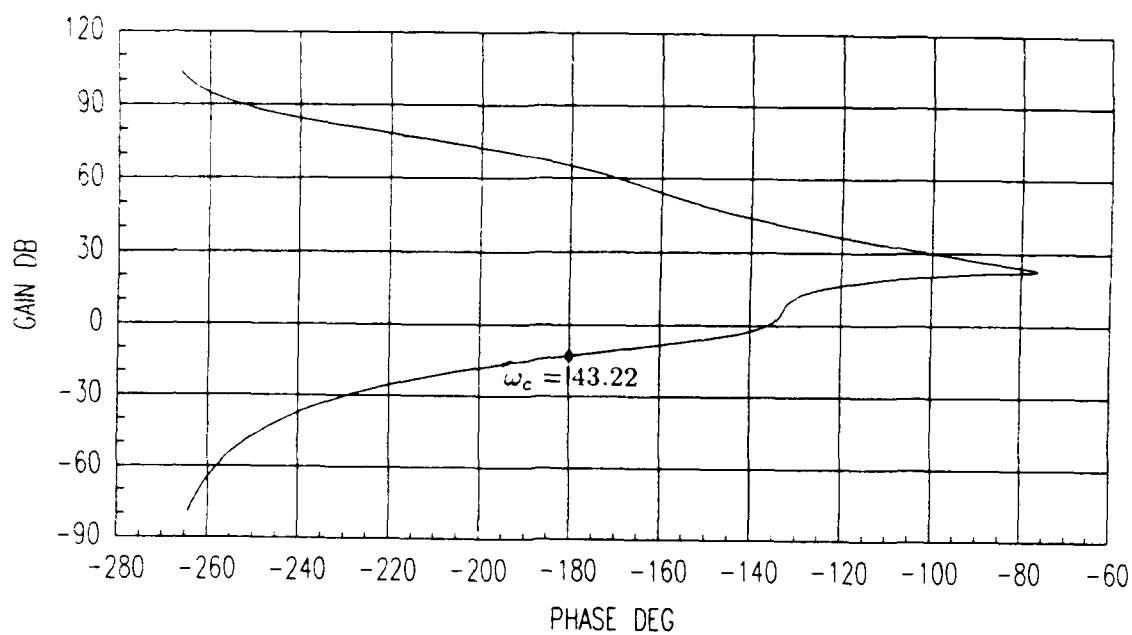


Figure 4.32. Discrete PI Nichols plot of  $\theta/\theta_{cmd}$  in TFTA

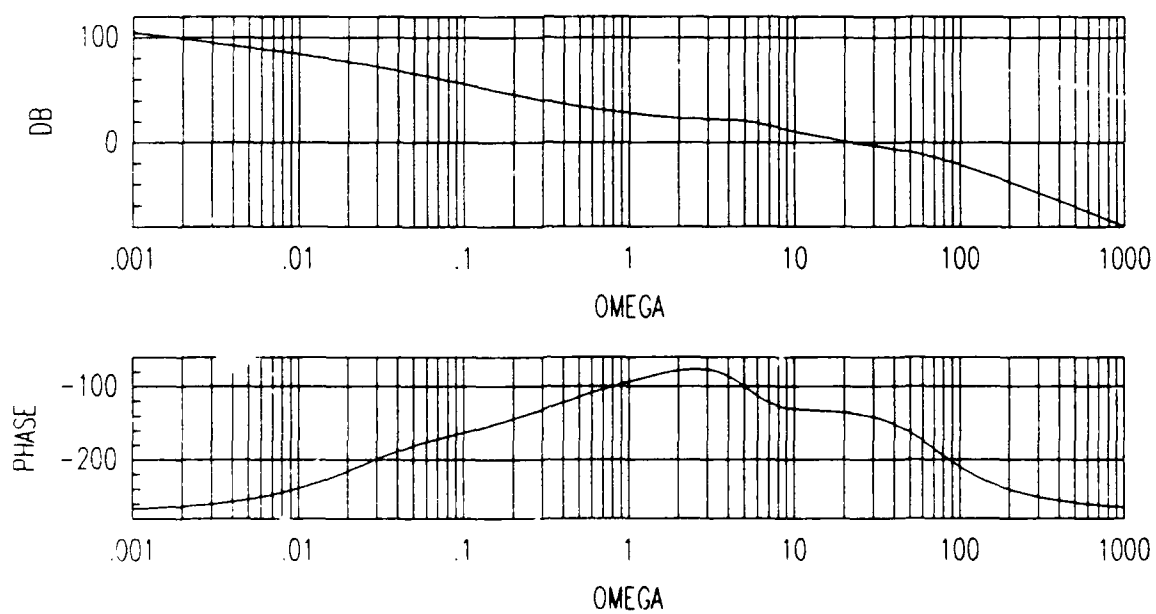


Figure 4.33. Discrete PI open loop Bode plot of  $\theta/\theta_{cmd}$  in TFTA

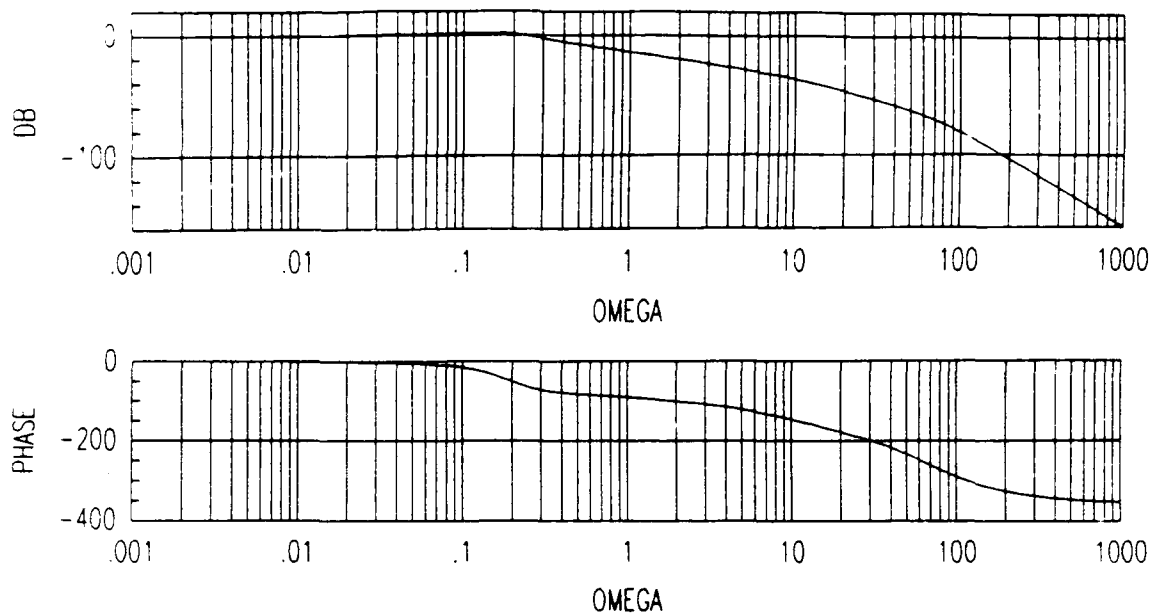


Figure 4.34. Discrete PI closed loop Bode plot of  $\beta/\beta_{cmd}$  in ACM Entry

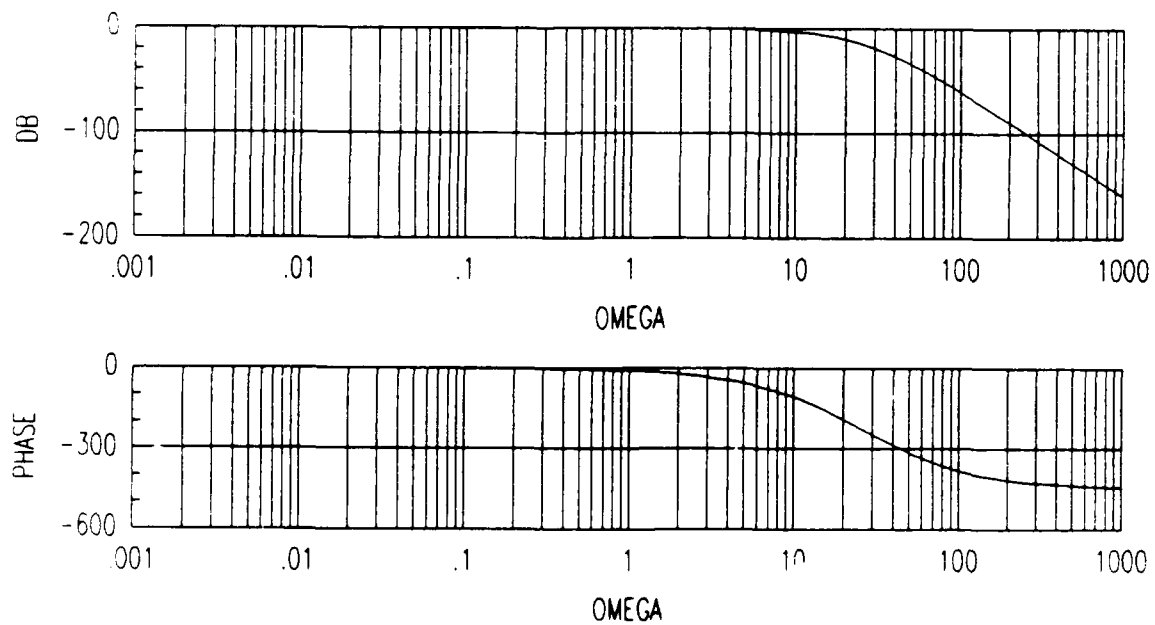


Figure 4.35. Discrete PI closed loop Bode plot of  $\theta/\theta_{cmd}$  in ACM Entry

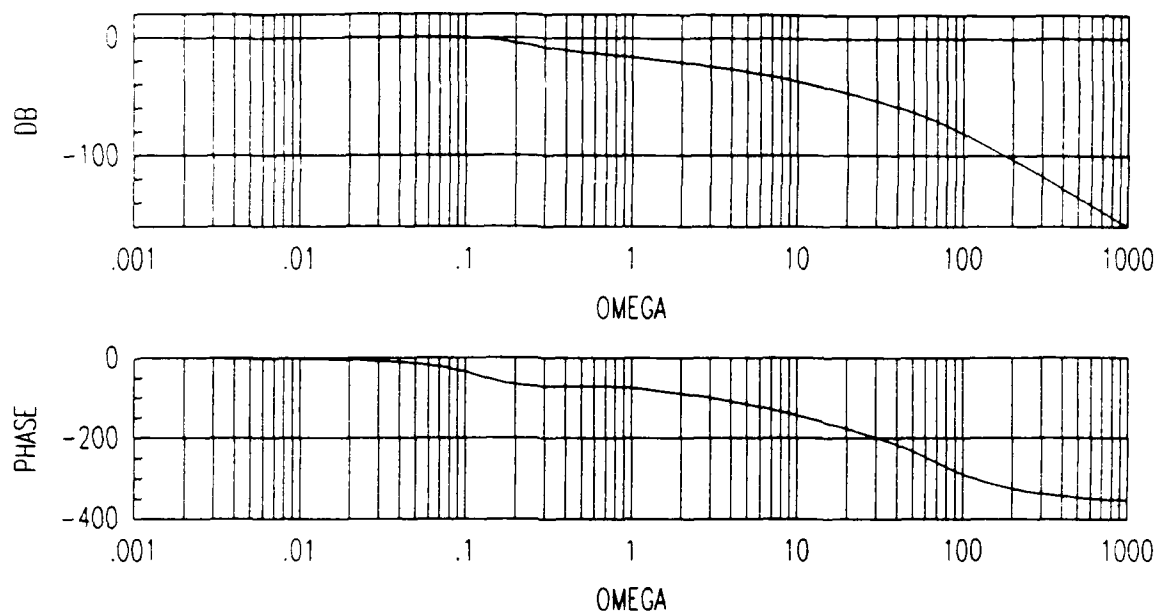


Figure 4.36. Discrete PI closed loop Bode plot of  $\beta/\beta_{cmd}$  in TFTA

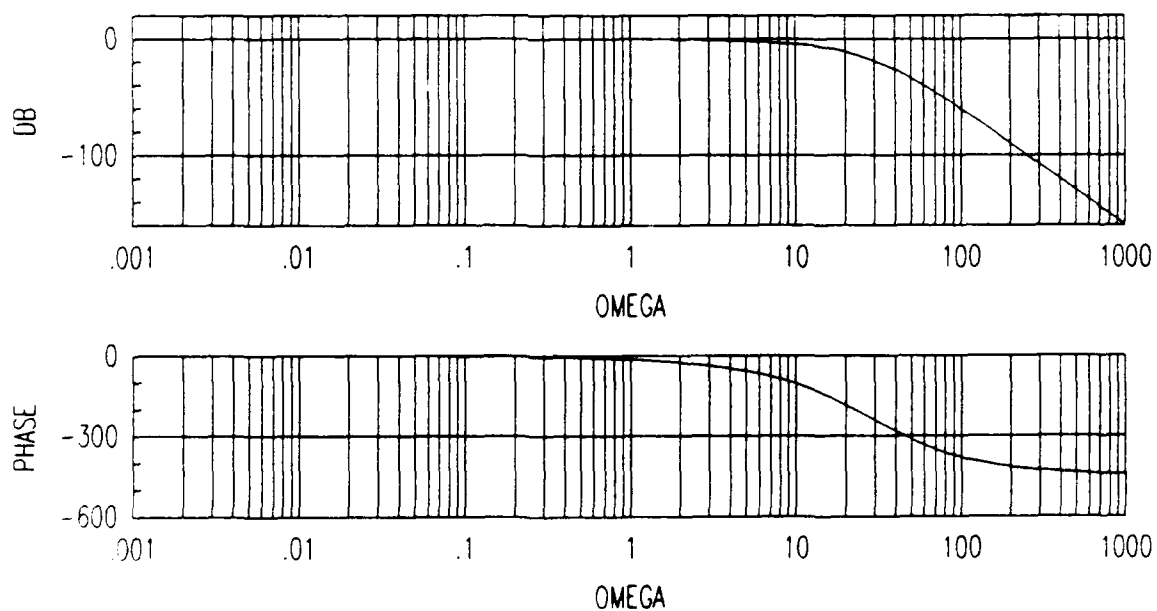


Figure 4.37. Discrete PI closed loop Bode plot of  $\theta/\theta_{cmd}$  in TFTA

The phase and gain margins for **ACM Entry** and **TFTA** are listed in Table 4.12.

Table 4.12. Gain and Phase Margins - Discrete PI Design

ACM Entry						
Transfer Function	Gain Margin (dB)		$\omega_c$ (rad/sec)		Phase Margin (deg)	$\omega_\phi$ (rad/sec)
	Low	High	Low	High		
$V$	(2)	14.26	(2)	70.62	74.64	8.07
$\beta$	(2)	48.54	(2)	50.54	(1)	(1)
$\theta$	-25.22	12.65	2.48	64.44	39.66	21.51
$\phi$	(2)	17.07	(2)	64.34	44.80	14.47
$r$	(2)	8.60	(2)	50.84	52.45	20.10

TF/TA						
Transfer Function	Gain Margin (dB)		$\omega_c$ (rad/sec)		Phase Margin (deg)	$\omega_\phi$ (rad/sec)
	Low	High	Low	High		
$V$	-39.18	16.51	0.24	50.40	70.61	7.21
$\beta$	(2)	48.54	(2)	50.69	(1)	(1)
$\theta$	-65.15	6.63	0.05	43.22	43.75	22.38
$\phi$	(2)	18.66	(2)	70.68	57.91	13.80
$r$	(2)	8.73	(2)	51.56	126.45	0.55
					180.03	0.74
					54.45	20.35

(1) = Response is always less than 0 dB

(2) = No low frequency gain margin (phase > -180 degrees)

This chapter contains a listing of the steady state control surface deflections to perform each maneuver in the chosen flight conditions. The design parameters and time responses for the discrete PI controller are presented for non failure and single failure conditions. Frequency analysis of the discrete design is presented for the non failed cases **ACM Entry** and **TFTA**. Chapter 5 contains the time responses for the step response controller and adaptive algorithm.

## V. STEP RESPONSE METHOD AND ADAPTIVE RESULTS

### 5.1 STEP RESPONSE METHOD

The time responses collected for the step response method use the same inputs displayed in Figures 4.1 through 4.5 and the following values of  $\sigma_i$ ,  $m_{31}$ ,  $m_{42}$ , and  $\gamma\pi_i$  in Equations 3.35 and 3.36.

$\sigma_1 = 0.1$	$\gamma\pi_1 = 0.2$
$\sigma_2 = 0.015$	$\gamma\pi_2 = 0.2$
$\sigma_3 = 0.01$	$\gamma\pi_3 = 0.2$
$\sigma_4 = 0.05$	$\gamma\pi_4 = 0.2$
$\sigma_5 = 0.075$	$\gamma\pi_5 = 0.2$
$m_{31} = 0.1$	$m_{42} = 0.1$

The  $w'$  plane roots are calculated for the step response method in the same fashion as discussed for the discrete PI controller in Section 4.3 and are included in Appendix C along with the fixed gain values of  $K_1$  and  $K_2$  used in the simulations for the no failure cases **ACM Entry** and **TFTA**. The computer simulations are conducted with a gain of 1. The gain factor in the control law of Equation 3.32,  $T$ , is already incorporated in the gain matrices listed in Appendix C.

Table 5.1 shows the stability results for all the possible maneuvers (see Section 4.1) in the various flight conditions for the step response method design parameters. The same time responses are shown here as have been presented for the discrete PI controller. The four responses on each plot are distinguished according to the same legend used in Chapter 4.

$$\begin{array}{l} \text{— } \beta \quad \dots \quad \theta \\ \text{-- } \phi \quad \text{-- } r \end{array}$$

Table 5.1. Stability Analysis Using step response design parameters

Flight Condition	Stable With Universal Gain	Requires Gain Change
ACMENTRY	X	
ACM30TL	X	
ACM50CL		X
ACM25RL		X
ACMEXIT	X (1)	
TFTA	X	
TFTA30TL	X	
TFTA50CL		X (2)
TFTA25RL		X

(1) = The responses are slightly divergent for ACM Exit over the 20 second simulation time.

(2) = All results have a distinct periodic oscillation and slowly diverge over the simulation duration.

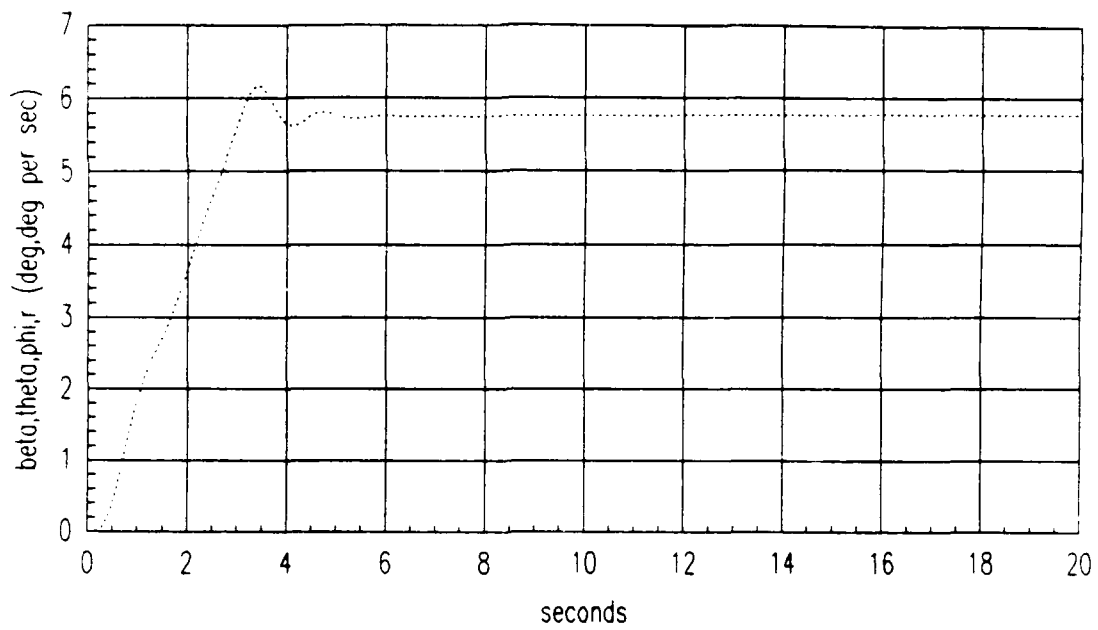


Figure 5.1. Step response method pitch rate tracking response in ACM Entry

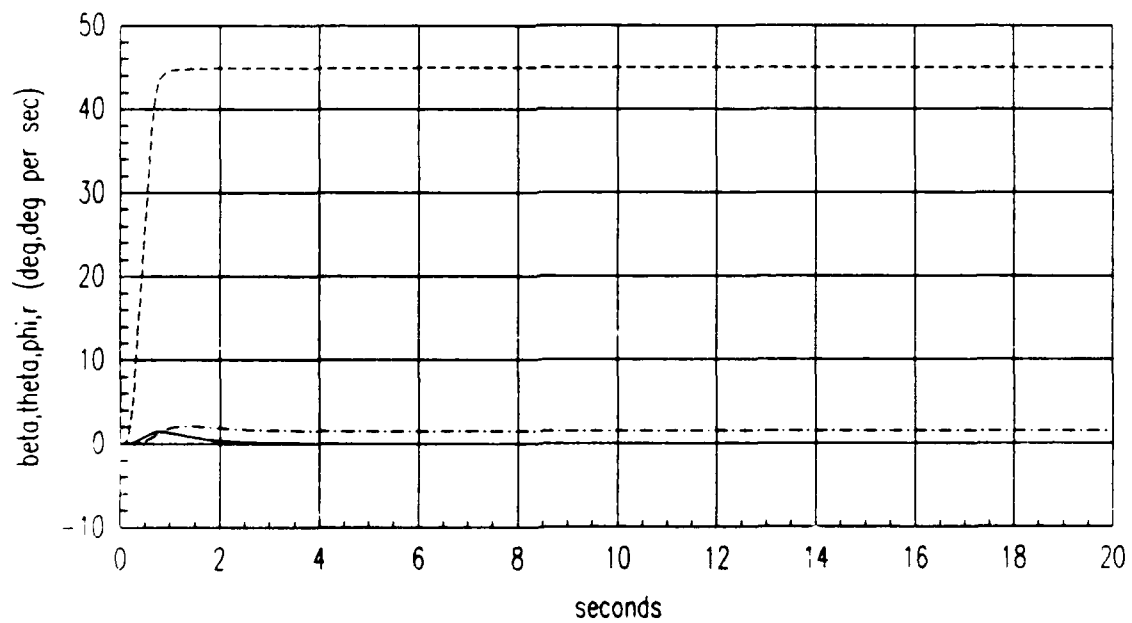


Figure 5.2. Step response method coordinated turn response in ACM Entry



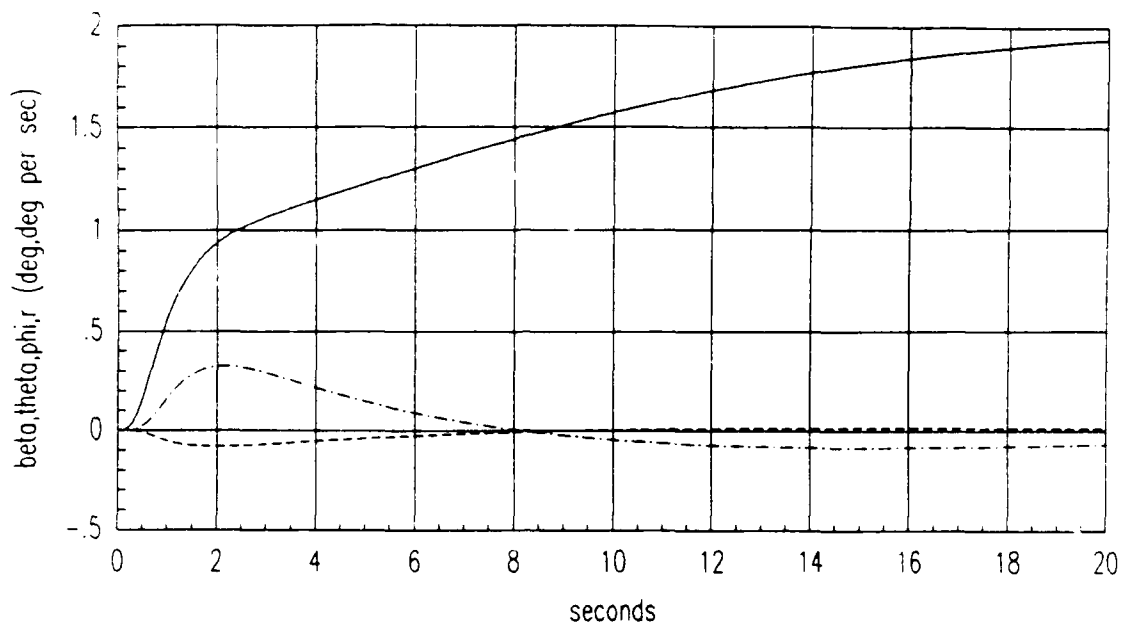


Figure 5.3. Step response method sideslip tracking response in ACM Entry

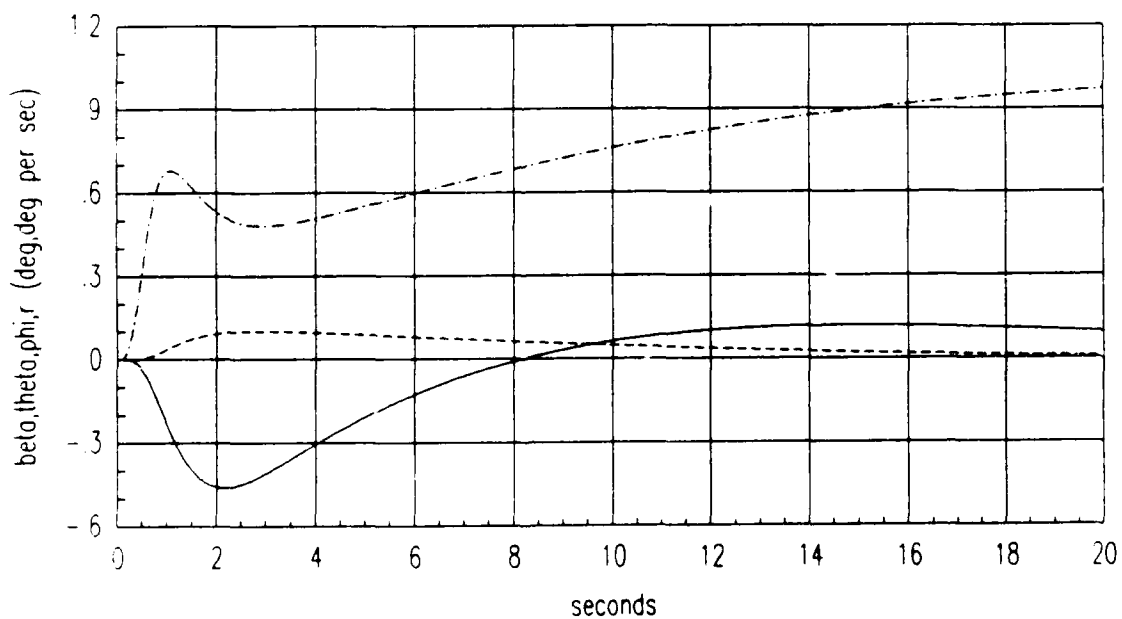


Figure 5.4. Step response method flat turn response in ACM Entry

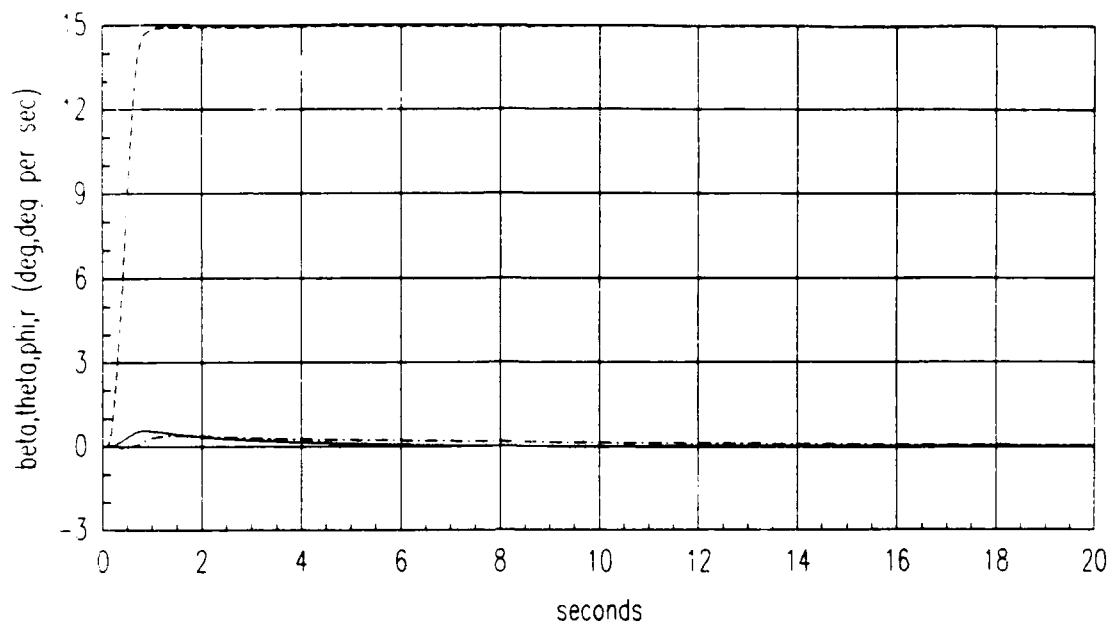


Figure 5.5. Step response method banked turn response in ACM Entry

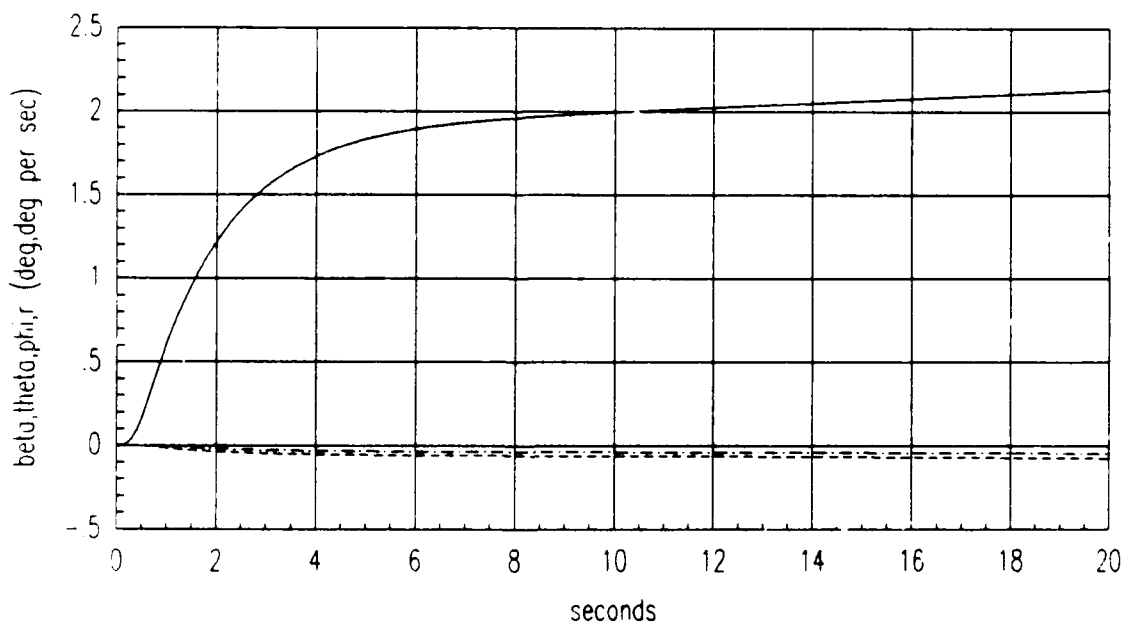


Figure 5.6. Step response method pitch sideslip tracking response in ACM Exit

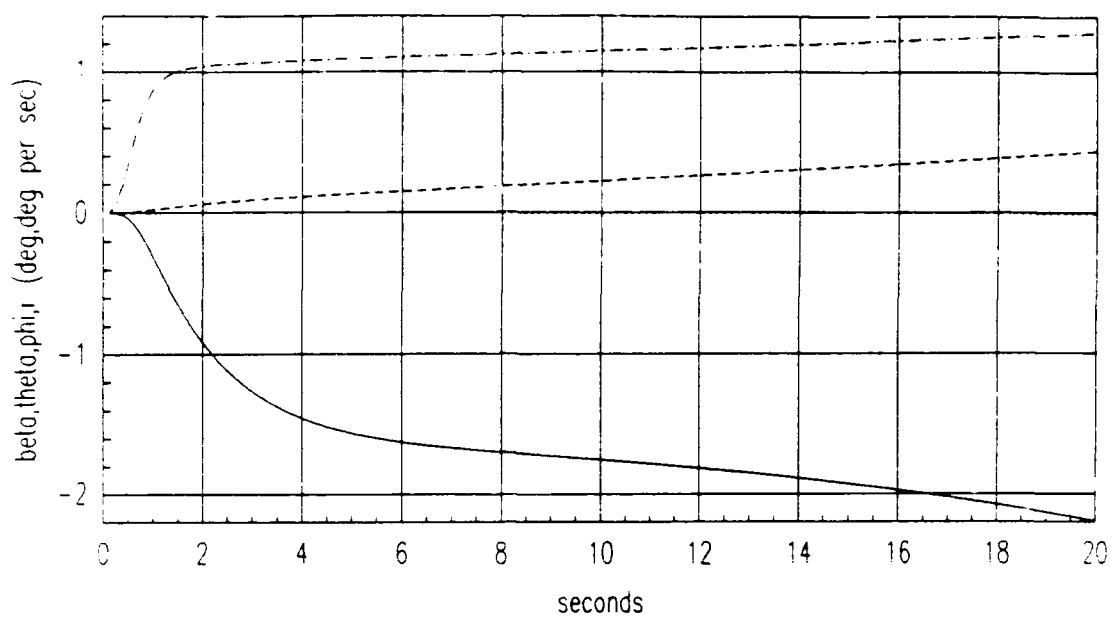


Figure 5.7. Step response method flat turn response in ACM Exit

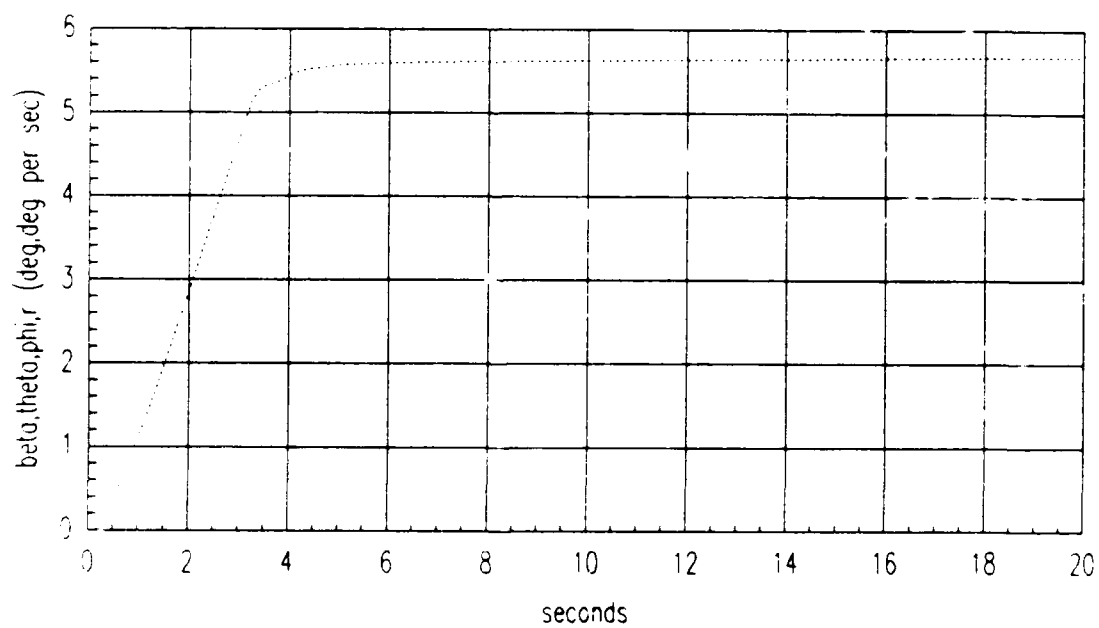


Figure 5.8. Step response method pitch rate tracking response in TFTA

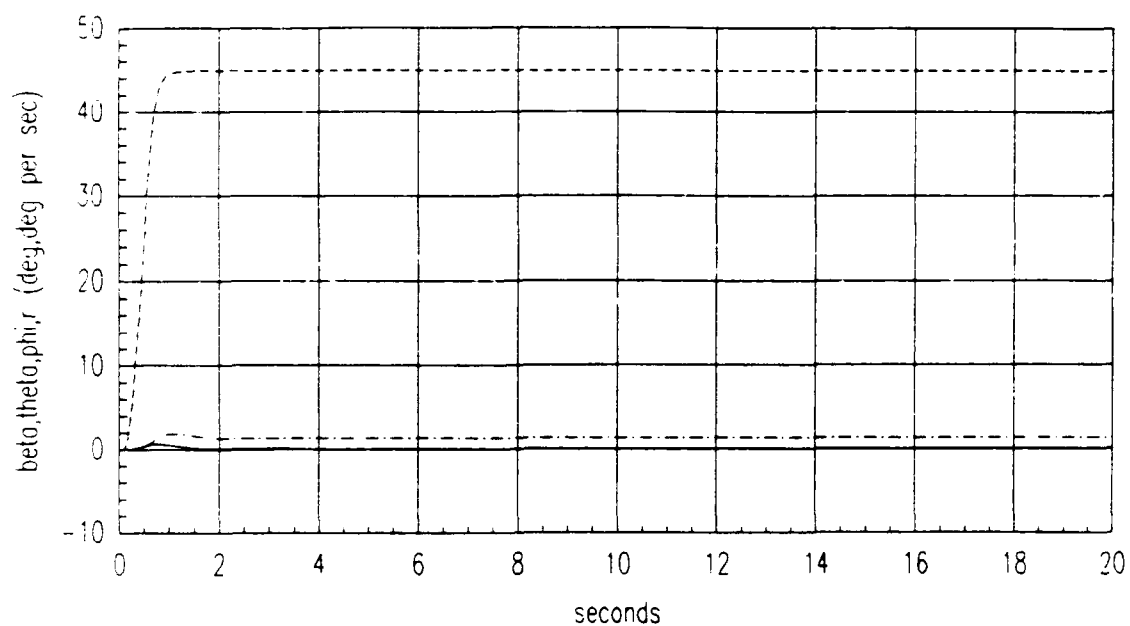


Figure 5.9. Step response method coordinated turn response in TFTA

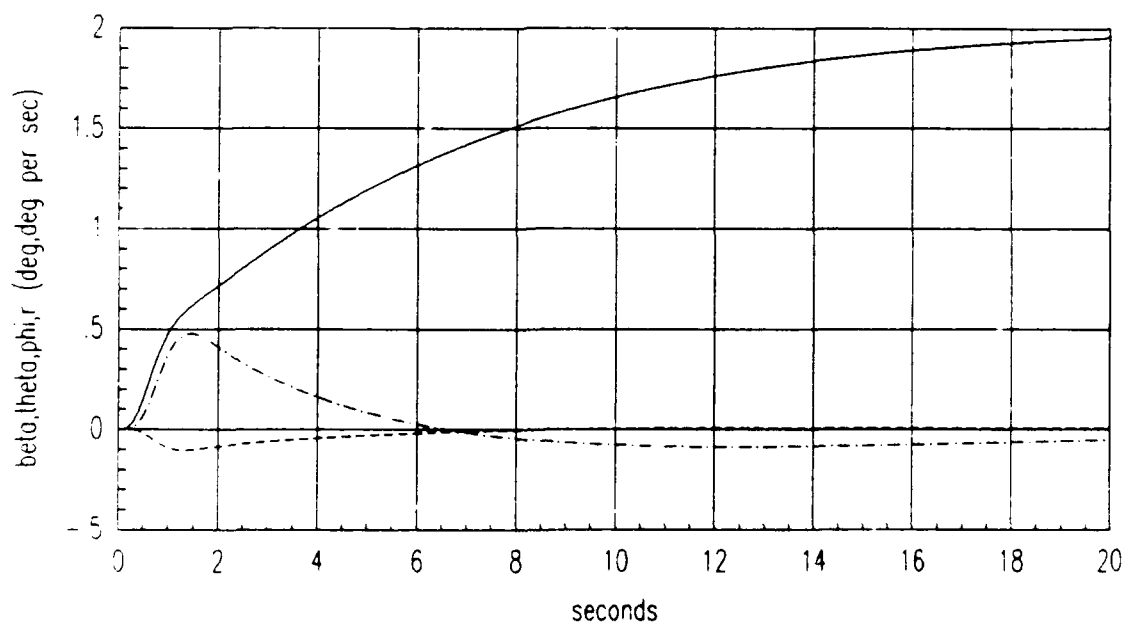


Figure 5.10. Step response method sideslip tracking response in TFTA

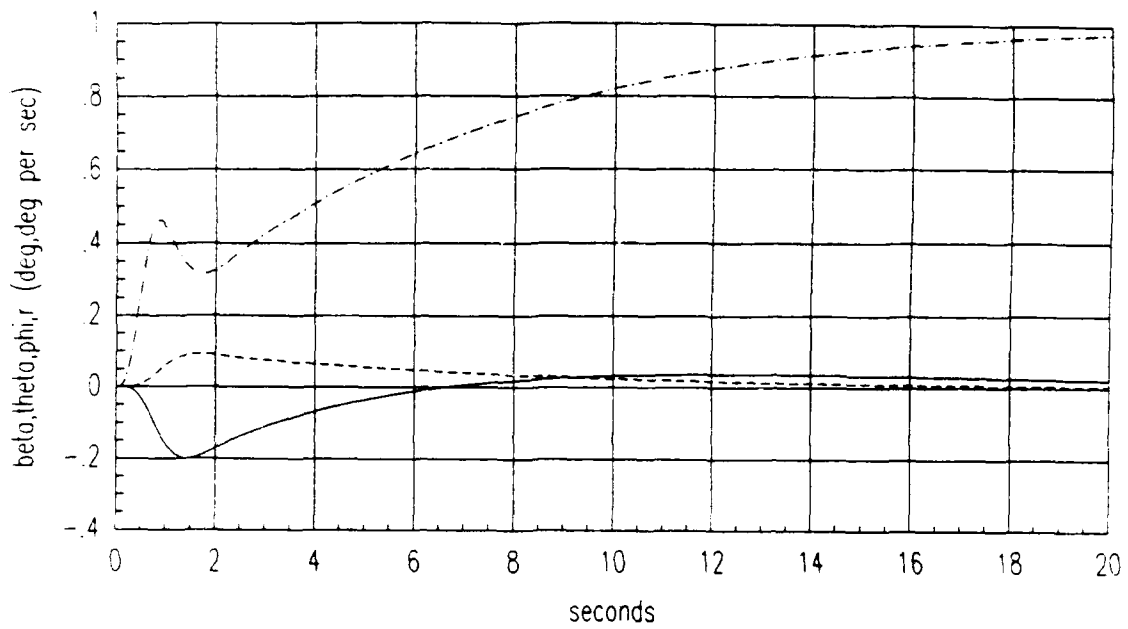


Figure 5.11. Step response method flat turn response in TFTA

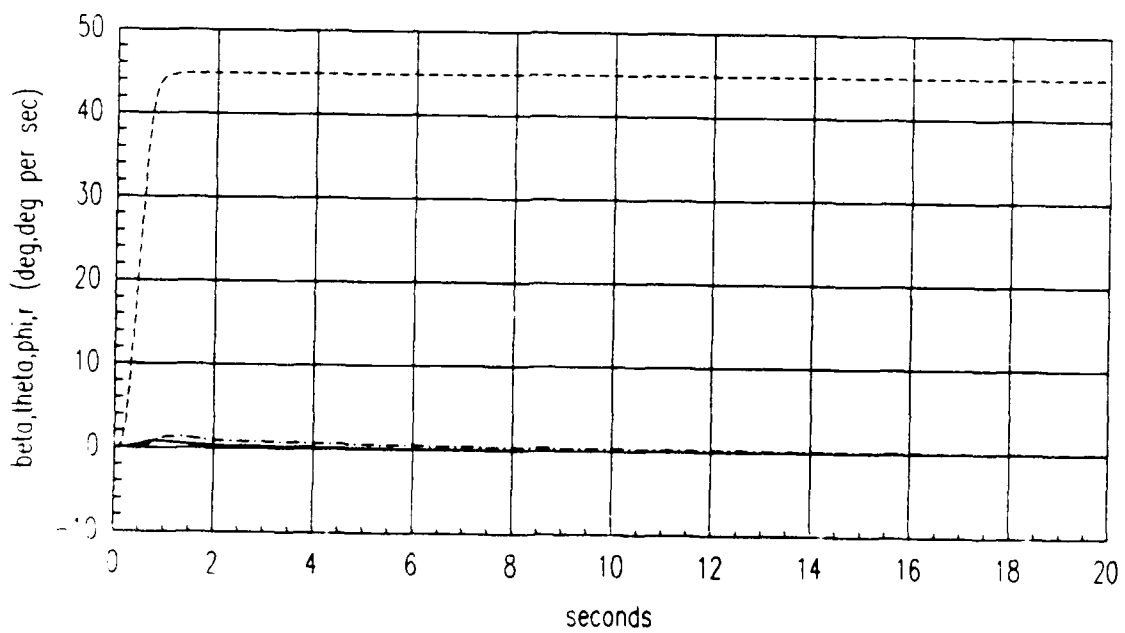


Figure 5.12. Step response method banked turn response in TFTA

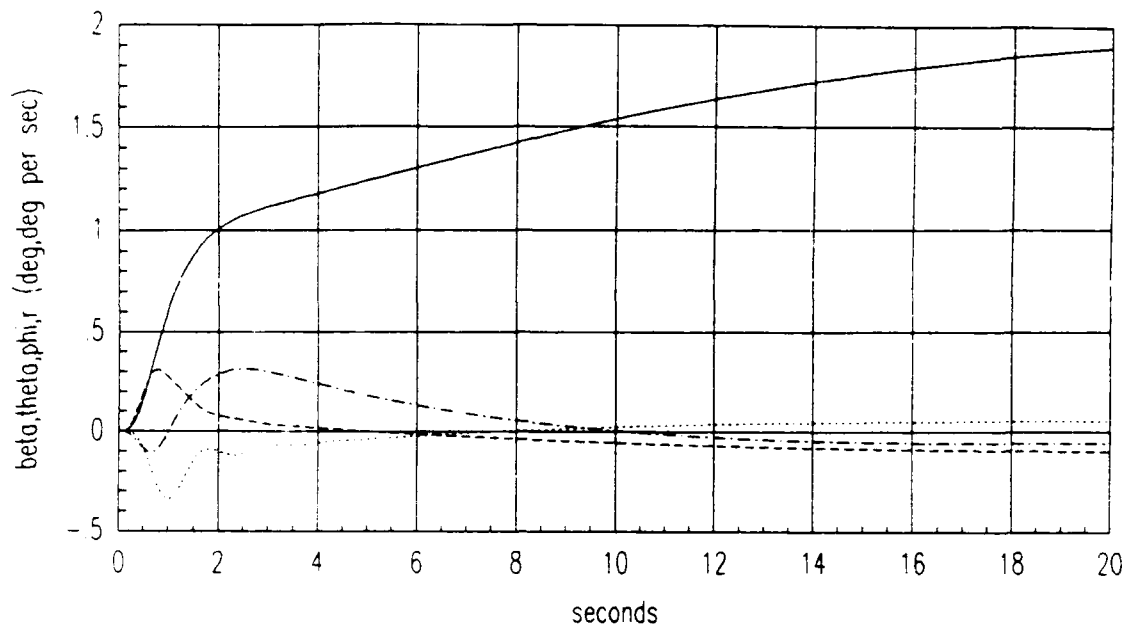


Figure 5.13. Step response method sideslip tracking response in ACM30TL

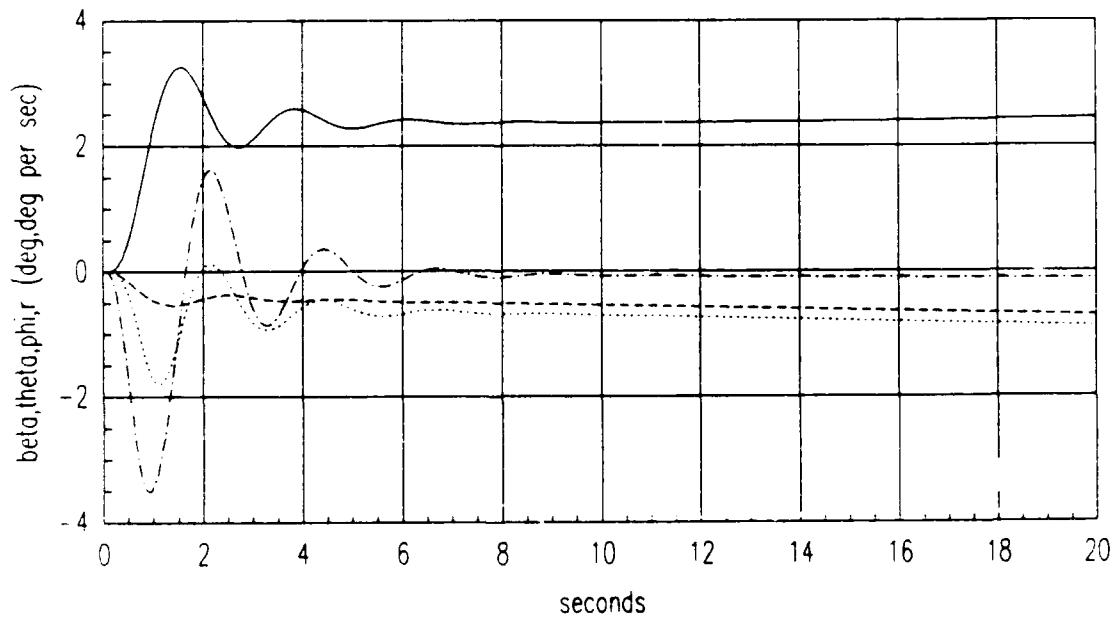


Figure 5.14. Step response method sideslip tracking response in ACM50CL

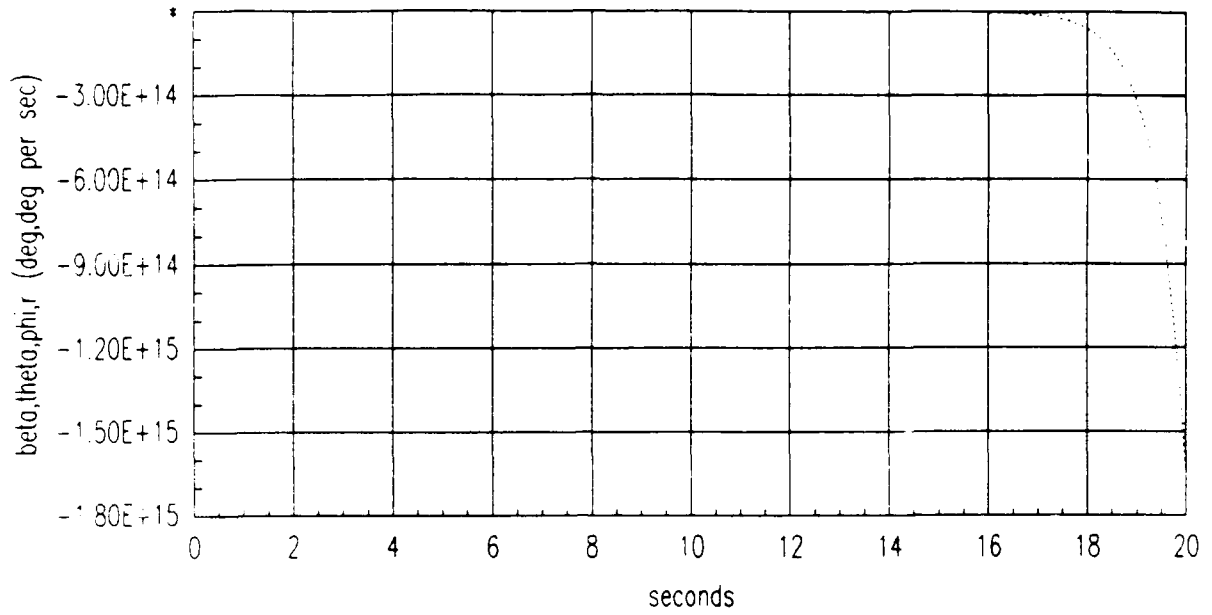


Figure 5.15. Step response method sideslip tracking response in ACM25RL

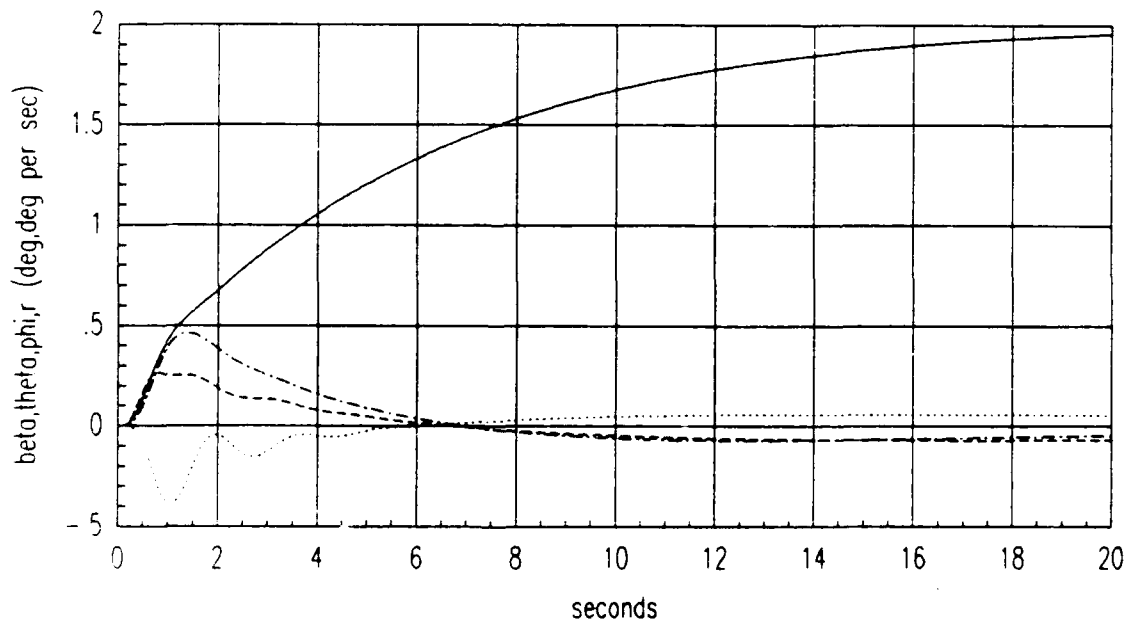


Figure 5.16. Step response method sideslip tracking response in TF TA30TL

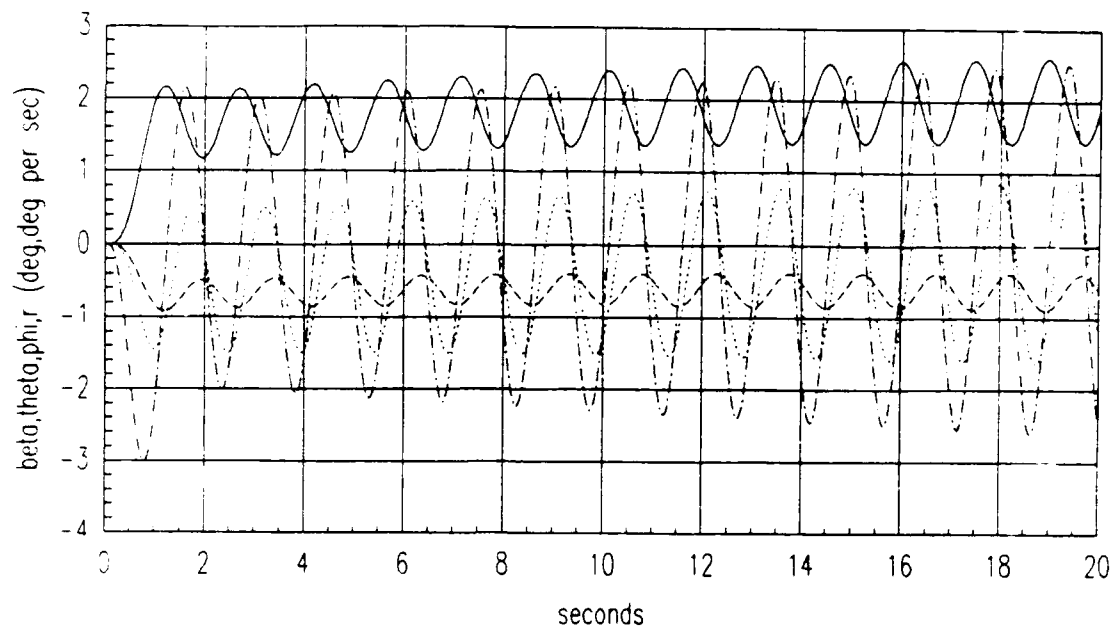


Figure 5.17. Step response method sideslip tracking response in TFTA50CL

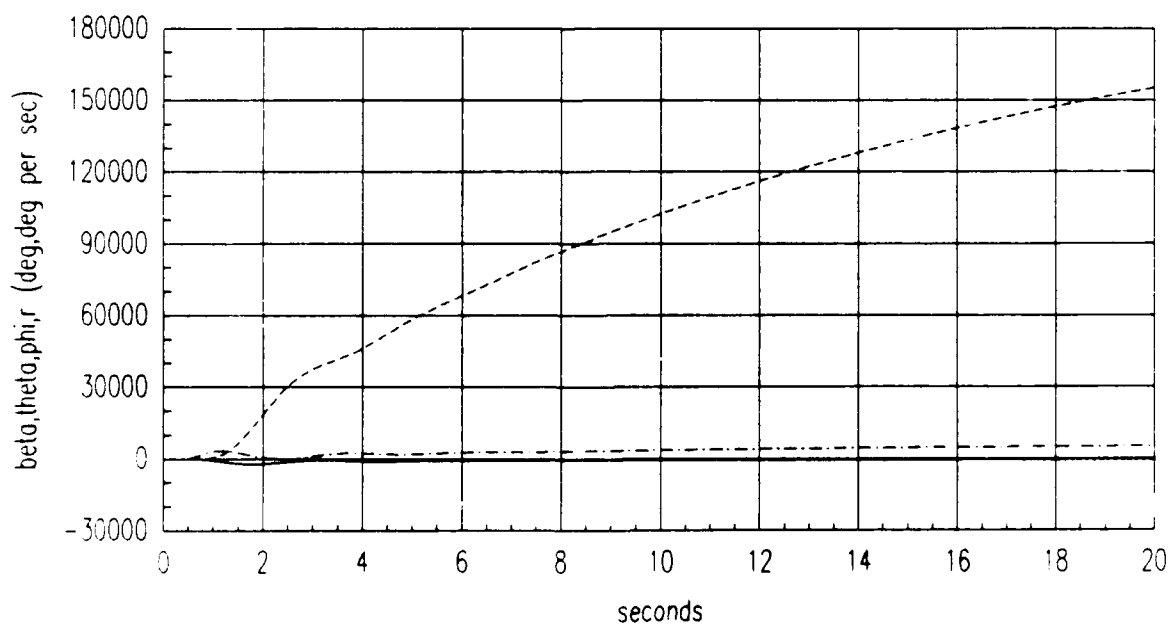


Figure 5.18. Step response method sideslip tracking response in TFTA25RL



## 5.2 ADAPTIVE CONTROLLER

When a single set of design parameters for a fixed-gain design do not adequately stabilize and control the aircraft, either gain scheduling or an adaptive algorithm can be used. Hammond's adaptive algorithm, which is built on the step response method, is examined.

Since the aircraft plant can be represented by a discrete difference equation for a given sampling time  $T$ , control law gains are calculated by manipulating the coefficients of this difference equation. By measuring input and output data, on-line, the coefficients that constitute the difference equation itself can be updated continuously and new PI controller gains calculated each time the measurements are taken. Predicting the new plant parameters allows gain calculations to be accurate and appropriate for the new flight condition or configuration. (4:6-1)

A recursive least squares (RLS) algorithm is used to update the ARMA coefficients each sampling period which are in turn used to determine the controller gain matrices.

The RLS algorithm is written in FORTRAN executable code and accessed each sample period in the MATRIX<sub>X</sub> simulation. The algorithm is initialized with a covariance matrix  $P(0)$  of  $I$  and the matrix containing the past output and input values,  $x(0) = 0$ . ARMA coefficients for either the non-failed **ACM Entry** or **TFTA** flight conditions are used for the first two sampling periods, 0.05 seconds, to ensure that the  $x(k+1)$  matrix is fully populated before the ARMA coefficients in  $\theta(k+1)$  are estimated. The rate of calculation of the varying ARMA coefficients is controlled by the choice of forgetting factor,  $\lambda$ . The applicable RLS Equations 3.38, 3.41, and 3.42 are repeated here with the weighting factor,  $\alpha_t = 1$ .

$$\begin{aligned}\theta(k+1) &= \theta(k) + P(k)x(k+1)\gamma(k+1)[y(k+1) - x^T(k+1)\theta(k)] \\ P(k+1) &= \frac{1}{\lambda} [P(k) - P(k)x(k+1)\gamma(k+1)x^T(k+1)P(k)] \\ \gamma(k+1) &= \frac{1}{[\lambda\alpha_t + x^T(k+1)P(k)x(k+1)]}\end{aligned}$$

The source code for the adaptive algorithm is listed in Appendix D.

The adaptive controller is initially evaluated by analyzing the results of all of the maneuvers performed in **ACM Entry** and **TFTA** with no failures. The forgetting factor,  $\lambda$  is set to one and the ARMA coefficients are monitored at the onset and upon completion of the maneuvers. The ARMA coefficients do not change when the adaptive algorithm is run, which is the expected result. The outputs are expected to closely resemble those obtained from the step response method, since the adaptive simulations start with the same ARMA plant models used in the step response simulations. The following time responses, however, do not show the desired decoupling of outputs that has been obtained from both the discrete PI and step response design methods.

The four responses on each of the next plots are defined as follows

—  $\beta$  ...  $\theta$   
 ---  $\phi$  - - -  $r$

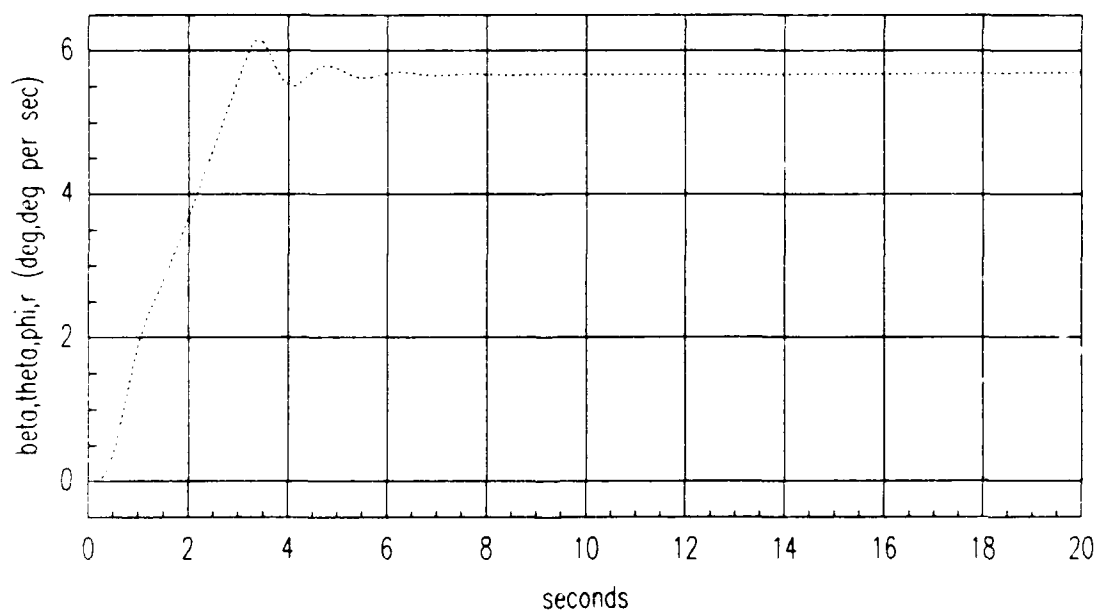


Figure 5.19. Adaptive pitch rate tracking response in ACM Entry

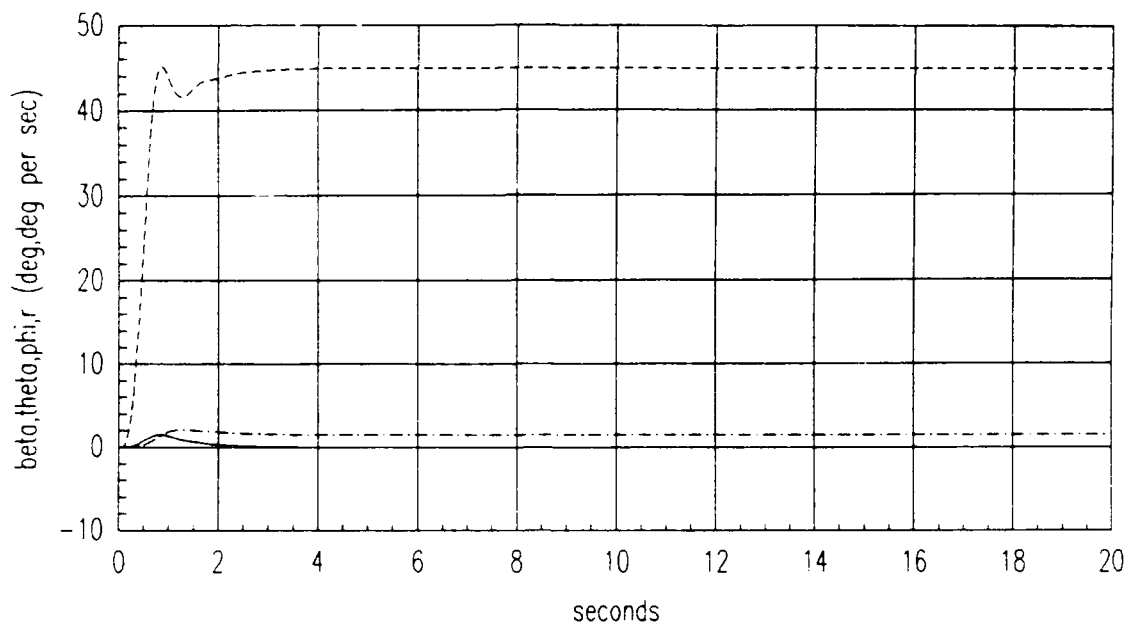


Figure 5.20. Adaptive coordinated turn response in ACM Entry

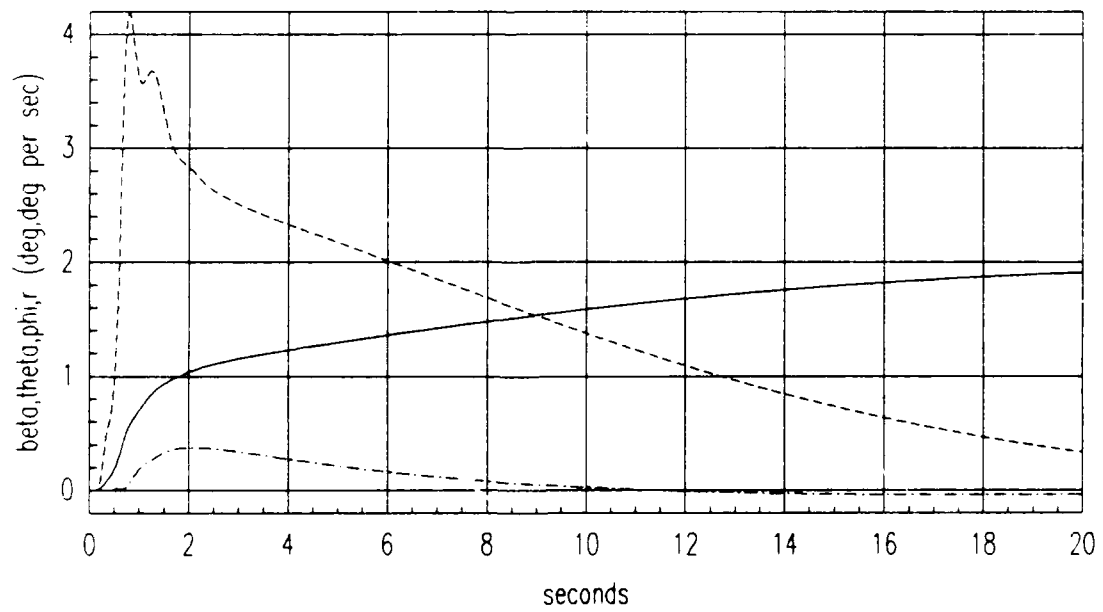


Figure 5.21. Adaptive sideslip tracking response in ACM Entry

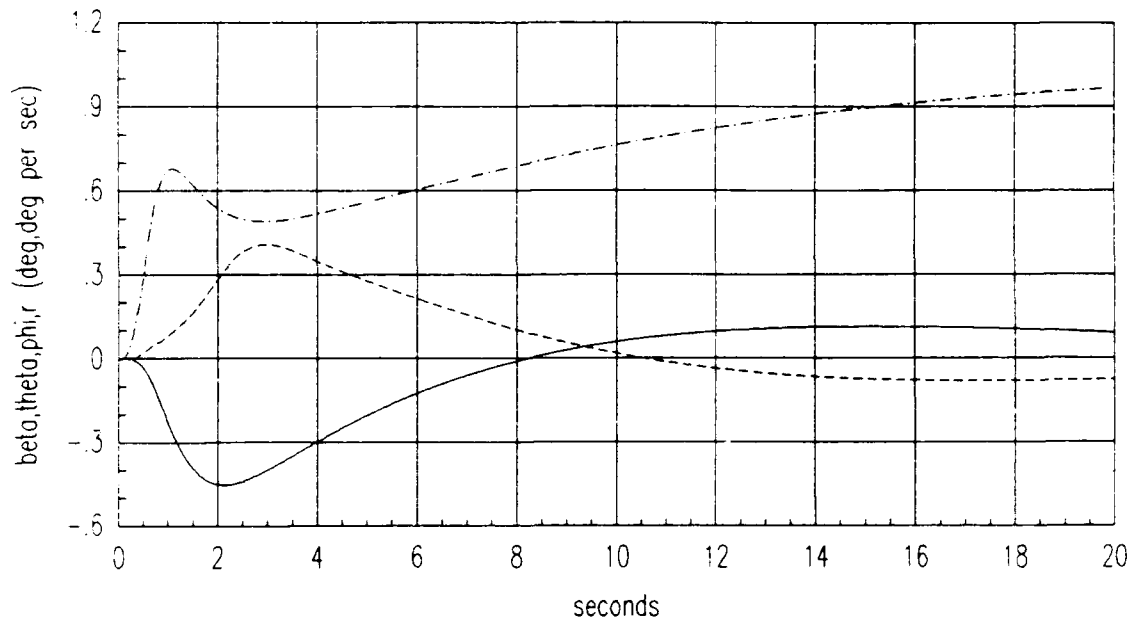


Figure 5.22. Adaptive flat turn response in ACM Entry

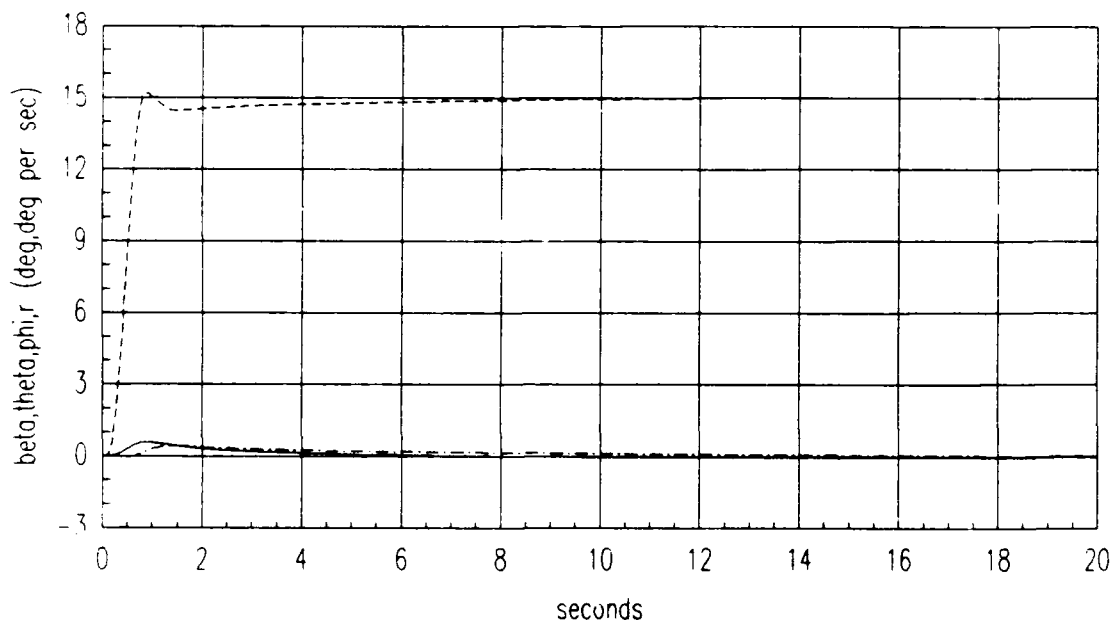


Figure 5.23. Adaptive banked turn response in ACM Entry

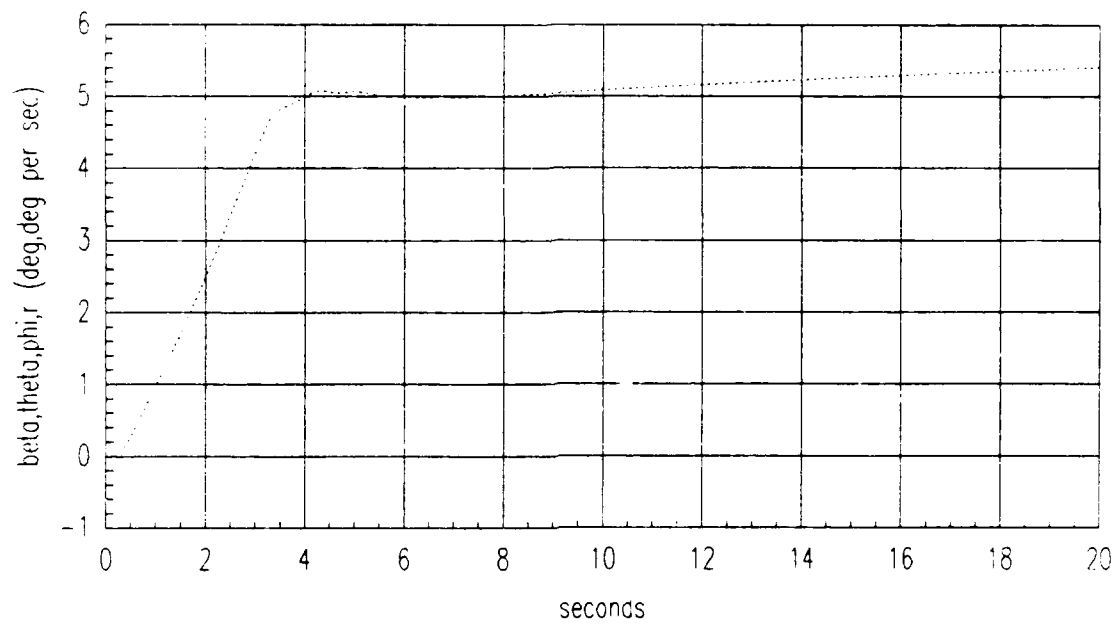


Figure 5.24. Adaptive pitch rate tracking response in TFTA

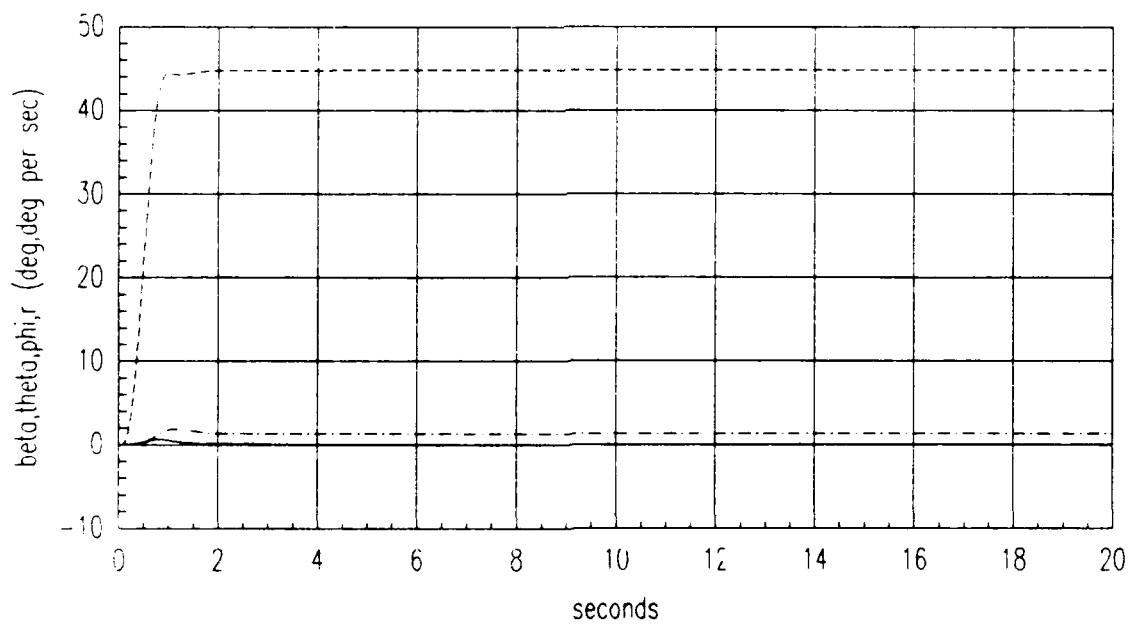


Figure 5.25. Adaptive coordinated turn response in TFTA

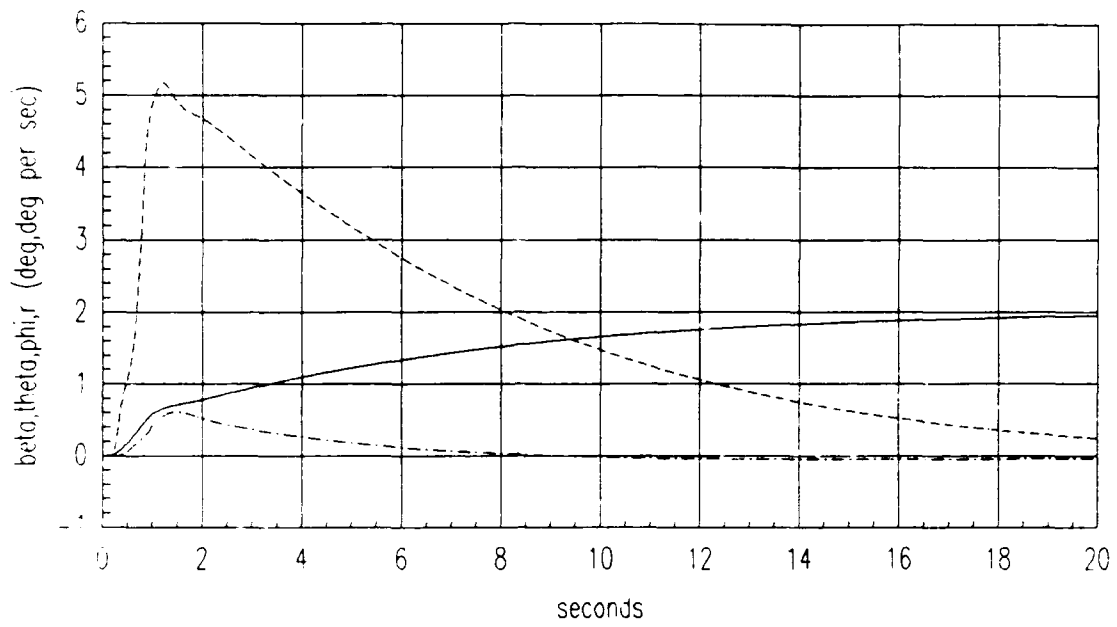


Figure 5.26. Adaptive sideslip tracking response in TFTA

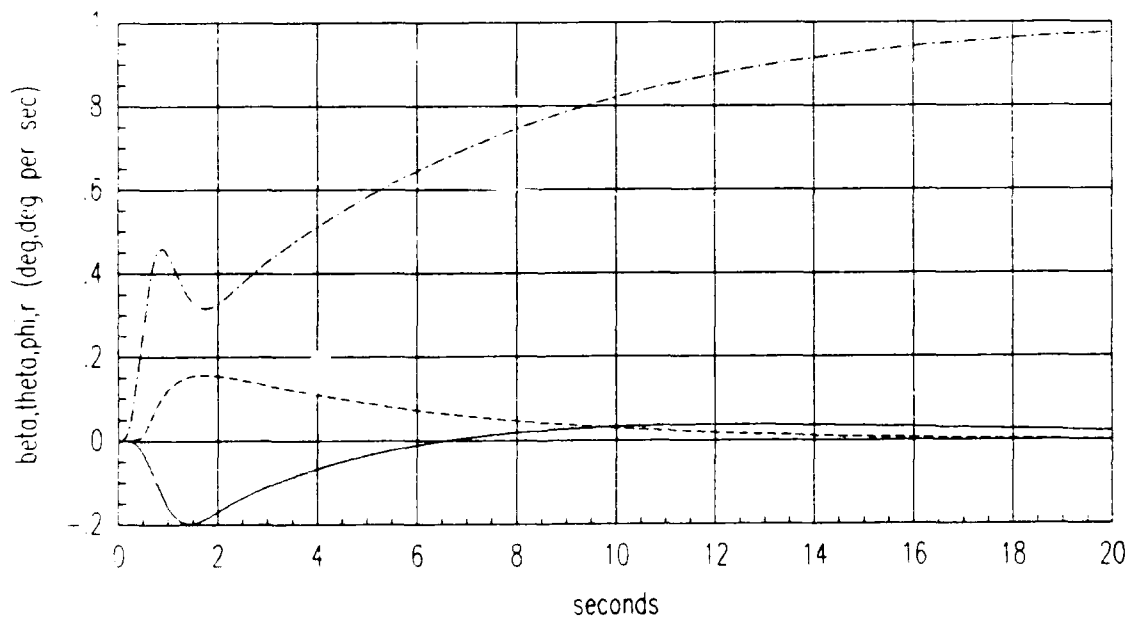


Figure 5.27. Adaptive flat turn response in TFTA

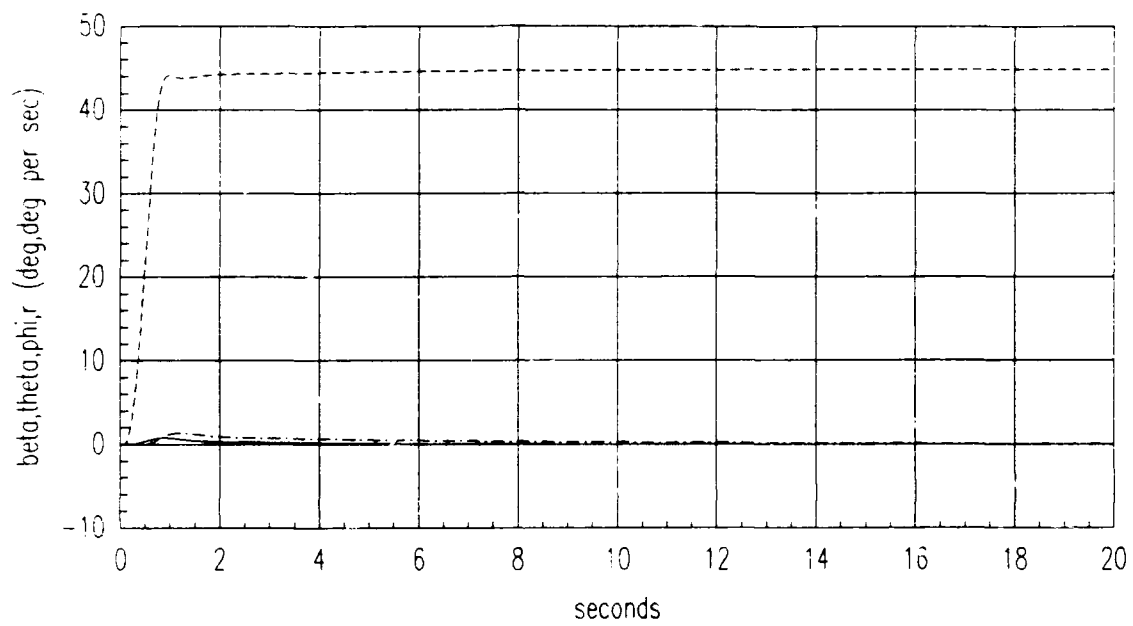


Figure 5.28. Adaptive banked turn response in TFTA

Adaptive simulations are now performed with a single failure occurring at either the beginning of the simulation or at two seconds. The ARMA values that are read into *MATRIX<sub>X</sub>* to initialize the  $\theta$  vector are for non-failed cases. The simulations are performed for a variety of  $\lambda$  values in the single failure cases of 30% left trailing edge loss and 50% left canard loss for the sideslip tracking and flat turn maneuvers. Only the responses generated in the failure condition ACM30TL are presented since the other cases produced divergent responses. For the two maneuvers tested in the two different failure onsets, the responses obtained from a  $\lambda = .90$  are the most stable. The responses were run for 30 seconds for the case of failure introduction at two seconds in order to allow the responses to settle.

The four responses on each plots are defined according to the following legend.

$\cdots \beta$     $\cdots \theta$   
 $---$   $\phi$     $---$   $r$

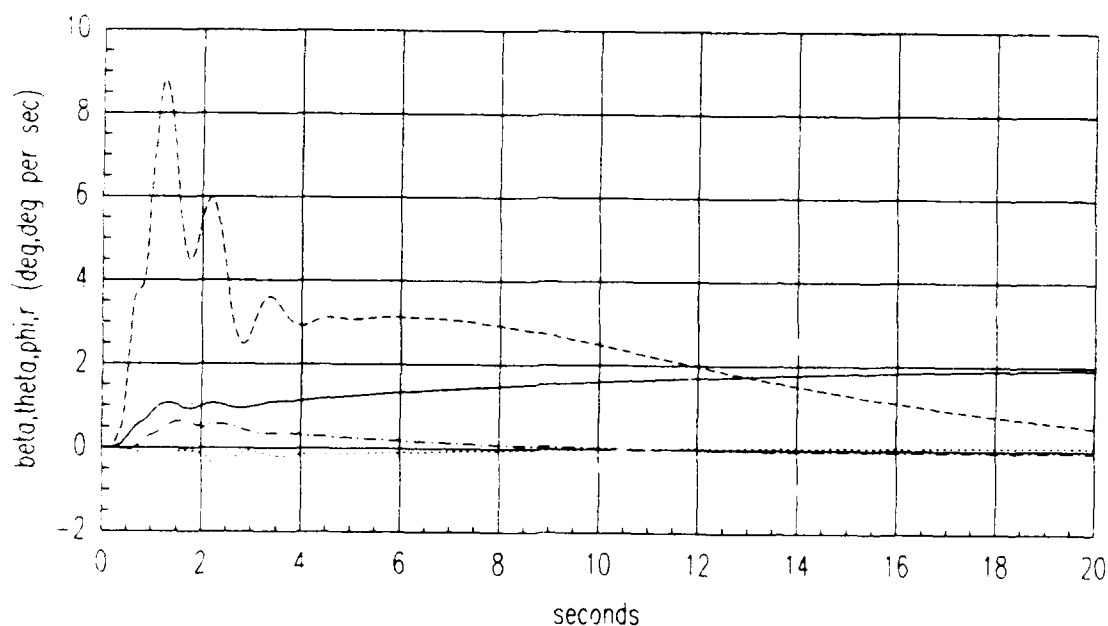


Figure 5.29. Adaptive sideslip tracking response in ACM30TEL with  $\lambda = .90$  and failure at  $t=0$



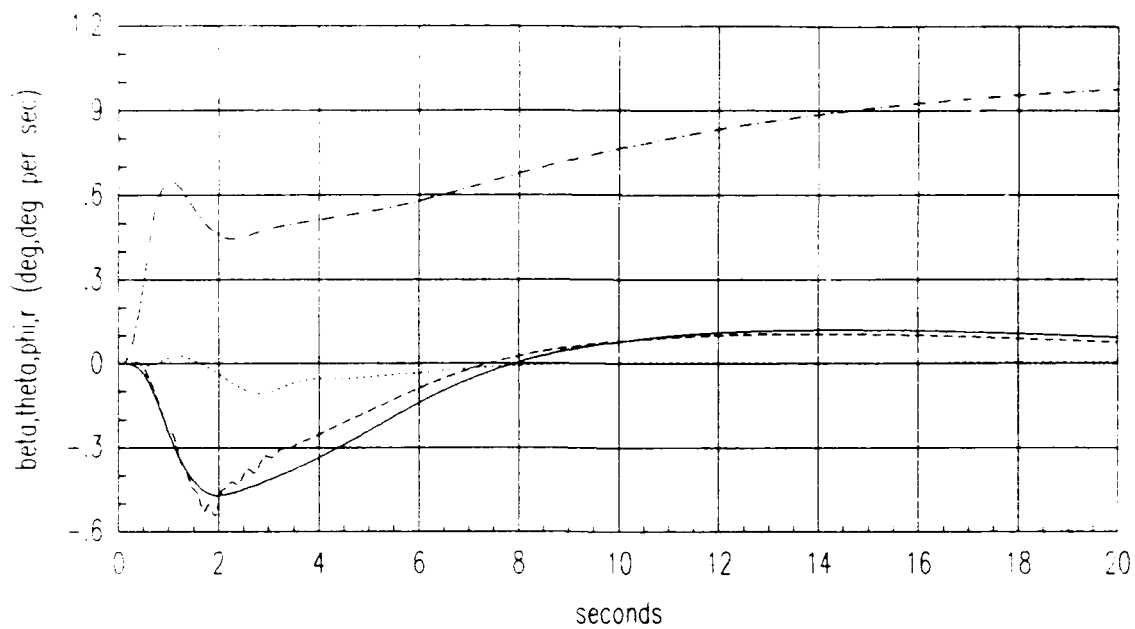


Figure 5.30. Adaptive flat turn response in ACM30TEL with  $\lambda=.90$  and failure at  $t=0$

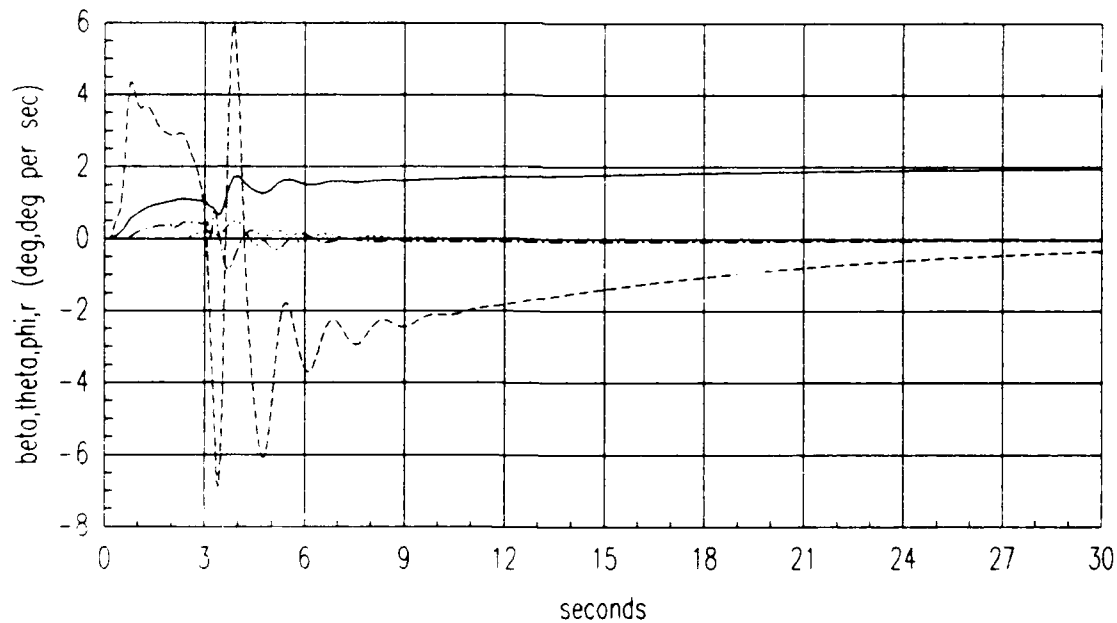


Figure 5.31. Adaptive sideslip tracking response in ACM30TEL with  $\lambda=.90$  and failure at  $t=2$

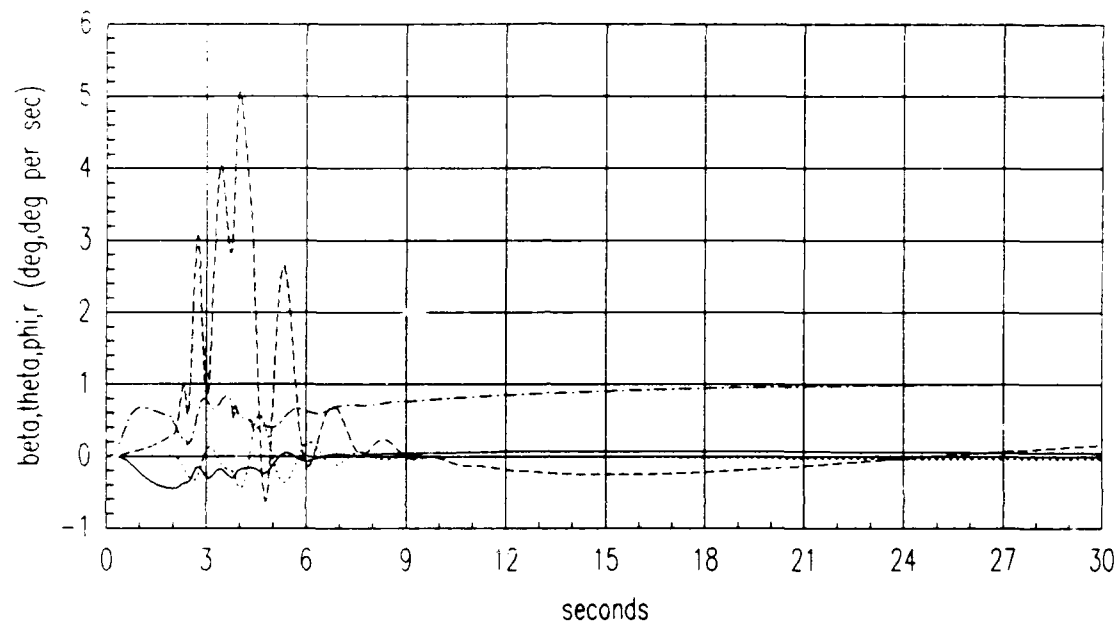


Figure 5.32. Adaptive flat turn response in ACM30TEL with  $\lambda=.90$  and failure at  $t=2$

The adaptive controller is initially evaluated by analyzing the results of all of the maneuvers performed in **ACM Entry** and **TFTA** with no failures. The forgetting factor,  $\lambda$ , is set to one and the ARMA coefficients are monitored at the onset and upon completion of the maneuvers. The ARMA coefficients do not change when the adaptive algorithm is run, which is the expected result. The outputs are expected to closely resemble those obtained from the step response method, since the adaptive simulations start with the same ARMA plant models used in the step response simulations. The following time responses, however, do not show the desired decoupling of outputs that has been obtained from both the discrete PI and step response design methods.

The four responses on each of the next plots are defined as follows

—  $\beta$  ...  $\theta$   
 --  $\phi$  - -  $r$

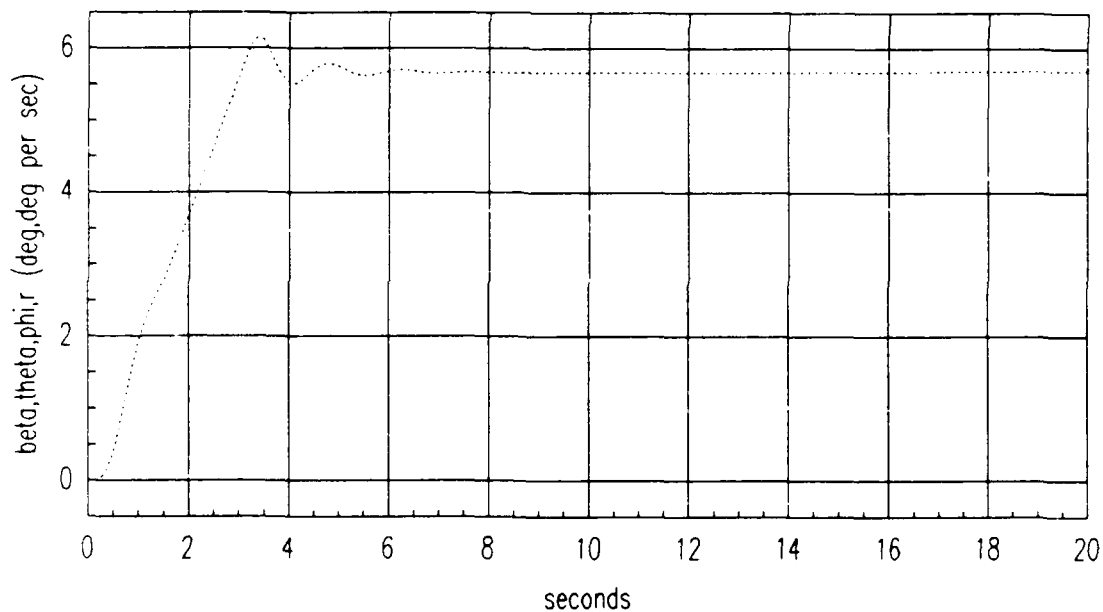


Figure 5.19. Adaptive pitch rate tracking response in ACM Entry

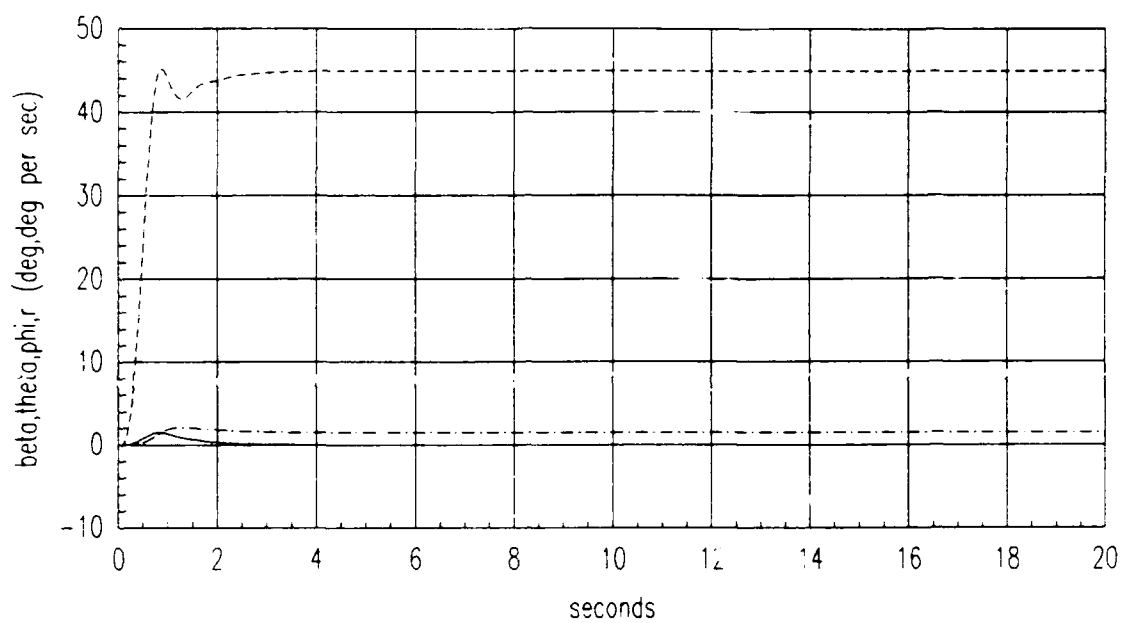


Figure 5.20. Adaptive coordinated turn response in ACM Entry

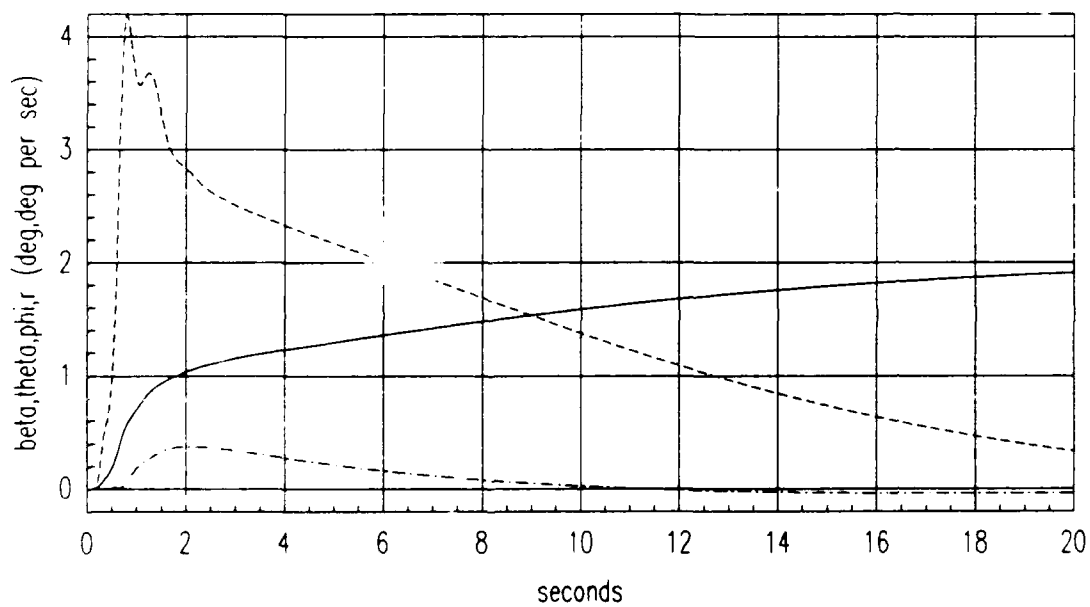


Figure 5.21. Adaptive sideslip tracking response in ACM Entry

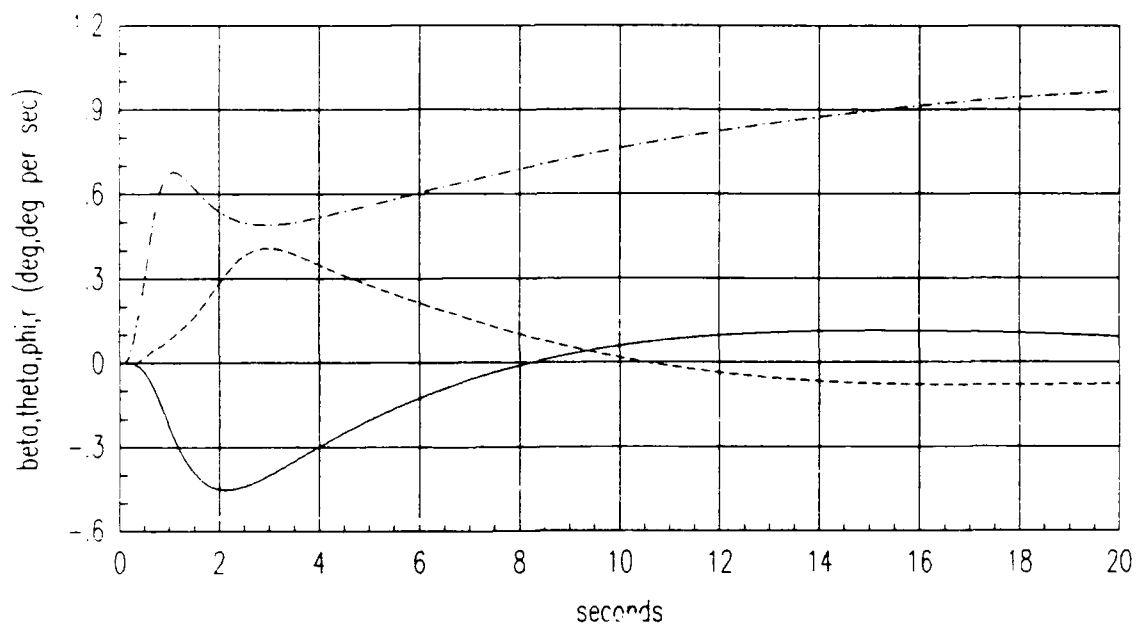


Figure 5.22. Adaptive flat turn response in ACM Entry

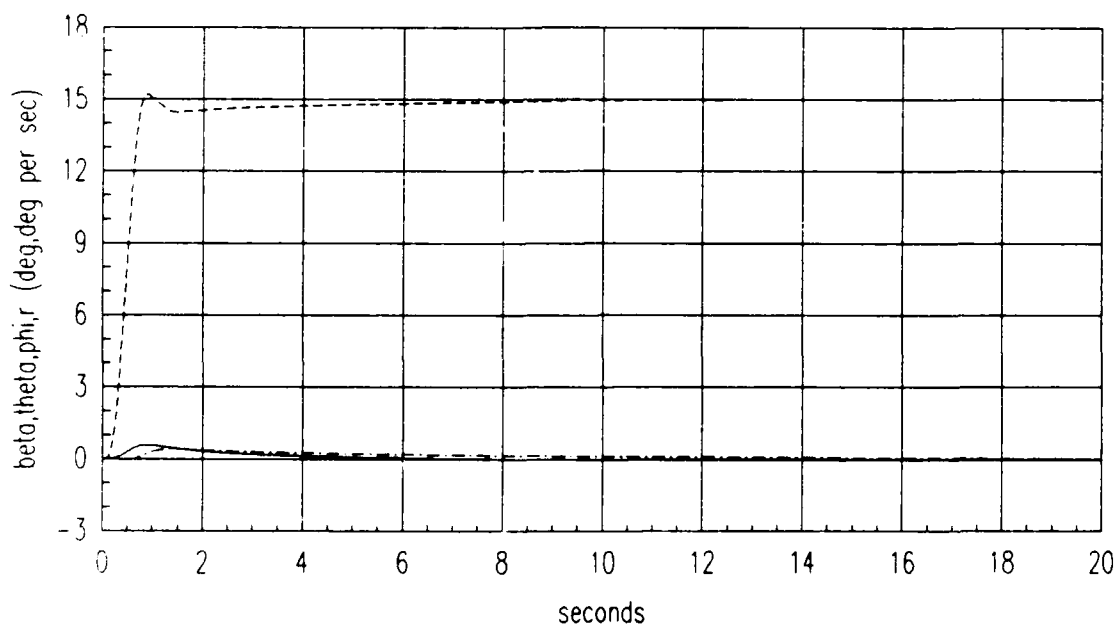


Figure 5.23. Adaptive banked turn response in ACM Entry

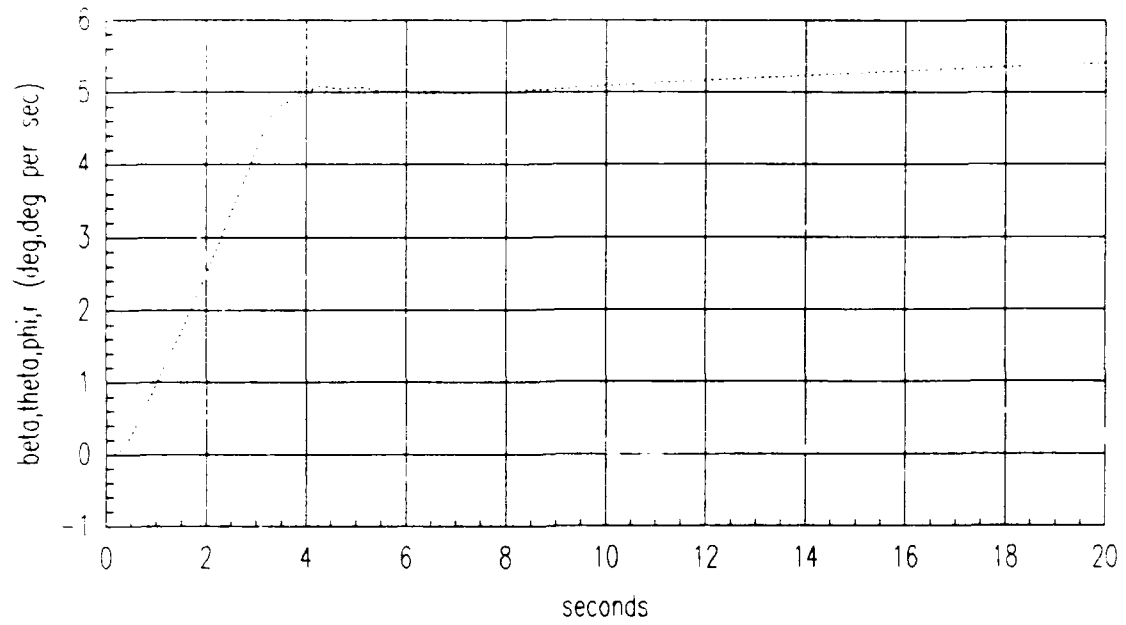


Figure 5.24. Adaptive pitch rate tracking response in TFTA

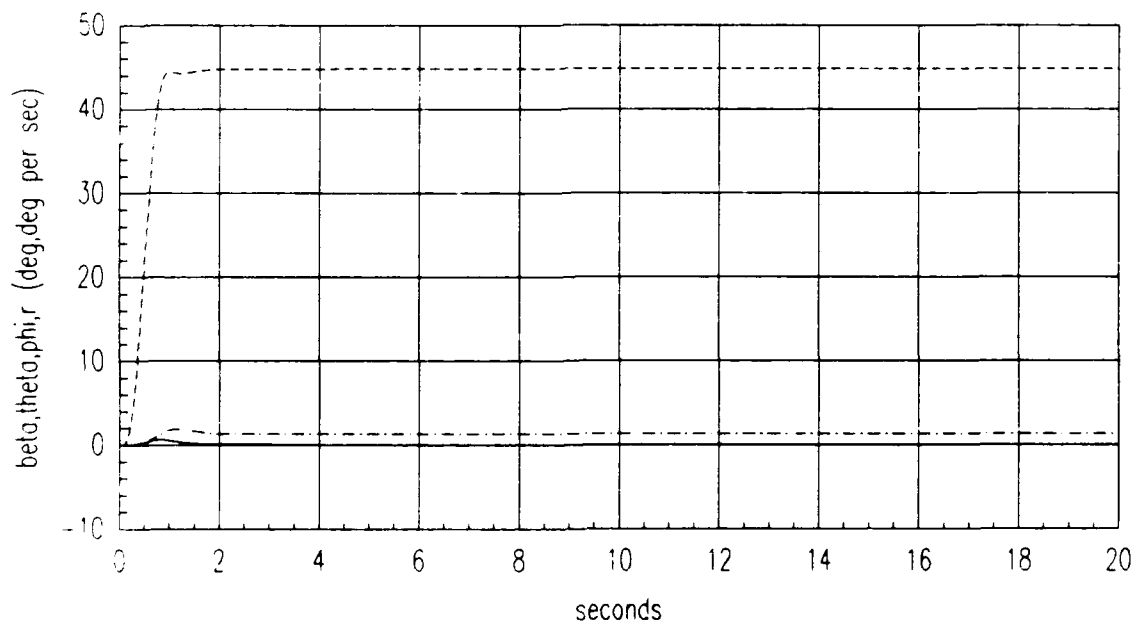


Figure 5.25. Adaptive coordinated turn response in TFTA

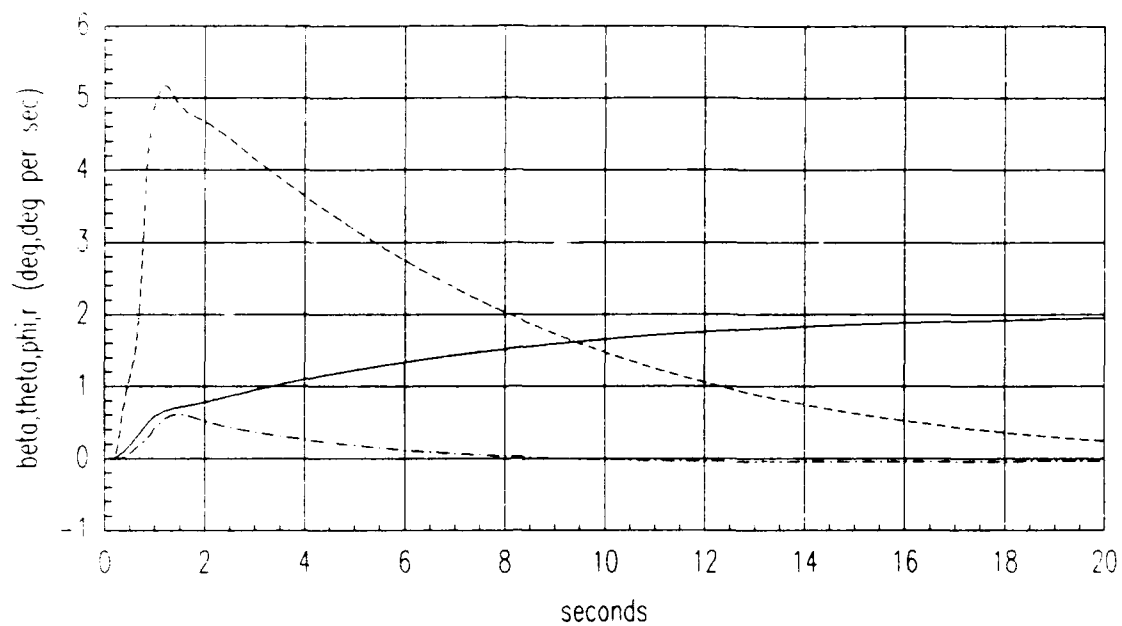


Figure 5.26. Adaptive sideslip tracking response in TFTA

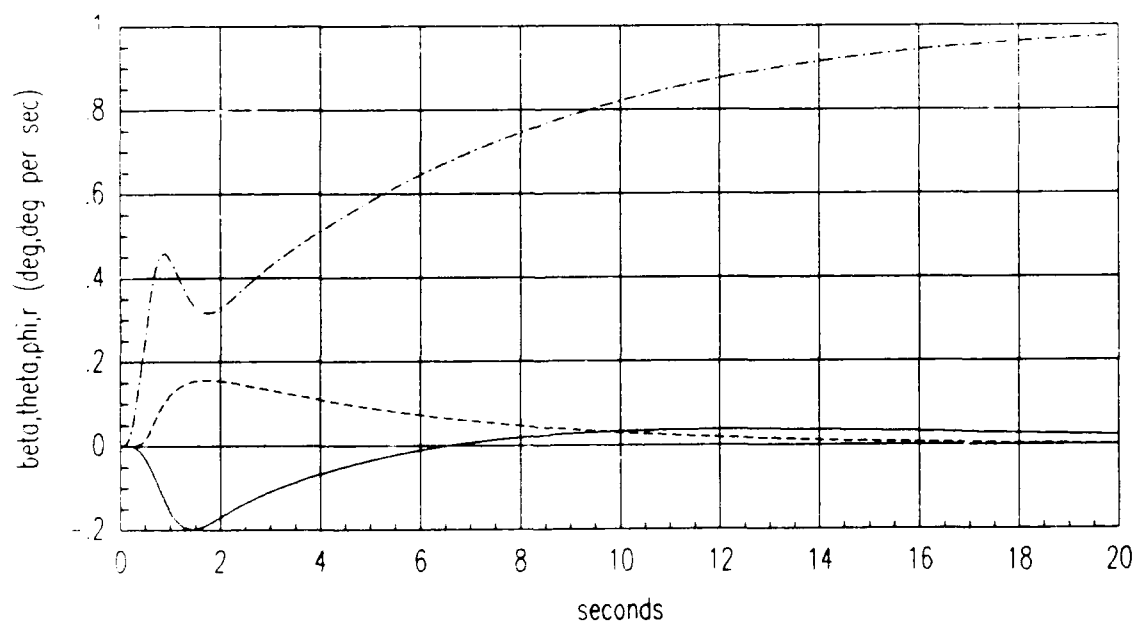


Figure 5.27. Adaptive flat turn response in TFTA

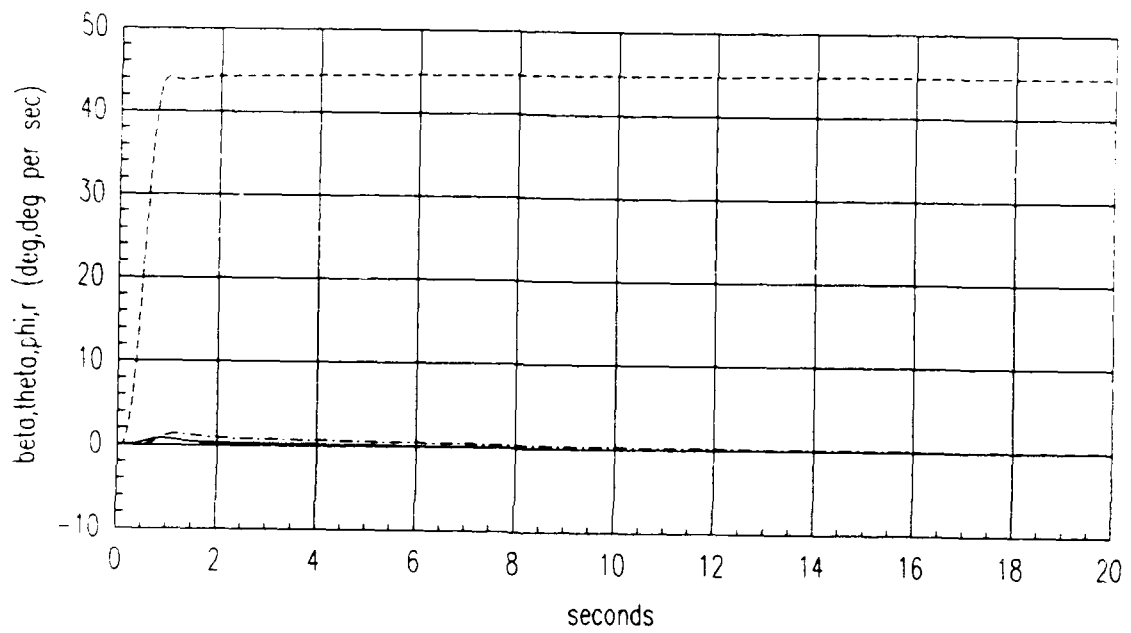


Figure 5.28. Adaptive banked turn response in TF1A



Adaptive simulations are now performed with a single failure occurring at either the beginning of the simulation or at two seconds. The ARMA values that are read into *MATRIX*<sub>X</sub> to initialize the  $\theta$  vector are for non-failed cases. The simulations are performed for a variety of  $\lambda$  values in the single failure cases of 30% left trailing edge loss and 50% left canard loss for the sideslip tracking and flat turn maneuvers. Only the responses generated in the failure condition ACM30TL are presented since the other cases produced divergent responses. For the two maneuvers tested in the two different failure onsets, the responses obtained from a  $\lambda = .90$  are the most stable. The responses were run for 30 seconds for the case of failure introduction at two seconds in order to allow the responses to settle.

The four responses on each plots are defined according to the following legend.

$$\begin{array}{lcl} \beta & \dots & \theta \\ - - & \phi & - - r \end{array}$$

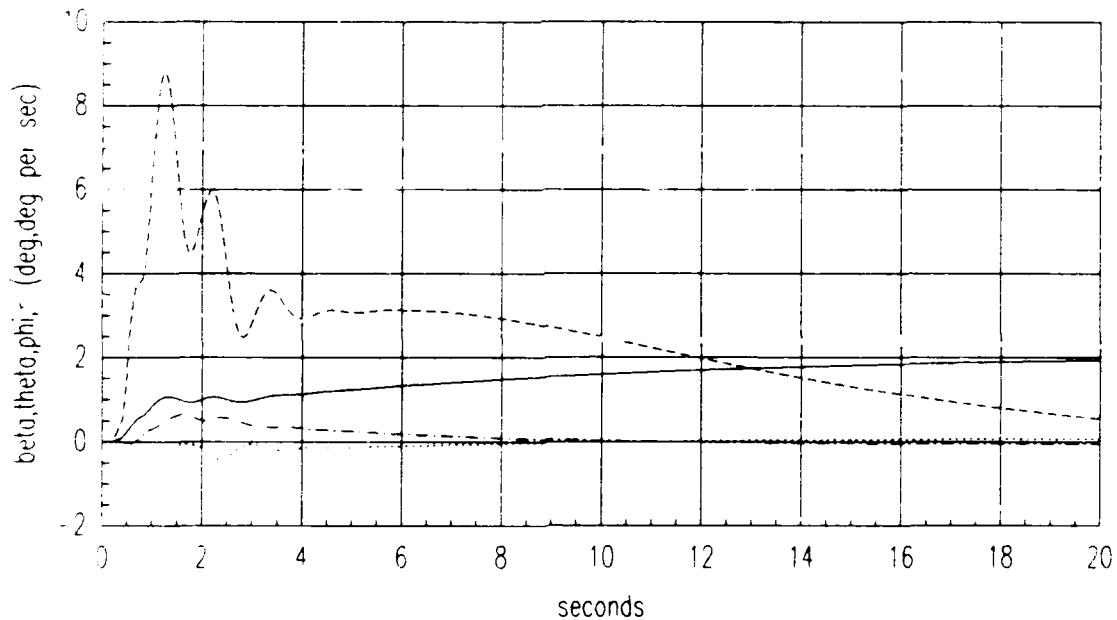


Figure 5.29. Adaptive sideslip tracking response in ACM30TEL with  $\lambda = .90$  and failure at  $t=0$

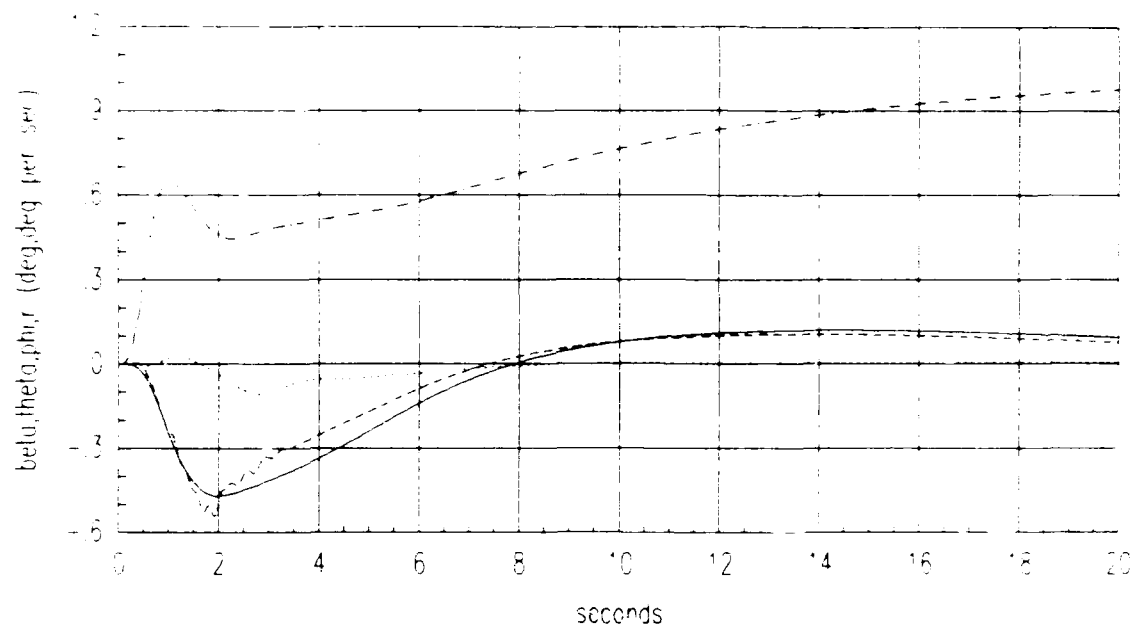


Figure 5.30. Adaptive flat turn response in ACM30TEL with  $\Lambda = 90$  and failure at  $t=0$

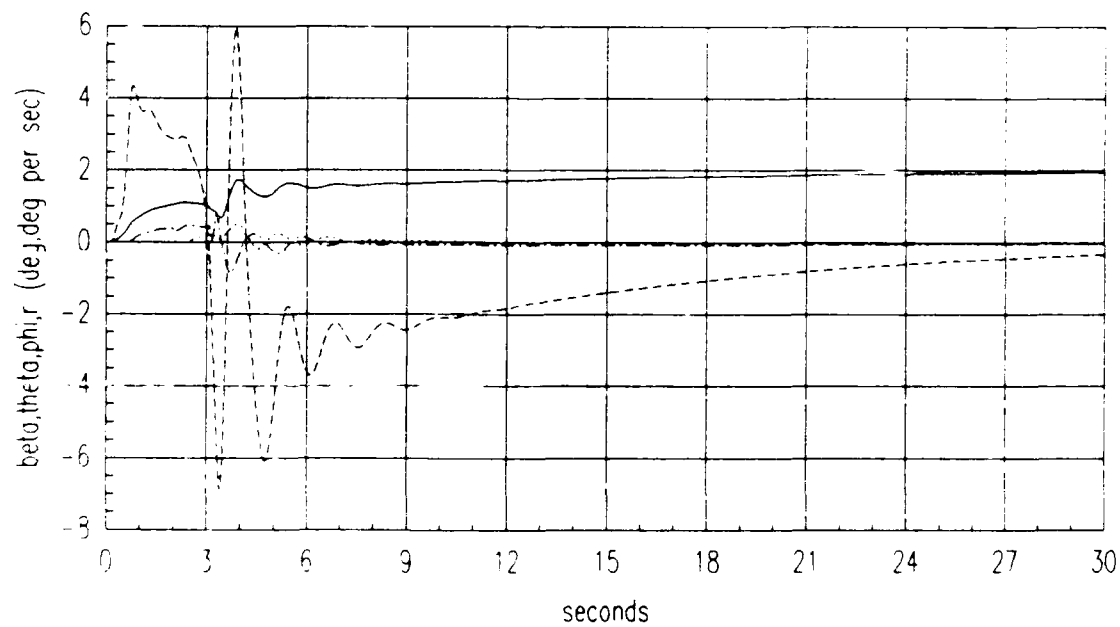


Figure 5.31. Adaptive sideslip tracking response in ACM30TEL with  $\Lambda = 90$  and failure at  $t=2$

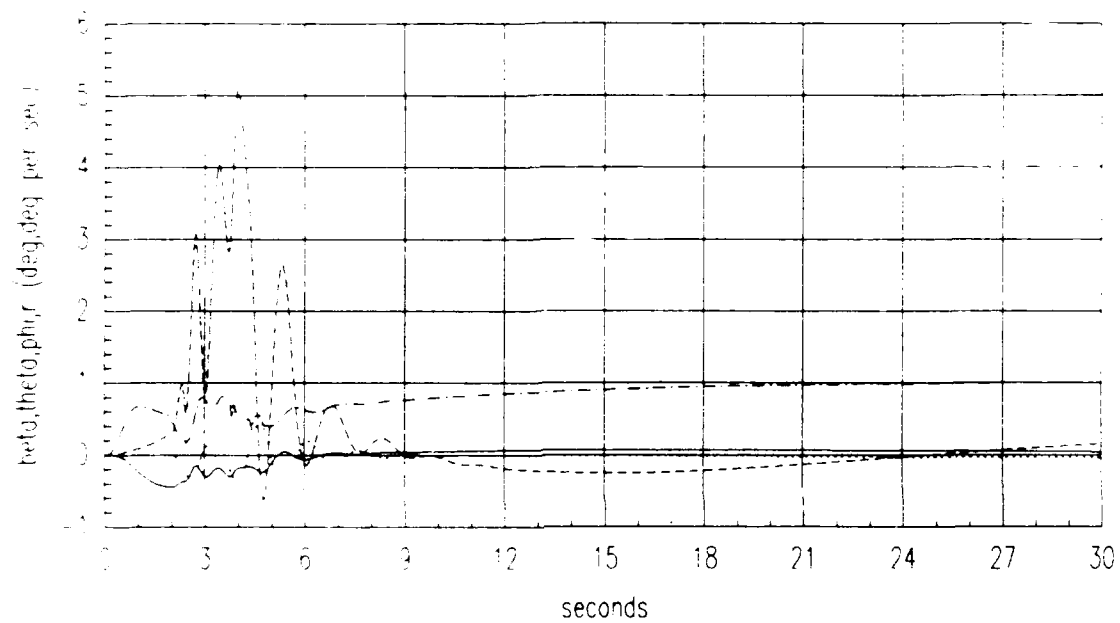


Figure 5.32. Adaptive flat turn response in ACM30TEI with  $\lambda=.90$  and failure at  $t=2$

This chapter contains the design parameters and time responses for the step response PI controller and results of the adaptive algorithm. The results of all work in this thesis are analyzed in Chapter 6.

## VI. CONCLUSIONS AND RECOMMENDATIONS

### 6.1 SUMMARY

**6.1.1 DISCRETE PI CONTROLLER** The time domain and frequency results obtained for the discrete PI controller, presented in Chapter 4, show that the outputs are indeed highly decoupled. The velocity results are not plotted in the same figures as the other four outputs because the  $180^\circ/\pi$  radian conversion factor is not applicable. The velocity responses are monitored and never peaked above 2 ft/sec, which is well within an acceptable range of variation. The time responses for the non failed flight conditions show that the design is very robust. The bandwidth of the system was increased by a factor of 100 over the previous design and is now just under 10 *rad/sec* for most of the five input/output pairs. The phase and gain margins specified by MIL - F - 9490D are met in almost all instances. The goal of determining one set of design parameters that can be used to determine fixed controller gains for all three flight conditions are met and robust results are obtained for **ACM Entry**, **TFTA**, and **ACM Exit**. An effort is made to limit the values of the individual elements in the  $K_1$  and  $K_2$  matrices. Examination of Appendix C demonstrates that the **ACM Entry** and **TFTA** gains are in a reasonable range and only a few of the elements in the **ACM Exit** gain matrices are larger than desired. The extension of the fixed-gain design to the cases of single failure conditions is fairly successful in that for three of the six failure conditions, the aircraft does remain stable and perform the maneuver with some degree of flying qualities intact. However, some type of gain scheduling scheme or adaptive control is deemed necessary by the fact that three failure conditions yield unstable responses.

**6.1.2 STEP RESPONSE METHOD PI** The step response method PI controller time domain results show the same degree of stability and decoupling between outputs, using one set of design parameters, as are obtained from the discrete PI controller. The step response method shows two improvements over the discrete PI controller design; the  $\beta$  undershoot in the flat turn is reduced by approximately one third in **ACM Entry** and **TFTA**, and the flat turn can now be successfully performed in **ACM30TL**. The goal of obtaining individual gain elements of less than 20 is not possible in this method

and the step response controller can only stabilize two of the six single failure conditions. Examination of the  $w'$  roots listed in Appendix C also shows that all roots are not in the LHP.

**6.1.3 ADAPTIVE CONTROLLER** The results of the adaptive controller are not all as expected. The simulations performed for the no failure cases show much larger  $\phi$  outputs in the sideslip tracking responses and slightly larger  $\phi$  responses in the flat turn maneuver than are in the step response method time responses. This result occurs even though the ARMA coefficients are invariant. This characteristic of the  $\phi$  output undoubtedly carries over into the single control surface failure simulations. The steady state values of the adaptive outputs are, however, very close to the steady state step response outputs.

Hammond had worked with the coordinated turn in **ACM30TL**, so two different maneuvers in two single failure conditions are attempted. However, the responses can not be stabilized in **ACM50CL**, **TFTA30TL**, and **TFTA50CL**. It is interesting to note that it is the  $\theta$  response which is consistently divergent in the **TFTA** failure cases. The steady state outputs for the two sets of failure onsets are reasonably decoupled at the completion of the simulation.

## **6.2 RECOMMENDATIONS FOR FUTURE RESEARCH**

There are many areas that can be examined using Porter's control law techniques on the CRCA. The first of which are areas of immediate interest and deal with the parameter adaptive algorithm.

1. Determine why there are differences between the sideslip tracking and flat turn maneuvers obtained from the step response PI method and adaptive simulations.
2. Stabilize the adaptive simulations in the two failure conditions attempted in this thesis.
3. Assess the effects noise in the output measurements have on the fixed-gain and adaptive designs.

4. Use non-linear aircraft equations to perform simulations with the design parameters determined from the linear point designs and compare the results.
5. Investigate the proportional plus integral plus derivative (PID) control law on the same set of maneuvers and failure conditions to remove the *slow* modes of the time responses.
6. Compare the results obtained from the PI design techniques to those obtained using the PID control law.

## Appendix A. *AIRCRAFT STATE SPACE MODELS*

The aircraft models used in the MATRIX<sub>X</sub> simulation are listed on the following pages.



Table A.1. ACM Entry Matrices - No Failures

$$A = \begin{bmatrix} .0000 & .0000 & .0000 & .0000 & 1.0000 & .0000 & .0000 & .0000 \\ .0000 & .0000 & .0000 & .0000 & .0000 & .0000 & 1.0000 & .0350 \\ -32.1804 & .0000 & -.0119 & -.0186 & -31.2350 & .0000 & .0000 & .0000 \\ -1.0634 & .0000 & -.0324 & -1.0634 & 894.4548 & .0000 & .0000 & .0000 \\ .0000 & .0000 & .0000 & .0069 & -.6015 & .0000 & .0000 & .0000 \\ .0000 & .0360 & .0000 & .0000 & .0000 & -.0929 & .0349 & -.9571 \\ .0000 & .0000 & .0000 & .0000 & .0000 & -27.8066 & -2.0376 & .4913 \\ .0000 & .0000 & .0000 & .0000 & .0000 & 2.4582 & -.0241 & -.4377 \end{bmatrix}$$

$$B = \begin{bmatrix} .0000 & .0000 & .0000 & .0000 & .0000 & .0000 & .0000 & .0000 & .0000 \\ .0000 & .0000 & .0000 & .0000 & .0000 & .0000 & .0000 & .0000 & .0000 \\ .0411 & .0411 & .1322 & .0866 & .1322 & .0866 & .1018 & .1018 & .0000 \\ -.3163 & -.3163 & -.9597 & -.6194 & -.9597 & -.6194 & -1.0183 & -1.0183 & .0000 \\ .1014 & .1014 & -.0284 & -.0215 & -.0284 & -.0215 & -.0200 & -.0200 & .0000 \\ .0003 & -.0003 & -.0002 & -.0001 & .0002 & .0001 & -.0001 & .0001 & .0006 \\ .0762 & -.0762 & .2219 & .2011 & -.2219 & -.2011 & .1109 & -.1109 & .1144 \\ .0486 & -.0486 & .0029 & .0021 & -.0029 & -.0021 & .0021 & -.0021 & -.0544 \end{bmatrix}$$

$$C = \begin{bmatrix} .0000 & .0000 & 1.0000 & .0349 & .0000 & .0000 & .0000 & .0000 \\ .0000 & .0000 & .0000 & .0000 & .0000 & 1.0000 & .0000 & .0000 \\ 1.0000 & .0000 & .0000 & .0000 & .0000 & .0000 & .0000 & .0000 \\ .0000 & 1.0000 & .0000 & .0000 & .0000 & .0000 & .0000 & .0000 \\ .0000 & .0000 & .0000 & .0000 & .0000 & .0000 & .0000 & 1.0000 \end{bmatrix}$$

B Matrix for Five Control Surfaces

$$B = \begin{bmatrix} .0000 & .0000 & .0000 & .0000 & .0000 \\ .0000 & .0000 & .0000 & .0000 & .0000 \\ .0411 & .0411 & .3206 & .3206 & .0000 \\ -.3163 & -.3163 & -2.5974 & -2.5974 & .0000 \\ .1014 & .1014 & -.0699 & -.0699 & .0000 \\ .0003 & -.0003 & -.0004 & .0004 & .0006 \\ .0762 & -.0762 & .5339 & -.5339 & .1144 \\ .0486 & -.0486 & .0071 & -.0071 & -.0544 \end{bmatrix}$$

$$x = \begin{bmatrix} \theta & \phi & u & w & q & \beta & p & r \end{bmatrix}^T \quad (A.1)$$

$$u = \begin{bmatrix} \delta_{cl} & \delta_{cr} & \delta_{tel} & \delta_{ter} & \delta_{rud} \end{bmatrix}^T \quad (A.2)$$

Table A.2. ACM Entry Matrices - 30% Loss Of Effectiveness Left Trailing Edge

$$A = \begin{bmatrix} .0000 & .0000 & .0000 & .0000 & 1.0000 & .0000 & .0000 & .0000 \\ .0000 & .0000 & .0000 & .0000 & .0000 & .0000 & 1.0000 & .0450 \\ -32.1420 & .0000 & -.0050 & .0550 & -39.9760 & .0000 & .0000 & .0000 \\ -1.4370 & .0000 & -.0240 & -1.0280 & 894.1070 & .0000 & .0000 & .0000 \\ .0000 & .0000 & .0000 & .0070 & -.6920 & .0000 & .0000 & .0000 \\ .0000 & .0360 & .0000 & .0000 & .0000 & -.0990 & .0450 & -.9990 \\ .0000 & .0000 & .0000 & .0000 & .0000 & -31.8340 & -2.1380 & .5160 \\ .0000 & .0000 & .0000 & .0000 & .0000 & 2.6670 & -.0310 & -.4420 \end{bmatrix}$$

$$B = \begin{bmatrix} .0000 & .0000 & .0000 & .0000 & .0000 & .0000 & .0000 & .0000 & .0000 \\ .0000 & .0000 & .0000 & .0000 & .0000 & .0000 & .0000 & .0000 & .0000 \\ .0520 & .0520 & .0000 & .0780 & .1040 & .0670 & .0930 & .0800 & .0000 \\ -.3300 & -.3300 & .0000 & -.6220 & -.9650 & -.6220 & -.7350 & -.7350 & .0000 \\ .1020 & .1020 & .0000 & -.0210 & -.0280 & -.0210 & -.0200 & -.0200 & .0000 \\ .0000 & .0000 & .0000 & .0000 & .0000 & .0000 & .0000 & .0000 & .0010 \\ .0800 & -.0760 & .0000 & .2010 & -.2220 & -.2010 & .1110 & -.1110 & .1150 \\ .0490 & -.0480 & .0000 & .0030 & -.0040 & -.0030 & .0030 & -.0030 & -.0550 \end{bmatrix}$$

$$C = \begin{bmatrix} .0000 & .0000 & 1.0000 & .0410 & .0000 & .0000 & .0000 & .0000 \\ .0000 & .0000 & .0000 & .0000 & .0000 & 1.0000 & .0000 & .0000 \\ 1.0000 & .0000 & .0000 & .0000 & .0000 & .0000 & .0000 & .0000 \\ .0000 & 1.0000 & .0000 & .0000 & .0000 & .0000 & .0000 & .0000 \\ .0000 & .0000 & .0000 & .0000 & .0000 & .0000 & .0000 & 1.0000 \end{bmatrix}$$

B Matrix for Five Control Surfaces

$$B = \begin{bmatrix} .0000 & .0000 & .0000 & .0000 & .0000 \\ .0000 & .0000 & .0000 & .0000 & .0000 \\ .0520 & .0520 & .1710 & .2510 & .0000 \\ -.3303 & -.3300 & -1.3570 & -2.3220 & .0000 \\ .1020 & .1020 & -.0410 & -.0690 & .0000 \\ .0000 & .0000 & .0000 & .0000 & .0010 \\ .0800 & -.0760 & .3120 & -.5340 & .1150 \\ .0490 & -.0480 & .0060 & -.0100 & -.0550 \end{bmatrix}$$

$$x = \begin{bmatrix} \theta & \phi & u & w & q & \beta & p & r \end{bmatrix}^T \quad (A.3)$$

$$u = \begin{bmatrix} \delta_{cl} & \delta_{cr} & \delta_{tel} & \delta_{ter} & \delta_{rud} \end{bmatrix}^T \quad (A.4)$$

Table A.3. ACM Entry Matrices - 50% Loss Of Effectiveness Left Canard

$$A = \begin{bmatrix} .0000 & .0000 & .0000 & .0000 & 1.0000 & .0000 & .0000 & .0000 \\ .0000 & .0000 & .0000 & .0000 & .0000 & .0000 & 1.0000 & .0390 \\ -32.1500 & .0000 & -.0080 & .0580 & -36.6690 & .0000 & .0000 & .0000 \\ -1.2460 & .0000 & -.0290 & -1.0450 & 894.3280 & .0000 & .0000 & .0000 \\ .0000 & .0000 & .0000 & .0040 & -.6460 & .0000 & .0000 & .0000 \\ .0000 & .0360 & .0000 & .0000 & .0000 & -.0820 & .0390 & -.9990 \\ .0000 & .0000 & .0000 & .0000 & .0000 & -23.8380 & -2.0700 & .4990 \\ .0000 & .0000 & .0000 & .0000 & .0000 & 2.4580 & -.0270 & -.4520 \end{bmatrix}$$

$$B = \begin{bmatrix} .0000 & .0000 & .0000 & .0000 & .0000 & .0000 & .0000 & .0000 & .0000 \\ .0000 & .0000 & .0000 & .0000 & .0000 & .0000 & .0000 & .0000 & .0000 \\ -.1560 & -.1150 & .1320 & .0840 & .1320 & .0840 & .1000 & .1000 & .0000 \\ -.1150 & -.2250 & -.9610 & -.6210 & -.9610 & -.6210 & -.7320 & -.7320 & .0000 \\ .0360 & .0720 & -.0280 & -.0220 & -.0280 & -.0220 & -.0200 & -.0200 & .0000 \\ .0000 & -.0010 & .0000 & .0000 & .0000 & .0000 & .0000 & .0000 & .0010 \\ .0350 & -.0690 & .2220 & .2010 & -.2220 & -.2010 & .1110 & -.1110 & .1140 \\ .0240 & -.0490 & .0030 & .0030 & -.0030 & -.0030 & .0020 & -.0020 & -.0550 \end{bmatrix}$$

$$C = \begin{bmatrix} .0000 & .0000 & 1.0000 & .0349 & .0000 & .0000 & .0000 & .0000 \\ .0000 & .0000 & .0000 & .0000 & .0000 & 1.0000 & .0000 & .0000 \\ 1.0000 & .0000 & .0000 & .0000 & .0000 & .0000 & .0000 & .0000 \\ .0000 & 1.0000 & .0000 & .0000 & .0000 & .0000 & .0000 & .0000 \\ .0000 & .0000 & .0000 & .0000 & .0000 & .0000 & .0000 & 1.0000 \end{bmatrix}$$

B Matrix for Five Control Surfaces

$$B = \begin{bmatrix} .0000 & .0000 & .0000 & .0000 & .0000 \\ .0000 & .0000 & .0000 & .0000 & .0000 \\ -.1560 & -.1150 & .3160 & .3160 & .0000 \\ -.1150 & -.2250 & -2.3140 & -2.3140 & .0000 \\ .0360 & .0720 & -.0700 & -.0700 & .0000 \\ .0000 & -.0010 & .0000 & .0000 & .0010 \\ .0350 & -.0690 & .5340 & -.5340 & .1140 \\ .0240 & -.0490 & .0080 & -.0080 & -.0550 \end{bmatrix}$$

$$x = \begin{bmatrix} \theta & \phi & u & w & q & \beta & p & r \end{bmatrix}^T \quad (A.5)$$

$$u = \begin{bmatrix} \delta_{cl} & \delta_{cr} & \delta_{tel} & \delta_{ter} & \delta_{rud} \end{bmatrix}^T \quad (A.6)$$

Table A.4. ACM Entry Matrices - 25% Loss Of Effectiveness Rudder

$$A = \begin{bmatrix} .0000 & .0000 & .0000 & .0000 & 1.0000 & .0000 & .0000 & .0000 \\ .0000 & .0000 & .0000 & .0000 & .0000 & .0000 & 1.0000 & .0350 \\ -32.1540 & .0000 & -.0080 & .0540 & -31.5470 & .0000 & .0000 & .0000 \\ -1.1349 & .0000 & -.0320 & -1.0580 & 894.4400 & .0000 & .0000 & .0000 \\ .0000 & .0000 & .0000 & .0070 & -.6740 & .0000 & .0000 & .0000 \\ .0000 & .0360 & .0000 & .0000 & .0000 & -.0920 & .0350 & -.9990 \\ .0000 & .0000 & .0000 & .0000 & .0000 & -27.8550 & -2.0330 & .4600 \\ .0000 & .0000 & .0000 & .0000 & .0000 & 2.0520 & -.0270 & -.4190 \end{bmatrix}$$

$$B = \begin{bmatrix} .0000 & .0000 & .0000 & .0000 & .0000 & .0000 & .0000 & .0000 & .0000 \\ .0000 & .0000 & .0000 & .0000 & .0000 & .0000 & .0000 & .0000 & .0000 \\ .0410 & .0410 & .1320 & .0870 & .1320 & .0870 & .1020 & .1020 & .0000 \\ -.3170 & -.3170 & -.9600 & -.6200 & -.9600 & -.6200 & -.7330 & -.7330 & .0000 \\ .1020 & .1020 & -.0280 & -.0220 & -.0280 & -.0220 & -.0200 & -.0200 & .0000 \\ .0000 & .0000 & .0000 & .0000 & .0000 & .0000 & .0000 & .0000 & .0000 \\ .0760 & -.0760 & .2220 & .2010 & -.2220 & -.2010 & .1110 & -.1110 & .0870 \\ .0000 & .0000 & .0000 & .0000 & .0000 & .0000 & -2.0520 & .0270 & .4190 \end{bmatrix}$$

$$C = \begin{bmatrix} .0000 & .0000 & 1.0000 & .0349 & .0000 & .0000 & .0000 & .0000 \\ .0000 & .0000 & .0000 & .0000 & .0000 & 1.0000 & .0000 & .0000 \\ 1.0000 & .0000 & .0000 & .0000 & .0000 & .0000 & .0000 & .0000 \\ .0000 & 1.0000 & .0000 & .0000 & .0000 & .0000 & .0000 & .0000 \\ .0000 & .0000 & .0000 & .0000 & .0000 & .0000 & .0000 & 1.0000 \end{bmatrix}$$

B Matrix for Five Control Surfaces

$$B = \begin{bmatrix} .0000 & .0000 & .0000 & .0000 & .0000 \\ .0000 & .0000 & .0000 & .0000 & .0000 \\ .0410 & .0410 & .3210 & .3210 & .0000 \\ -.3170 & -.3170 & -2.3130 & -2.3130 & .0000 \\ .1020 & .1020 & -.0700 & -.0700 & .0000 \\ .0000 & .0000 & .0000 & .0000 & .0000 \\ .0760 & -.0760 & .5340 & -.5340 & .0870 \\ .0000 & .0000 & -2.0520 & .0270 & .4190 \end{bmatrix}$$

$$x = \begin{bmatrix} \theta & \phi & u & w & q & \beta & p & r \end{bmatrix}^T \quad (A.7)$$

$$u = \begin{bmatrix} \delta_{cl} & \delta_{cr} & \delta_{tel} & \delta_{ter} & \delta_{rud} \end{bmatrix}^T \quad (A.8)$$

Table A.5. ACM Exit Matrices - No Failures

$$A = \begin{bmatrix} .0000 & .0000 & .0000 & .0000 & 1.0000 & .0000 & .0000 & .0000 \\ .0000 & .0000 & .0000 & .0000 & .0000 & .0000 & 1.0000 & .5184 \\ -28.5877 & .0000 & -.2762 & -.0283 & -136.2190 & .0000 & .0000 & .0000 \\ -4.9465 & 26.9479 & .1330 & -.6753 & 262.7934 & .0000 & .0000 & .0000 \\ .0000 & .0000 & -.0018 & .0035 & -.6511 & .0000 & .0000 & .0000 \\ .0472 & .0322 & .0000 & .0000 & .0000 & -.0245 & .4602 & -.8878 \\ .0000 & .0000 & .0000 & .0000 & .0000 & -7.7280 & -1.4530 & .9687 \\ .0000 & .0000 & .0000 & .0000 & .0000 & -.0889 & -.0543 & .0456 \end{bmatrix}$$

$$B = \begin{bmatrix} .0000 & .0000 & .0000 & .0000 & .0000 & .0000 & .0000 & .0000 & .0000 \\ .0000 & .0000 & .0000 & .0000 & .0000 & .0000 & .0000 & .0000 & .0000 \\ -.0253 & -.0281 & .0206 & .0131 & .0206 & .0131 & .0154 & .0154 & .0000 \\ -.1512 & -.1471 & -.1302 & -.0848 & -.1302 & -.0848 & -.0997 & -.0997 & .0000 \\ .0161 & -.0156 & -.0024 & -.0018 & -.0024 & -.0018 & -.0016 & -.0016 & .0000 \\ .0007 & -.0007 & -.0001 & -.0001 & .0001 & .0001 & -.0001 & .0001 & .0004 \\ .0113 & -.0337 & .0270 & .0240 & -.0270 & -.0240 & .0135 & -.0135 & .0277 \\ .0133 & -.0121 & -.0005 & -.0004 & .0005 & .0004 & -.0004 & .0004 & -.0130 \end{bmatrix}$$

$$C = \begin{bmatrix} .0000 & .0000 & 1.0000 & .4600 & .0000 & .0000 & .0000 & .0000 \\ .0000 & .0000 & .0000 & .0000 & .0000 & 1.0000 & .0000 & .0000 \\ 1.0000 & .0000 & .0000 & .0000 & .0000 & .0000 & .0000 & .0000 \\ .0000 & 1.0000 & .0000 & .0000 & .0000 & .0000 & .0000 & .0000 \\ .0000 & .0000 & .0000 & .0000 & .0000 & .0000 & .0000 & 1.0000 \end{bmatrix}$$

B Matrix for Five Control Surfaces

$$B = \begin{bmatrix} .0000 & .0000 & .0000 & .0000 & .0000 \\ .0000 & .0000 & .0000 & .0000 & .0000 \\ -.0253 & -.0281 & .0491 & .0491 & .0000 \\ -.1512 & -.1471 & -.3147 & -.3147 & .0000 \\ .0161 & .0156 & -.0058 & -.0058 & .0000 \\ .0007 & -.0007 & -.0003 & .0003 & .0004 \\ .0113 & -.0337 & .0645 & -.0645 & .0277 \\ .0133 & -.0121 & -.0013 & .0013 & -.0130 \end{bmatrix}$$

$$x = \begin{bmatrix} \theta & \phi & u & w & q & \beta & p & r \end{bmatrix}^T \quad (A.9)$$

$$u = \begin{bmatrix} \delta_{cl} & \delta_{cr} & \delta_{tel} & \delta_{ter} & \delta_{rud} \end{bmatrix}^T \quad (A.10)$$

Table A.6. TF/TA Matrices - No Failures

$$A = \begin{bmatrix} .0000 & .0000 & .0000 & .0000 & 1.0000 & .0000 & .0000 & .0000 \\ .0000 & .0000 & .0000 & .0000 & .0000 & .0000 & 1.0000 & .0153 \\ -32.1961 & .0000 & -.0355 & .0357 & -15.6105 & .0000 & .0000 & .0000 \\ -.5002 & .0000 & -.0071 & -3.2056 & 1004.8788 & .0000 & .0000 & .0000 \\ .0000 & .0000 & -.0003 & .0202 & -1.6773 & .0000 & .0000 & .0000 \\ .0000 & .0320 & .0000 & .0000 & .0000 & -.2538 & .0155 & -.9999 \\ .0000 & .0000 & .0000 & .0000 & .0000 & -66.9300 & -5.4612 & 1.0349 \\ .0000 & .0000 & .0000 & .0000 & .0000 & 8.2821 & -.0299 & -1.2709 \end{bmatrix}$$

$$B = \begin{bmatrix} .0000 & .0000 & .0000 & .0000 & .0000 & .0000 & .0000 & .0000 & .0000 \\ .0000 & .0000 & .0000 & .0000 & .0000 & .0000 & .0000 & .0000 & .0000 \\ -.3284 & -.3284 & .2548 & .1679 & .2548 & .1679 & .1975 & .1975 & .0000 \\ -.6788 & -.6788 & -1.7517 & -1.1313 & -1.7517 & -1.1313 & -1.3351 & -1.3351 & .0000 \\ .2387 & .2387 & -.0534 & -.0406 & -.0534 & -.0406 & -.0372 & -.0372 & .0000 \\ .0012 & -.0012 & -.0001 & -.0001 & .0001 & .0001 & -.0001 & .0003 & .0018 \\ .2336 & -.2336 & .4200 & .3737 & -.4200 & -.3737 & .2100 & -.2100 & .3737 \\ .1590 & -.1590 & .0024 & .0012 & -.0024 & -.0012 & -.0012 & -.0012 & -.1795 \end{bmatrix}$$

$$C = \begin{bmatrix} .0000 & .0000 & 1.0000 & .0138 & .0000 & .0000 & .0000 & .0000 \\ .0000 & .0000 & .0000 & .0000 & .0000 & 1.0000 & .0000 & .0000 \\ 1.0000 & .0000 & .0000 & .0000 & .0000 & .0000 & .0000 & .0000 \\ .0000 & 1.0000 & .0000 & .0000 & .0000 & .0000 & .0000 & .0000 \\ .0000 & .0000 & .0000 & .0000 & .0000 & .0000 & .0000 & 1.0000 \end{bmatrix}$$

B Matrix for Five Control Surfaces

$$B = \begin{bmatrix} .0000 & .0000 & .0000 & .0000 & .0000 \\ .0000 & .0000 & .0000 & .0000 & .0000 \\ -.3284 & -.3284 & .6202 & .6202 & .0000 \\ -.6788 & -.6788 & -4.2181 & -4.2181 & .0000 \\ .2387 & .2387 & -.1312 & -.1312 & .0000 \\ .0012 & -.0012 & -.0003 & .0005 & .0018 \\ .2336 & -.2336 & 1.0037 & -1.0037 & .3737 \\ .1590 & -.1590 & .0048 & -.0048 & -.1795 \end{bmatrix}$$

$$x = \begin{bmatrix} \theta & \phi & u & w & q & \beta & p & r \end{bmatrix}^T \quad (A.11)$$

$$u = \begin{bmatrix} \delta_{cl} & \delta_{cr} & \delta_{tel} & \delta_{ter} & \delta_{rud} \end{bmatrix}^T \quad (A.12)$$

Table A.7. TF/TA Matrices - 30% Loss of Effectiveness Left Trailing Edge

$$A = \begin{bmatrix} .0000 & .0000 & .0000 & .0000 & 1.0000 & .0000 & .0000 & .0000 \\ .0000 & .0000 & .0000 & .0000 & .0000 & .0000 & 1.0000 & .0160 \\ -32.1704 & .0000 & -.0330 & -.0200 & -15.2961 & .0000 & .0000 & .0000 \\ -.5110 & .0000 & -.0080 & -3.0620 & 1004.8730 & .0000 & .0000 & .0000 \\ .0000 & .0000 & .0000 & .0210 & -1.8240 & .0000 & .0000 & .0000 \\ .0000 & .0320 & .0000 & .0000 & .0000 & -.2460 & .0160 & -1.0000 \\ .0000 & .0000 & .0000 & .0000 & .0000 & -65.9740 & -5.4310 & 1.2860 \\ .0000 & .0000 & .0000 & .0000 & .0000 & 8.1650 & -.0340 & -1.2630 \end{bmatrix}$$

$$B = \begin{bmatrix} .0000 & .0000 & .0000 & .0000 & .0000 & .0000 & .0000 & .0000 & .0000 \\ .0000 & .0000 & .0000 & .0000 & .0000 & .0000 & .0000 & .0000 & .0000 \\ -.3450 & -.3450 & .0930 & .1580 & .2520 & .1580 & .1340 & .1940 & .0000 \\ -.6760 & -.6760 & .0000 & -1.1140 & -1.7250 & -1.1140 & -1.3160 & -1.3160 & .0000 \\ .2360 & .2360 & .0000 & -.0400 & -.0520 & -.0400 & -.0360 & -.0360 & .0000 \\ .0010 & -.0010 & .0000 & .0000 & .0000 & .0000 & .0000 & .0000 & .0020 \\ .2300 & -.2300 & .0000 & .3680 & -.4150 & -.3680 & .2070 & -.2070 & .3800 \\ .1570 & -.1570 & .0000 & .0010 & -.0020 & -.0010 & .0010 & -.0010 & -.1770 \end{bmatrix}$$

$$C = \begin{bmatrix} .0000 & .0000 & 1.0000 & .0160 & .0000 & .0000 & .0000 & .0000 \\ .0000 & .0000 & .0000 & .0000 & .0000 & 1.0000 & .0000 & .0000 \\ 1.0000 & .0000 & .0000 & .0000 & .0000 & .0000 & .0000 & .0000 \\ .0000 & 1.0000 & .0000 & .0000 & .0000 & .0000 & .0000 & .0000 \\ .0000 & .0000 & .0000 & .0000 & .0000 & .0000 & .0000 & 1.0000 \end{bmatrix}$$

B Matrix for Five Control Surfaces

$$B = \begin{bmatrix} .0000 & .0000 & .0000 & .0000 & .0000 \\ .0000 & .0000 & .0000 & .0000 & .0000 \\ -.3450 & -.3450 & .4450 & .6042 & .0000 \\ -.6760 & -.6760 & -2.4300 & -4.1550 & .0000 \\ .2360 & .2360 & -.0760 & -.1280 & .0000 \\ .0010 & -.0010 & .0000 & .0000 & .0020 \\ .2300 & -.2300 & .5750 & .9900 & .3800 \\ .1570 & -.1570 & .0020 & -.0040 & -.1770 \end{bmatrix}$$

$$x = \begin{bmatrix} \theta & \phi & u & w & q & \beta & p & r \end{bmatrix}^T \quad (A.13)$$

$$u = \begin{bmatrix} \delta_{cl} & \delta_{cr} & \delta_{tel} & \delta_{ter} & \delta_{rud} \end{bmatrix}^T \quad (A.14)$$

Table A.8. TF/TA Matrices - 50% Loss of Effectiveness Left Canard

$$A = \begin{bmatrix} .0000 & .0000 & .0000 & .0000 & 1.0000 & .0000 & .0000 & .0000 \\ .0000 & .0000 & .0000 & .0000 & .0000 & .0000 & 1.0000 & .0110 \\ -32.1720 & .0000 & -.0380 & -.0290 & -11.0560 & .0000 & .0000 & .0000 \\ -.3540 & .0000 & -.0160 & -3.6430 & 1005.4390 & .0000 & .0000 & .0000 \\ .0000 & .0000 & .0000 & .0140 & -2.1070 & .0000 & .0000 & .0000 \\ .0000 & .0320 & .0000 & .0000 & .0000 & -.2780 & .0110 & -1.0000 \\ .0000 & .0000 & .0000 & .0000 & .0000 & -77.1970 & -6.1840 & 1.4760 \\ .0000 & .0000 & .0000 & .0000 & .0000 & 8.7570 & -.0290 & -1.4650 \end{bmatrix}$$

$$B = \begin{bmatrix} .0000 & .0000 & .0000 & .0000 & .0000 & .0000 & .0000 & .0000 & .0000 \\ .0000 & .0000 & .0000 & .0000 & .0000 & .0000 & .0000 & .0000 & .0000 \\ -.5220 & -.3790 & .2940 & .1930 & .2940 & .1930 & .2270 & .2270 & .0000 \\ -.3950 & -.7740 & -2.0190 & -1.3040 & -2.0190 & -1.3040 & -1.5390 & -1.5390 & .0000 \\ .1390 & .2750 & -.0610 & -.0470 & -.0610 & -.0470 & -.0430 & -.0430 & .0000 \\ .0010 & -.0020 & .0000 & .0000 & .0000 & .0000 & .0000 & .0000 & .0018 \\ .1210 & -.2830 & .4850 & .4310 & -.4850 & -.4310 & .2430 & -.2430 & .4310 \\ .0920 & -.1820 & .0010 & .0010 & -.0010 & -.0010 & .0010 & -.0010 & -.2070 \end{bmatrix}$$

$$C = \begin{bmatrix} .0000 & .0000 & 1.0000 & .0110 & .0000 & .0000 & .0000 & .0000 \\ .0000 & .0000 & .0000 & .0000 & .0000 & 1.0000 & .0000 & .0000 \\ 1.0000 & .0000 & .0000 & .0000 & .0000 & .0000 & .0000 & .0000 \\ .0000 & 1.0000 & .0000 & .0000 & .0000 & .0000 & .0000 & .0000 \\ .0000 & .0000 & .0000 & .0000 & .0000 & .0000 & .0000 & 1.0000 \end{bmatrix}$$

B Matrix for Five Control Surfaces

$$B = \begin{bmatrix} .0000 & .0000 & .0000 & .0000 & .0000 \\ .0000 & .0000 & .0000 & .0000 & .0000 \\ -.5220 & -.3790 & .7140 & .7140 & .0000 \\ -.3950 & -.7740 & -4.8620 & -4.8620 & .0000 \\ .1390 & .2750 & -.1510 & -.1510 & .0000 \\ .0010 & -.0020 & .0000 & .0000 & .0020 \\ .1210 & -.2830 & 1.1590 & -1.1590 & .4310 \\ .0920 & -.1820 & .0030 & -.0030 & -.2070 \end{bmatrix}$$

$$x = \begin{bmatrix} \theta & \phi & u & w & q & \beta & p & r \end{bmatrix}^T \quad (A.15)$$

$$u = \begin{bmatrix} \delta_{cl} & \delta_{cr} & \delta_{tel} & \delta_{ter} & \delta_{rud} \end{bmatrix}^T \quad (A.16)$$



Table A.9. TF/TA Matrices - 25% Loss of Effectiveness Rudder

$$A = \begin{bmatrix} .0000 & .0000 & .0000 & .0000 & 1.0000 & .0000 & .0000 & .0000 \\ .0000 & .0000 & .0000 & .0000 & .0000 & .0000 & 1.0000 & .0140 \\ -32.1710 & .0000 & -.0340 & .0050 & -13.8570 & .0000 & .0000 & .0000 \\ -4440 & .0000 & -.0140 & -3.1400 & 1004.9000 & .0000 & .0000 & .0000 \\ .0000 & .0000 & .0000 & -.0200 & -1.8190 & .0000 & .0000 & .0000 \\ .0000 & .0320 & .0000 & .0000 & .0000 & -.2300 & .0140 & -1.0000 \\ .0000 & .0000 & .0000 & .0000 & .0000 & -65.9740 & -5.3590 & -1.1910 \\ .0000 & .0000 & .0000 & .0000 & .0000 & 6.1230 & -.0390 & -1.2160 \end{bmatrix}$$

$$B = \begin{bmatrix} .0000 & .0000 & .0000 & .0000 & .0000 & .0000 & .0000 & .0000 & .0000 \\ .0000 & .0000 & .0000 & .0000 & .0000 & .0000 & .0000 & .0000 & .0000 \\ -.3240 & -.3240 & .2520 & .1650 & .2520 & .1650 & .1940 & .1940 & .0000 \\ -.6690 & -.6690 & -1.7250 & -1.1140 & -1.7250 & -1.1140 & -1.3160 & -1.3160 & .0000 \\ .2350 & .2350 & -.0520 & -.0400 & -.0520 & -.0400 & -.0360 & -.0360 & .0000 \\ .0010 & -.0010 & .0000 & .0000 & .0000 & .0000 & .0000 & .0000 & .0010 \\ .2300 & -.2300 & .4150 & .3680 & -.4150 & -.3680 & .2070 & -.2070 & .2760 \\ .0000 & .0000 & .0000 & .0000 & .0000 & .0000 & -6.1230 & .0390 & 1.2160 \end{bmatrix}$$

$$C = \begin{bmatrix} .0000 & .0000 & 1.0000 & .0138 & .0000 & .0000 & .0000 & .0000 & .0000 \\ .0000 & .0000 & .0000 & .0000 & .0000 & 1.0000 & .0000 & .0000 & .0000 \\ 1.0000 & .0000 & .0000 & .0000 & .0000 & .0000 & .0000 & .0000 & .0000 \\ .0000 & 1.0000 & .0000 & .0000 & .0000 & .0000 & .0000 & .0000 & .0000 \\ .0000 & .0000 & .0000 & .0000 & .0000 & .0000 & .0000 & .0000 & 1.0000 \end{bmatrix}$$

B Matrix for Five Control Surfaces

$$B = \begin{bmatrix} .0000 & .0000 & .0000 & .0000 & .0000 \\ .0000 & .0000 & .0000 & .0000 & .0000 \\ -.3240 & -.3240 & .6110 & .6110 & .0000 \\ -.6690 & -.6690 & -4.1550 & -4.1550 & .0000 \\ .2350 & .2350 & -.1280 & -.1280 & .0000 \\ .0010 & -.0010 & .0000 & .0000 & .0010 \\ .2300 & -.2300 & .9900 & -.9900 & .2760 \\ .0000 & .0000 & -6.1230 & .0390 & 1.2160 \end{bmatrix}$$

$$x = \begin{bmatrix} \theta & \phi & u & w & q & \beta & p & r \end{bmatrix}^T \quad (A.17)$$

$$u = \begin{bmatrix} \delta_{cv} & \delta_{cr} & \delta_{tel} & \delta_{ter} & \delta_{rud} \end{bmatrix}^T \quad (A.18)$$

## Appendix B. ARMA MODEL GENERATION

### B.1 INTRODUCTION

This appendix contains a summary of the ARMA model conversion technique developed by Bokor and Keviczky and the MATRIX<sub>r</sub> macro used to accomplish this transformation for all the plant matrices (1, 11). Detailed mathematical development of the procedure is contained in reference (1).

### B.2 ARMA MODEL

The method used to generate the ARMA model representation from a state-space model representation is based upon using constructibility invariants. This method eliminates some of the problems associated with the observability matrix technique when the state transition matrix is singular. Recall that the state-space representation of the continuous time system is expressed by

$$\dot{x} = Ax(t) + Bu(t) \quad \text{B.1}$$

$$y(t) = Cx(t) \quad \text{B.2}$$

where

$A$  = the continuous time plant matrix ( $n \times n$ )

$B$  = the continuous time control matrix ( $n \times m$ ) with the rank of  $B = m$

$C$  = the continuous time output matrix ( $l \times n$ )

$x$  = the state variable vector with  $n$  states

$u$  = the control input vector with  $m$  inputs

$y$  = the output vector with  $l$  outputs

The state-space matrices of Equation B.1 and Equation B.2 are discretized for a given sampling time  $T$  and expressed in the discrete time domain by

$$\dot{x}(T) = Fx(T) + Gu(T) \quad (\text{B.3})$$

$$y(T) = Hx(T) \quad (\text{B.4})$$

where

$F$  = the discrete plant matrix ( $n \times n$ )

$G$  = the discrete control matrix ( $n \times m$ ) with the rank =  $m$

$H$  = the discrete output matrix ( $l \times n$ )

$x$  = the state variable vector with  $n$  states

$u$  = the control input vector with  $m$  inputs

$y$  = the output vector with  $l$  outputs

For this technique, the discrete time representation given in Equations B.3 and B.4 must have no poles at the origin, i.e. the inverse matrix  $F^{-1}$  exists. The constructibility matrix  $C_o$  is defined as

$$C_o = \begin{bmatrix} HF^{-1} \\ HF^{-2} \\ HF^{-3} \\ \vdots \\ HF^{-n} \end{bmatrix} \quad (\text{B.5})$$

and must have rank  $C_o = n$ .

A new matrix,  $TT$ , is formed from the linearly independent rows of  $C_o$  in Equation B.5 (where each block  $HF^{-i}$  is  $l \times n$ ). The first row of the new matrix is the first row of  $C_o$ . The second row of  $T$  is the next linearly independent row of  $C_o$ . The process continues until the matrix  $TT$  has full rank  $n$ .

The transformation matrix  $T$  is formed by rearranging the rows of matrix  $TT$  into the following form

$$T = \left[ \begin{array}{c} h_1 F^{-1} \\ \vdots \\ h_1 F^{-V_1} \\ \hline \vdots \\ h_l F^{-1} \\ \vdots \\ h_l F^{-V_l} \end{array} \right] \quad (\text{B.6})$$

where  $h_i$  is the  $i$ th row of the  $H$  matrix.

For  $1 \leq i \leq l$ , the  $i$ th constructibility index  $V_i$  is defined as the smallest positive integer such that  $h_i F^{-V_i-1}$  is a linear combination of the rows before it. Then the constructibility indices satisfy the relation

$$V_1 + V_2 + \dots + V_l = n \quad (\text{B.7})$$

and are arranged in descending order

$$V_1 \geq V_2 \geq V_3 > \dots V_l \quad (\text{B.8})$$

If Equation B.8 is *not* satisfied, permute the output matrix,  $H$ , to satisfy the relationship of the constructibility indices.

Then the following matrices are defined:

$$R = T^{-1} \quad (\text{B.9})$$

$$\bar{H} = HR \quad (\text{B.10})$$

$$\bar{F} = R^{-1}FR \quad (\text{B.11})$$

$$\bar{G} = R^{-1}G \quad (\text{B.12})$$

A reduced order ARMA model is used where, instead of having  $n$  coefficients, only  $N = n/m$  (rounded to the largest integer) are needed. The  $A_i$  coefficients of the ARMA model are calculated from the relationship

$$A_i = -\bar{H} S_{p_i}(k-i) \quad (\text{B.13})$$

where  $i = 1, \dots, N$ ,  $(k-i)$  is a delay operator, and

$$S_{p_i}(k) = \begin{bmatrix} (k-1) & 0 & \dots & 0 \\ (k-2) & 0 & \dots & 0 \\ \vdots & \vdots & \dots & \vdots \\ (k-V_1) & 0 & \dots & 0 \\ 0 & (k-1) & \dots & 0 \\ 0 & (k-2) & \dots & 0 \\ \vdots & \vdots & \dots & \vdots \\ 0 & (k-V_2) & \dots & 0 \\ 0 & 0 & \dots & (k-1) \\ 0 & 0 & \dots & (k-2) \\ \vdots & \vdots & \dots & \vdots \\ 0 & 0 & \dots & (k-V_l) \end{bmatrix} \in R^{n \times l} \quad (\text{B.14})$$

As an example, to find the  $A_1$  coefficients using Equation B.13 and Equation B.14, the  $S_{p_i}(k)$  matrix elements associated with the  $(k-1)$  terms in Equation B.14 would be set equal to 1 and all other matrix elements equal to zero. The  $A_2$  coefficients would require  $S_{p_i}(k)$  matrix elements associated with the  $(k-2)$  terms in Equation B.14 be set equal to 1 and all other matrix elements equal to zero, etc.

The  $B_i$  coefficients of the ARMA model are calculated from the relationship

$$B_i = \bar{H} S_{q_i}(k-i) \bar{G} \quad (\text{B.15})$$

where,

$$S_{q_i} = \sum_{i=1}^N S^{i-1} \quad (\text{B.16})$$

where

$$S = \text{block diagonal } [S_1, S_j, \dots, S_l] \quad (\text{B.17})$$

and  $S_j$  is the block-diagonal Toeplitz matrix given by

$$S_j = \begin{bmatrix} 0 & \dots & 0 \\ 1 & \dots & \vdots \\ 0 & 1 & 0 \end{bmatrix} \in R^{V_j \times V_j} \quad (\text{B.18})$$

for  $j = 1, \dots, l$

### B.3 ARMA IMPLEMENTATION

The implementation of the theory presented in the previous section is executed in MATRIX<sub>X</sub> using a modification of a macro developed by Velez in his thesis (11). For this design,

$$V_1 = 2$$

$$V_2 = 2$$

$$V_3 = 2$$

$$V_4 = 1$$

$$V_5 = 1$$

$$S_{p_1} = \begin{bmatrix} 1 & 0 & 0 & 0 & 0 & 0 \\ 0 & 0 & 0 & 0 & 0 & 0 \\ 0 & 1 & 0 & 0 & 0 & 0 \\ 0 & 0 & 0 & 0 & 0 & 0 \\ 0 & 0 & 1 & 0 & 0 & 0 \\ 0 & 0 & 0 & 0 & 0 & 0 \\ 0 & 0 & 0 & 1 & 0 & 0 \\ 0 & 0 & 0 & 0 & 1 & 0 \end{bmatrix} \quad (\text{B.19})$$

$$S_{p_2} = \begin{bmatrix} 0 & 0 & 0 & 0 & 0 & 0 \\ 1 & 0 & 0 & 0 & 0 & 0 \\ 0 & 0 & 0 & 0 & 0 & 0 \\ 0 & 1 & 0 & 0 & 0 & 0 \\ 0 & 0 & 0 & 0 & 0 & 0 \\ 0 & 0 & 1 & 0 & 0 & 0 \\ 0 & 0 & 0 & 0 & 0 & 0 \\ 0 & 0 & 0 & 0 & 0 & 0 \end{bmatrix} \quad (\text{B.20})$$

$$S_{q_1} = \begin{bmatrix} 1 & 0 & 0 & 0 & 0 & 0 & 0 & 0 \\ 0 & 1 & 0 & 0 & 0 & 0 & 0 & 0 \\ 0 & 0 & 1 & 0 & 0 & 0 & 0 & 0 \\ 0 & 0 & 0 & 1 & 0 & 0 & 0 & 0 \\ 0 & 0 & 0 & 0 & 1 & 0 & 0 & 0 \\ 0 & 0 & 0 & 0 & 0 & 1 & 0 & 0 \\ 0 & 0 & 0 & 0 & 0 & 0 & 1 & 0 \\ 0 & 0 & 0 & 0 & 0 & 0 & 0 & 1 \end{bmatrix} = S^0 \quad (\text{B.21})$$

$$S_{q_2} = \begin{bmatrix} 0 & 0 & 0 & 0 & 0 & 0 & 0 & 0 \\ 1 & 0 & 0 & 0 & 0 & 0 & 0 & 0 \\ 0 & 0 & 0 & 0 & 0 & 0 & 0 & 0 \\ 0 & 0 & 1 & 0 & 0 & 0 & 0 & 0 \\ 0 & 0 & 0 & 0 & 0 & 0 & 0 & 0 \\ 0 & 0 & 0 & 0 & 1 & 0 & 0 & 0 \\ 0 & 0 & 0 & 0 & 0 & 0 & 0 & 0 \\ 0 & 0 & 0 & 0 & 0 & 0 & 0 & 0 \end{bmatrix} = S^1 \quad (\text{B.22})$$

*B.3.1 MATRIX<sub>X</sub> ARMA Macro* The following MATRIX<sub>X</sub> macro listing can be directly typed into MATRIX<sub>X</sub> and implemented by using the command "EXEC('filename')".

```
//ENSURE THAT A/C MATRICES FOR DESIRED FLIGHT CONDITION HAVE BEEN
//LOADED IN MATRIXX.
//THIS PROGRAM WAS MODIFIED FROM VELEZ'S AND HAMMOND'S THESES AND IS
//WRITTEN FOR AN 8 STATE PLANT WITH 5 OUTPUTS

N=8;           //DEFINE THE NUMBER OF STATES
L=5;           //INDICATE NUMBER OF OUTPUTS

CDUM=C([1 2 3 4 5],:); //THE C MATRIX FOR THIS MODEL HAS
                        //10 OUTS, 5 OF WHICH ARE COMMANDED
                        //FORM THE S PLANE SYSTEM MATRIX

SDUM=<A,B;CDUM,0*EYE(5)>; //CONTINUOUS SYSTEM MATRIX

SD=DISC(SDUM,N,.025);   //DISCRETIZES THE SYSTEM MATRIX
                        //TSAMP=.025

[F G H D]=SPLIT(SD,N); //SEPARATES DISCRETE MATRICES
```



```

//*****
//FORM CONSTRUCTABILITY MATRIX

J=N-L;                                //J+1 IS THE LARGEST POSSIBLE VALUE
                                        //OF INDEX V1
                                        //THE REMAINING SECTIONS OF THE CODE
                                        //ARE WRITTEN FOR THE UNDER THE
                                        //ASSUMPTION THAT J>0.

CO=<H*INV(F)>;                          //THIS LINE FORMS THE COMPLETE
                                        //CONSTRUCTABILITY MATRIX IF J=0.

FOR I=2:J+1,...                        //ONLY J*L+1 ROWS OF CO ARE NEEDED
    CO=<CO;H*INV(F)**I>;...            //TO SELECT BASIS VECTORS. THIS
END;                                   //FORMS THE REMAINING BLOCKS OF CO

RCO=RANK(CO)                           //MAKE SURE THAT CO HAS RANK N

//*****
//FORM TEMPORARY TRANSFORMATION MATRIX

KEEP=1;                                //TRACKS WHICH ROWS OF CO WHICH GO IN
CR=0;                                  //TEMP INITIALIZES COUNTER
TT=<CO(1,:)>;                          //INITIALIZES TEMPORARY VECTOR 1ST ROW
TEMP=TT;                               //INITIALIZES TEMPORARY VECTOR

                                        //LOOP FOR GENERATING
                                        //TEMPORARY TRANSFORMATION MATRIX
FOR I=2:J*L+1,...                      //LOOK THROUGH THE ROWS OF CO FOR
    TEMP=<TT;CO(I,:)>;...              //THE 1ST N LINEARLY INDEPENDENT ROWS.
    RN=RANK(TEMP);...                 //THIS ENSURES THAT EACH ROW OF THE
    IF RN=I-CR THEN TT=TEMP;...//H MATRIX IS REPRESENTED.
    KEEPERS=<KEEP;I>;...              //"KEEP" LISTS ROWS OF CO WHICH ARE
    KEEP=KEEPERS;...                 //INCLUDED IN "TEMP".
    ELSEIF RN<I-CR THEN TEMP=TT;...
    CR=CR+1;...
END,...
END;

RN                                     //MAKE SURE THAT RANK OF TEMP IS N

```

```

//*****
//CALCULATE INDICES

V=O*ONES(L,1);          //INITIALIZES INDEX MATRIX

FOR I=1:L,...
    K=KEEP(I,1);...
    IF K=I THEN V(I,1)=1;... //ROWS 1-L OF CO MUST BE LINEARLY
    END;...                //INDEPENDENT FOR THE L INDICES TO
    END;                    //EACH EQUAL AT LEAST 1.

FOR I=L+1:N,...          //THIS LOOP IS NOT NEEDED FOR J=0
    K=KEEP(I,1);...      //CASE.
    IF K<(J-1)*L+1 THEN V(K-L,1)=V(K-L,1)+1;...
    ELSEIF K<J*L+1 THEN V(K-(J-1)*L)=V(K-(J-1)*L)+1;...
    END;...

    IF K=J*L+1 THEN V(1,1)=V(1,1)+1;...
    END;...              //PLEASE NOTE THAT ADDITIONAL LOOPS
    END;                  //MUST BE ADDED FOR CASE WHERE J>3
                          //OR SUBTRACTED WHEN J<3.

KEEP                      //ENSURE THAT ALL L INDICES AT LEAST
                          //ARE EQUAL 1, THEIR SUM IS N, AND
V                          //THEY ARRANGED IN DESCENDING ORDER.
                          //OTHERWISE, THE H MATRIX MUST BE
                          //RESTRUCTURED.

//*****

//THE FOLLOWING PORTION OF THIS MACRO WORKS FOR THE 5 INDICES HAVING
//VALUES OF 2,2,2,1,1 RESPECTIVELY. OTHERWISE, THE "T" MATRIX AND
//SP'S AND SQ MAY HAVE A DIFFERENT FORM. REFER TO BOKOR AND
//KEVICZKY ARTICLE FOR SPECIFIC GUIDANCE.

T=<TEMP(1,:);TEMP(6,:);TEMP(2,:);TEMP(7,:);TEMP(3,:);TEMP(8,:);...
    TEMP(4,:);TEMP(5,:)>; //ROWS OF TEMP ARE ARRANGED IN ORDER
                          //OF CALCULATED INDICES

//T=<H(1,:)*F**1;...;H(1,:)*F**V1;|...;|...;|
//                                H(L,:)*F**1;...;H(L,:)*F**VL>

```

```

R=INV(T);
HBAR=H*R;
FBAR=INV(R)*F*R;
GBAR=INV(R)*G;

SQ1=EYE(8);                                //SQ1=S**0

SQ2=<0 0 0 0 0 0 0 0;...                //SQi IS AN NXN BLOCK DIAGONAL MATRIX
    1 0 0 0 0 0 0 0;...                //WITH L ENTRIES DIMENSIONED ViXVi
    0 0 0 0 0 0 0 0;...                //HAVING 1'S ON THE LOWER SUB-
    0 0 1 0 0 0 0 0;...                //DIAGONAL (A VERSION OF A TOEPLITZ
    0 0 0 0 0 0 0 0;...                //MATRIX).  SQi=S**(i-1)
    0 0 0 0 1 0 0 0;...
    0 0 0 0 0 0 0 0;...                //S=BLOCK DIAGONAL{TOEPLITZ(V1XV1),
    0 0 0 0 0 0 0 0>;                // ...,TOEPLITZ(VLXVL)}.

//THE NUMBER OF ARMA COEFFICIENTS NEEDED FOR A REDUCED ORDER MODEL
//IS APPROXIMATELY K=N/L (ROUND UP TO NEXT INTEGER FOR ANY REMAINDER)

//FOR THE N=8 L=5 CASE, 2 ARMA COEFF'S AND 2 SP MATRICES ARE NEEDED.

//FOR THE K=1 CASE

SP1=<1 0 0 0 0;...                        //THE NXL SP MATRICES HAVE THE
    0 0 0 0 0;...                        //SAME FORM.  THE FIRST COLUMN IS
    0 1 0 0 0;...                        //[K-1;...;K-V1;0*(V2,1);...;0*(VL,1)]
    0 0 0 0 0;...                        //THE SECOND COL ENTRIES START ON THE
    0 0 1 0 0;...                        //ROW UNDER THE FIRST COL ENTRIES
    0 0 0 0 0;...                        //[0*(V1,1);K-1,...;K-V2;0*(V3,1);...]
    0 0 0 1 0;...                        //THIS TREND IS CONTINUED FOR ALL L
    0 0 0 0 1>;                        //COLUMNS.

//AND FOR THE K=2 CASE

SP2=<0 0 0 0 0;...                        //THE SP MATRICES HAVE A TIME
    1 0 0 0 0;...                        //SHIFT OPERATOR (K-i).
    0 0 0 0 0;...
    0 1 0 0 0;...
    0 0 0 0 0;...
    0 0 1 0 0;...
    0 0 0 0 0;...
    0 0 0 0 0>;

//NOW ALL THE PRELIMINARY VARIABLES HAVE BEEN DETERMINED AND
//CALCULATION OF THE ARMA COEFFICIENTS CAN PROCEED.

```

```
B1ARMA=HBAR*SQ1*GBAR;           //B1 COEFFICIENT
B2ARMA=HBAR*SQ2*GBAR;           //B2 COEFFICIENT

A1ARMA=-HBAR*SP1;                //A1 COEFFICIENT
A2ARMA=-HBAR*SP2;                //A2 COEFFICIENT

GO=INV(EYE(5)+A1ARMA+A2ARMA)*(B1ARMA+B2ARMA);

CLEAR CDUM SDUM
```

## B.4 AUTO REGRESSIVE MOVING AVERAGE MODELS

Table B.1. ACM Entry ARMA Model - No Failures

$$\begin{aligned}
 A_1 &= \begin{bmatrix} -1.9766D - 00 & 0.0000D - 00 & 2.0200D - 00 & 0.0000D - 00 & 0.0000D - 00 \\ 0.0000D - 00 & -1.9877D - 00 & 0.0000D - 00 & -7.0718D - 06 & -8.7077D - 05 \\ 3.0638D - 03 & 0.0000D - 00 & -1.9857D - 00 & 0.0000D - 00 & 0.0000D - 00 \\ 0.0000D - 00 & -27.8260D - 00 & 0.0000D - 00 & -9.7496D - 01 & -7.0019D - 01 \\ 0.0000D - 00 & 5.7549D - 01 & 0.0000D - 00 & -6.0038D - 04 & -9.7326D - 01 \end{bmatrix} \\
 A_2 &= \begin{bmatrix} 9.7666D - 01 & 0.0000D - 00 & -2.0015D - 00 & 0.0000D - 00 & 0.0000D - 00 \\ 0.0000D - 00 & 9.8983D - 01 & 0.0000D - 00 & 0.0000D - 00 & 0.0000D - 00 \\ -3.0627D - 03 & 0.0000D - 00 & 9.8814D - 01 & 0.0000D - 00 & 0.0000D - 00 \\ 0.0000D - 00 & 27.7994D - 00 & 0.0000D - 00 & 0.0000D - 00 & 0.0000D - 00 \\ 0.0000D - 00 & -6.3593D - 01 & 0.0000D - 00 & 0.0000D - 00 & 0.0000D - 00 \end{bmatrix} \\
 B_1 &= \begin{bmatrix} 7.3484D - 04 & 7.3484D - 04 & 5.8075D - 03 & 5.8075D - 03 & 0.0000D - 00 \\ -6.7897D - 06 & 6.7897D - 06 & -6.3897D - 06 & 6.3897D - 06 & 3.3130D - 05 \\ 3.1534D - 05 & 3.1534D - 05 & -2.1788D - 05 & -2.1788D - 05 & 0.0000D - 00 \\ 2.4002D - 05 & -2.4002D - 05 & 1.6415D - 04 & -1.6415D - 04 & 3.4422D - 05 \\ 1.2078D - 03 & -1.2078D - 03 & 1.7236D - 04 & -1.7236D - 04 & -1.3526D - 03 \end{bmatrix} \\
 B_2 &= \begin{bmatrix} -7.7184D - 04 & -7.7184D - 04 & -5.5416D - 03 & -5.5416D - 03 & 0.0000D - 00 \\ -2.1695D - 05 & 2.1695D - 05 & 1.3484D - 05 & -1.3484D - 05 & 3.2708D - 06 \\ 3.3706D - 05 & 3.3706D - 05 & -4.1380D - 06 & -4.1380D - 06 & 0.0000D - 00 \\ -6.0930D - 04 & 6.0930D - 04 & 3.7870D - 04 & -3.7870D - 04 & 9.1860D - 05 \\ 1.3938D - 05 & -1.3938D - 05 & -8.6630D - 06 & 8.6630D - 06 & -2.1013D - 06 \end{bmatrix}
 \end{aligned}$$

$$\begin{aligned}
 \theta^T &= [A_1(1,1), A_1(1,2), \dots, A_1(5,5), A_2(1,1), \dots, A_2(5,5), \\
 &\quad B_1(1,1), \dots, B_1(5,5), B_2(1,1), \dots, B_2(5,5)]
 \end{aligned}$$

Table B.2. ACM Entry ARMA Model - 30% Loss of Effectiveness Left Trailing Edge

$$\begin{aligned}
 A_1 &= \begin{bmatrix} -1.9278D-00 & 0.0000D-00 & 7.2958D-01 & 0.0000D-00 & 0.0000D-00 \\ 0.0000D-00 & -1.9879D-00 & 0.0000D-00 & -1.4482D-05 & 1.1316D-04 \\ -1.3075D-02 & 0.0000D-00 & -2.0334D-00 & 0.0000D-00 & 0.0000D-00 \\ 0.0000D-00 & -21.4570D-00 & 0.0000D-00 & -9.8068D-01 & -5.4042D-01 \\ 0.0000D-00 & 5.6254D-01 & 0.0000D-00 & -5.9587D-04 & -9.7238D-01 \end{bmatrix} \\
 A_2 &= \begin{bmatrix} 9.2777D-01 & 0.0000D-00 & -6.7154D-01 & 0.0000D-00 & 0.0000D-00 \\ 0.0000D-00 & 9.8145D-01 & 0.0000D-00 & 0.0000D-00 & 0.0000D-00 \\ 1.3073D-02 & 0.0000D-00 & 1.0229D-00 & 0.0000D-00 & 0.0000D-00 \\ 0.0000D-00 & 21.4414D-00 & 0.0000D-00 & 0.0000D-00 & 0.0000D-00 \\ 0.0000D-00 & -6.2829D-01 & 0.0000D-00 & 0.0000D-00 & 0.0000D-00 \end{bmatrix} \\
 B_1 &= \begin{bmatrix} 8.4875D-04 & 8.4975D-04 & 2.9229D-03 & 3.9602D-03 & 0.0000D-00 \\ -1.4104D-05 & 1.3849D-05 & 2.4955D-06 & -4.3548D-06 & 9.4794D-06 \\ 3.1696D-05 & 3.1696D-05 & -1.2768D-05 & -2.1488D-05 & 0.0000D-00 \\ 2.5335D-05 & -2.4091D-05 & 9.5873D-05 & -1.6409D-04 & 3.6092D-05 \\ 1.2172D-03 & -1.1924D-03 & 1.4627D-04 & -2.4366D-04 & 1.3668D-03 \end{bmatrix} \\
 B_2 &= \begin{bmatrix} -1.0088D-03 & -1.0088D-03 & -2.6349D-03 & -3.5456D-03 & 0.0000D-00 \\ -1.3970D-05 & 1.3718D-05 & 2.4858D-06 & 1.3371D-06 & -7.9887D-05 \\ 1.8899D-05 & 1.8899D-05 & -5.0412D-05 & -7.2305D-05 & 0.0000D-00 \\ -3.0520D-04 & 2.9969D-04 & 5.4302D-05 & -9.4750D-05 & -8.7139D-04 \\ 8.9433D-06 & -8.7818D-06 & -1.5912D-06 & 2.7765D-06 & 2.5534D-05 \end{bmatrix}
 \end{aligned}$$

Table B.3. ACM Entry ARMA Model - 50% Loss of Effectiveness Left Canard

$$\begin{aligned}
 A_1 &= \begin{bmatrix} -1.9488D - 00 & 0.0000D - 00 & 5.3735D - 01 & 0.0000D - 00 & 0.0000D - 00 \\ 0.0000D - 00 & -1.9845D - 00 & 0.0000D - 00 & -1.0175D - 05 & -1.0880D - 05 \\ -4.4830D - 03 & 0.0000D - 00 & -2.0113D - 00 & 0.0000D - 00 & 0.0000D - 00 \\ 0.0000D - 00 & -24.8440D - 00 & 0.0000D - 00 & -9.7764D - 01 & -6.2532D - 01 \\ 0.0000D - 00 & 5.7566D - 01 & 0.0000D - 00 & -6.0059D - 04 & -9.7200D - 01 \end{bmatrix} \\
 A_2 &= \begin{bmatrix} 9.4885D - 01 & 0.0000D - 00 & -4.9634D - 01 & 0.0000D - 00 & 0.0000D - 00 \\ 0.0000D - 00 & 9.8666D - 01 & 0.0000D - 00 & 0.0000D - 00 & 0.0000D - 00 \\ 4.4820D - 03 & 0.0000D + 00 & 1.0077D - 00 & 0.0000D - 00 & 0.0000D - 00 \\ 0.0000D - 00 & 24.8260D - 00 & 0.0000D - 00 & 0.0000D - 00 & 0.0000D - 00 \\ 0.0000D - 00 & -6.3624D - 01 & 0.0000D - 00 & 0.0000D - 00 & 0.0000D - 00 \end{bmatrix} \\
 B_1 &= \begin{bmatrix} -4.0629D - 03 & -3.1970D - 03 & 5.9859D - 03 & 5.9859D - 03 & 0.0000D - 00 \\ -7.0321D - 06 & -1.0579D - 05 & 3.9925D - 06 & -3.9925D - 06 & 4.3437D - 05 \\ 1.1191D - 05 & 2.2381D - 05 & -2.1786D - 05 & -2.1786D - 05 & 0.0000D - 00 \\ 1.1082D - 05 & -2.1809D - 05 & 1.6413D - 04 & -1.6413D - 04 & 3.4196D - 05 \\ 5.9619D - 04 & -1.2180D - 03 & 1.9454D - 04 & -1.9454D - 04 & -1.3671D - 03 \end{bmatrix} \\
 B_2 &= \begin{bmatrix} 3.7323D - 03 & 2.7869D - 03 & -5.4731D - 03 & -5.4734D - 03 & 0.0000D - 00 \\ -7.0028D - 06 & 3.9010D - 05 & 3.9740D - 06 & -3.9740D - 06 & -6.2894D - 06 \\ 2.9058D - 05 & 3.6021D - 05 & -4.8049D - 05 & -4.8049D - 05 & 0.0000D - 00 \\ -1.7621D - 04 & 9.8158D - 04 & 9.9993D - 05 & -9.9993D - 05 & -1.5826D - 04 \\ 4.5157D - 06 & -2.5156D - 05 & -2.5626D - 06 & 2.5626D - 06 & 1.0557D - 06 \end{bmatrix}
 \end{aligned}$$

Table B.4. ACM Entry ARMA Model - 25% Loss of Effectiveness Rudder

$$\begin{aligned}
 A_1 &= \begin{bmatrix} -1.9684D + 00 & 0.0000D + 00 & 4.3587D - 01 & 0.0000D + 00 & 0.0000D + 00 \\ 0.0000D + 00 & -1.9900D + 00 & 0.0000D + 00 & -5.2378D - 06 & -1.2597D - 04 \\ -9.8466D - 03 & 0.0000D + 00 & -1.9924D + 00 & 0.0000D + 00 & 0.0000D + 00 \\ 0.0000D + 00 & -2.7779D + 01 & 0.0000D + 00 & -9.7500D - 01 & -6.9850D - 01 \\ 0.0000D + 00 & 6.6970D - 01 & 0.0000D + 00 & -6.7151D - 04 & -9.7985D - 01 \end{bmatrix} \\
 A_2 &= \begin{bmatrix} 9.6838D - 01 & 0.0000D + 00 & -4.1059D - 01 & 0.0000D + 00 & 0.0000D + 00 \\ 0.0000D + 00 & 9.9189D - 01 & 0.0000D + 00 & 0.0000D + 00 & 0.0000D + 00 \\ 9.8443D - 03 & 0.0000D + 00 & 9.8452D - 01 & 0.0000D + 00 & 0.0000D + 00 \\ 0.0000D + 00 & 2.7750D + 01 & 9.6000D + 00 & 0.0000D + 00 & 0.0000D + 00 \\ 0.0000D + 00 & -7.1991D - 01 & 0.0000D + 00 & 0.0000D + 00 & 0.0000D + 00 \end{bmatrix} \\
 B_1 &= \begin{bmatrix} 7.3170D - 04 & 7.3170D - 04 & 6.0040D - 03 & 6.0040D - 03 & 0.0000D + 00 \\ 8.2887D - 07 & -8.2887D - 07 & 6.4352D - 04 & -1.4215D - 05 & -1.2926D - 04 \\ 3.1701D - 05 & 3.1701D - 05 & -2.1801D - 05 & -2.1801D - 05 & 0.0000D + 00 \\ 2.3351D - 05 & -2.3351D - 05 & 1.3837D - 04 & -1.6374D - 04 & 3.1979D - 05 \\ -6.1414D - 07 & 6.1414D - 07 & -5.1026D - 02 & 6.7565D - 04 & 1.0417D - 02 \end{bmatrix} \\
 B_2 &= \begin{bmatrix} -7.4570D - 04 & -7.4570D - 04 & -5.8168D - 03 & -5.8168D - 03 & 0.0000D + 00 \\ 8.2662D - 07 & -8.2662D - 07 & 6.4393D - 04 & -1.4204D - 05 & -1.2935D - 04 \\ 2.4128D - 05 & 2.4128D - 05 & -8.0847D - 05 & -8.0847D - 05 & 0.0000D + 00 \\ 2.3126D - 05 & -2.3126D - 05 & 1.8015D - 02 & -3.9739D - 04 & -3.6188D - 03 \\ -5.9996D - 07 & 5.9996D - 07 & -4.6736D - 04 & 1.0310D - 05 & 9.3883D - 05 \end{bmatrix}
 \end{aligned}$$



Table B.5. ACM Exit ARMA Model - No Failures

$$\begin{aligned}
 A_1 &= \begin{bmatrix} -1.9837D-00 & -6.5693D-01 & 2.2386D-00 & 1.1610D-03 & -1.8660D-02 \\ 2.6268D-07 & -1.9658D-00 & -1.1845D-03 & -2.5388D-05 & 4.3827D-04 \\ 4.4540D-04 & 1.4892D-04 & -1.9772D-00 & -1.3834D-04 & 4.2016D-06 \\ 9.3315D-08 & -2.0952D-00 & 1.2440D-03 & -9.9831D-01 & -6.0140D-02 \\ -5.2666D-09 & 1.1718D-01 & -6.6512D-05 & -9.1823D-05 & -9.9858D-01 \end{bmatrix} \\
 A_2 &= \begin{bmatrix} 9.8377D-01 & 6.5725D-01 & -2.2302D-00 & 0.0000D-00 & 0.0000D-00 \\ -2.6062D-07 & 9.6796D-01 & 1.1476D-03 & 0.0000D-00 & 0.0000D-00 \\ -4.4191D-04 & -1.4888D-04 & 9.7758D-01 & 0.0000D-00 & 0.0000D-00 \\ -9.2583D-08 & 2.0986D-00 & 1.2332D-03 & 0.0000D-00 & 0.0000D-00 \\ 5.2253D-09 & -1.1514D-01 & -6.8092D-05 & 0.0000D-00 & 0.0000D-00 \end{bmatrix} \\
 B_1 &= \begin{bmatrix} -2.4336D-03 & -2.4560D-03 & -2.3306D-03 & -2.3347D-03 & 6.6196D-07 \\ 1.5424D-05 & -1.8937D-05 & 2.0378D-06 & -2.0392D-05 & 1.7525D-05 \\ 5.0031D-06 & 4.8478D-06 & -1.8059D-06 & -1.8059D-06 & 1.5819D-13 \\ 5.6635D-06 & -1.2379D-05 & 1.9698D-05 & -1.9698D-05 & 6.4000D-06 \\ 3.3248D-04 & -3.0209D-04 & -3.3599D-05 & 3.3599D-05 & -3.2566D-04 \end{bmatrix} \\
 B_2 &= \begin{bmatrix} 2.2530D-03 & 2.3031D-03 & 2.4219D-03 & 2.4033D-03 & -2.2257D-06 \\ -1.8931D-05 & 1.5462D-05 & 1.6683D-05 & -1.6687D-05 & -2.2764D-06 \\ 3.9268D-06 & 3.7560D-06 & -2.8621D-06 & -2.8588D-06 & 6.5541D-10 \\ -4.1049D-05 & 3.3518D-05 & 3.6174D-05 & -3.6176D-05 & -4.9354D-06 \\ 2.2522D-06 & -1.8390D-06 & -1.9847D-06 & 1.9848D-06 & 2.7078D-07 \end{bmatrix}
 \end{aligned}$$

Table B.6. TF/TA ARMA Model - No Failures

$$\begin{aligned}
 A_1 &= \begin{bmatrix} -3.6847D-00 & 0.0000D-00 & -51.1370D-00 & 0.0000D-00 & 0.0000D-00 \\ 0.0000D-00 & -1.9519D-00 & 0.0000D-00 & -2.8733D-05 & 1.0815D-01 \\ 5.9207D-02 & 0.0000D-00 & -1.8445D-01 & 0.0000D-00 & 0.0000D-00 \\ 0.0000D-00 & -59.2300D-00 & 0.0000D-00 & -9.5265D-01 & -1.5044D-00 \\ 0.0000D-00 & 1.4404D-00 & 0.0000D-00 & -1.3954D-03 & -9.2447D-01 \end{bmatrix} \\
 A_2 &= \begin{bmatrix} 2.6832D-00 & 0.0000D-00 & 49.7810D-00 & 0.0000D-00 & 0.0000D-00 \\ 0.0000D-00 & 9.5785D-01 & 0.0000D-00 & 0.0000D-00 & 0.0000D-00 \\ -5.9154D-02 & 0.0000D-00 & -7.6791D-01 & 0.0000D-00 & 0.0000D-00 \\ 0.0000D-00 & 59.0480D-00 & 0.0000D-00 & 0.0000D-00 & 0.0000D-00 \\ 0.0000D-00 & -1.6383D-00 & 0.0000D-00 & 0.0000D-00 & 0.0000D-00 \end{bmatrix} \\
 B_1 &= \begin{bmatrix} 1.0618D-02 & -1.0618D-02 & 1.5259D-02 & 1.5259D-02 & 0.0000D-00 \\ -1.8033D-05 & 1.8033D-05 & -4.1580D-06 & 9.1373D-06 & 1.0194D-04 \\ 7.3451D-05 & 7.3451D-05 & -4.0607D-05 & -4.0607D-05 & 0.0000D-00 \\ 7.1020D-05 & -7.1020D-05 & 2.9993D-04 & -2.9997D-04 & 1.0971D-04 \\ 3.9102D-03 & -3.9102D-03 & 1.0870D-04 & -1.0819D-04 & -4.4117D-03 \end{bmatrix} \\
 B_2 &= \begin{bmatrix} 2.0494D-02 & 2.0494D-02 & -3.6496D-02 & -3.6496D-02 & 0.0000D-00 \\ -7.5883D-05 & 7.5883D-05 & 1.0468D-05 & -1.5268D-05 & 1.2956D-05 \\ -4.2691D-04 & -4.2691D-04 & 7.9098D-04 & 7.9098D-04 & 0.0000D-00 \\ -4.6779D-03 & 4.6779D-03 & 6.4531D-04 & -9.4120D-04 & 7.9867D-04 \\ 1.2979D-04 & -1.2979D-04 & -1.7904D-05 & 2.6114D-05 & -2.2160D-05 \end{bmatrix}
 \end{aligned}$$

Table B.7. TF/TA ARMA Model - 30% Loss of Effectiveness Left Trailing Edge

$$\begin{aligned}
 A_1 &= \begin{bmatrix} -1.9289D-00 & 0.0000D-00 & 2.4122D-00 & 0.0000D-00 & 0.0000D-00 \\ 0.0000D-00 & -1.9561D-00 & 0.0000D-00 & -2.5617D-05 & 1.3755D-05 \\ 7.2371D-03 & 0.0000D-00 & -1.9644D-00 & 0.0000D+00 & 0.0000D-00 \\ 0.0000D-00 & 57.5160D-00 & 0.0000D-00 & -9.5402D-01 & -1.4610D-00 \\ 0.0000D-00 & 1.6261D-00 & 0.0000D-00 & -1.5406D-03 & -9.2005D-01 \end{bmatrix} \\
 A_2 &= \begin{bmatrix} 9.2900D-01 & 0.0000D-00 & -2.3558D-00 & 0.0000D-00 & 0.0000D-00 \\ 0.0000D-00 & 9.6193D-01 & 0.0000D-00 & 0.0000D-00 & 0.0000D-00 \\ -7.2311D-03 & 0.0000D-00 & 9.7021D-01 & 0.0000D-00 & 0.0000D-00 \\ 0.0000D-00 & 57.7350D-00 & 0.0000D-00 & 0.0000D-00 & 0.0000D-00 \\ 0.0000D-00 & -1.8209D-00 & 0.0000D-00 & 0.0000D-00 & 0.0000D-00 \end{bmatrix} \\
 B_1 &= \begin{bmatrix} -8.8814D-03 & -8.8814D-03 & 1.0201D-02 & 1.3521D-02 & 0.0000D-00 \\ -2.2384D-05 & 2.2384D-05 & 2.2204D-06 & -3.6512D-06 & 1.0626D-04 \\ 7.2684D-05 & 7.2684D-05 & -2.3547D-05 & -3.9662D-05 & 0.0000D-00 \\ 7.0004D-05 & -7.0004D-05 & 1.7183D-04 & -2.9585D-04 & 1.1159D-04 \\ 3.8607D-03 & -3.8607D-03 & 4.3589D-05 & -8.8733D-05 & -4.3508D-03 \end{bmatrix} \\
 B_2 &= \begin{bmatrix} 8.2180D-03 & 8.2180D-03 & -9.3663D-03 & -1.2370D-02 & 0.0000D-00 \\ -7.0757D-05 & 7.0757D-05 & 2.1920D-06 & -3.6047D-06 & 7.5178D-06 \\ 7.4294D-06 & 7.4294D-06 & 5.0055D-05 & 5.7807D-05 & 0.0000D-00 \\ -4.2185D-03 & 4.2185D-03 & 1.3069D-04 & -2.1491D-04 & 4.4821D-04 \\ 1.3394D-04 & -1.3394D-04 & -4.1495D-06 & 6.8238D-06 & -1.1231D-05 \end{bmatrix}
 \end{aligned}$$

Table B.8. TF/TA ARMA Model - 50% Loss of Effectiveness Left Canard

$$\begin{aligned}
 A_1 &= \begin{bmatrix} -1.9180D-00 & 0.0000D-00 & 2.4247D-00 & 0.0000D-00 & 0.0000D-00 \\ 0.0000D-00 & -1.9713D-00 & 0.0000D-00 & -1.2614D-05 & -5.2084D-04 \\ 4.7557D-03 & 0.0000D-00 & -1.9509D-00 & 0.0000D-00 & 0.0000D-00 \\ 0.0000D-00 & -83.6540D-00 & 0.0000D-00 & -9.3315D-01 & -2.1289D-00 \\ 0.0000D-00 & 2.0604D-00 & 0.0000D-00 & -1.9038D-03 & -9.0350D-01 \end{bmatrix} \\
 A_2 &= \begin{bmatrix} 9.1806D-01 & 0.0000D-00 & -2.3596D-00 & 0.0000D-00 & 0.0000D-00 \\ 0.0000D-00 & 9.7736D-01 & 0.0000D-00 & 0.0000D-00 & 0.0000D-00 \\ -4.7512D-03 & 0.0000D-00 & 9.5472D-01 & 0.0000D-00 & 0.0000D-00 \\ 0.0000D-00 & 83.3500D-00 & 0.0000D-00 & 0.0000D-00 & 0.0000D-00 \\ 0.0000D-00 & -2.2661D-00 & 0.0000D-00 & 0.0000D-00 & 0.0000D-00 \end{bmatrix} \\
 B_1 &= \begin{bmatrix} -1.3180D-02 & -9.7372D-03 & 1.6645D-02 & 1.6645D-02 & 0.0000D-00 \\ -3.0171D-06 & 5.2788D-06 & 3.0283D-06 & -3.0283D-06 & 1.1496D-04 \\ 4.2701D-05 & 8.4482D-05 & -4.6574D-05 & -4.6574D-05 & 0.0000D-00 \\ 3.6503D-05 & -8.5166D-05 & 3.4423D-04 & -3.4423D-04 & 1.2590D-04 \\ 2.2580D-03 & -4.4667D-03 & 6.4002D-05 & -6.4002D-05 & -5.0749D-03 \end{bmatrix} \\
 B_2 &= \begin{bmatrix} 1.2025D-02 & 8.7762D-03 & -1.4993D-02 & -1.4993D-02 & 0.0000D-00 \\ -5.2586D-05 & 1.0441D-04 & 2.9923D-06 & -2.9923D-06 & 1.6596D-05 \\ -2.9516D-05 & 3.7108D-05 & 3.2466D-05 & 3.2466D-05 & 0.0000D-00 \\ -4.4845D-03 & 8.9044D-03 & 2.5519D-04 & -2.5519D-04 & 1.4153D-03 \\ 1.2193D-04 & -2.4210D-04 & -6.9381D-06 & 6.9381D-06 & -3.8481D-05 \end{bmatrix}
 \end{aligned}$$

Table B.9. TF/TA ARMA Model - 25% Loss of Effectiveness Rudder

$$\begin{aligned}
 A_1 &= \begin{bmatrix} -1.9129D + 00 & 0.0000D + 00 & 1.7108D + 00 & 0.0000D + 00 & 0.0000D + 00 \\ 0.0000D + 00 & -1.9828D + 00 & 0.0000D + 00 & -5.6997D - 06 & -5.6667D - 04 \\ -1.2382D - 02 & 0.0000D + 00 & -1.9545D + 00 & 0.0000D + 00 & 0.0000D + 00 \\ 0.0000D + 00 & -6.6691D + 01 & 0.0000D + 00 & -9.4670D - 01 & -1.6908D + 00 \\ 0.0000D + 00 & 2.3355D + 00 & 0.0000D + 00 & -2.0471D - 03 & -9.0518D - 01 \end{bmatrix} \\
 A_2 &= \begin{bmatrix} 9.1298D - 01 & 0.0000D + 00 & -1.6414D + 00 & 0.0000D + 00 & 0.0000D + 00 \\ 0.0000D + 00 & 9.8717D - 01 & 0.0000D + 00 & 0.0000D + 00 & 0.0000D + 00 \\ 1.2371D - 02 & 0.0000D + 00 & 9.4454D - 01 & 0.0000D + 00 & 0.0000D + 00 \\ 0.0000D + 00 & 6.6475D + 01 & 0.0000D + 00 & 0.0000D + 00 & 0.0000D + 00 \\ 0.0000D + 00 & -2.4777D + 00 & 0.0000D + 00 & 0.0000D + 00 & 0.0000D + 00 \end{bmatrix} \\
 B_1 &= \begin{bmatrix} -8.3608D - 03 & -8.3608D - 03 & 1.3906D - 02 & 1.3906D - 02 & 0.0000D + 00 \\ 2.5912D - 05 & -2.5912D - 05 & 1.8944D - 03 & -1.6350D - 05 & -3.4926D - 04 \\ 7.2296D - 05 & 7.2296D - 05 & -3.9150D - 05 & -3.9150D - 05 & 0.0000D + 00 \\ 6.8601D - 05 & -6.8601D - 05 & 2.8136D - 04 & -2.9590D - 04 & 8.5261D - 05 \\ -7.0756D - 07 & 7.0756D - 07 & -1.5069D - 01 & 9.7093D - 04 & 2.9922D - 02 \end{bmatrix} \\
 B_2 &= \begin{bmatrix} 7.5351D - 03 & 7.5351D - 03 & -1.2552D - 02 & -1.2552D - 02 & 0.0000D + 00 \\ -2.3735D - 05 & 2.3735D - 05 & 1.9152D - 03 & -1.6463D - 05 & -4.0302D - 04 \\ 1.7408D - 04 & 1.7408D - 04 & -2.0952D - 04 & -2.0952D - 04 & 0.0000D + 00 \\ -1.5983D - 03 & 1.5983D - 03 & 1.2897D - 01 & -1.1086D - 03 & -2.7139D - 02 \\ 5.9572D - 05 & -5.9572D - 05 & -4.8068D - 03 & 4.1321D - 05 & 1.0115D - 03 \end{bmatrix}
 \end{aligned}$$

## Appendix C. *GAIN MATRICES AND STEP RESPONSE ROOTS*

This Appendix contains the fixed-gain matrices for the no failure flight conditions and the  $w$  roots for the step response PI controller design.

Table C.1. Discrete PI Controller Gain Matrices - ACMENTRY

$$K_1 = \begin{bmatrix} 0.2750 & 2.6579 & 22.6167 & 0.9347 & 3.2537 \\ 0.2750 & -2.6579 & 22.6167 & -0.9347 & -3.2537 \\ 0.3989 & -0.8640 & -2.9566 & 2.4292 & -0.1156 \\ 0.3939 & 0.8640 & -2.9566 & -2.4292 & 0.1156 \\ 0.0000 & 4.5235 & 0.0000 & 2.3043 & -3.4078 \end{bmatrix}$$

$$K_2 = \begin{bmatrix} 0.0825 & 0.7974 & 6.7850 & 0.2804 & 0.9761 \\ 0.0825 & -0.7974 & 6.7850 & -0.2804 & -0.9761 \\ 0.1197 & -0.2592 & -0.8870 & 0.7288 & -0.0347 \\ 0.1197 & 0.2592 & -0.8870 & -0.7288 & 0.0347 \\ 0.0000 & 1.3570 & 0.0000 & 0.6913 & -1.0223 \end{bmatrix}$$

Table C.2. Discrete PI Controller Gain Matrices - ACMEXIT

$$K_1 = \begin{bmatrix} -0.2877 & 1.8139 & 118.6223 & 5.9943 & 7.1919 \\ -0.2728 & -1.8515 & 112.4901 & -6.1188 & -7.3413 \\ -0.8052 & -1.4469 & -99.0041 & 19.5178 & 0.7930 \\ -0.7271 & 1.5019 & -131.2262 & -19.3359 & -0.5747 \\ -0.0326 & 3.8739 & 13.4352 & 7.9424 & -24.4074 \end{bmatrix}$$

$$K_2 = \begin{bmatrix} -0.0863 & 0.5442 & 35.5867 & 1.7983 & 2.1576 \\ -0.0818 & -0.5555 & 33.7470 & -1.8356 & -2.2024 \\ -0.2416 & -0.4341 & -29.7012 & 5.8553 & 0.2379 \\ -0.2181 & 0.4506 & -39.3679 & -5.8008 & -0.1724 \\ -0.0098 & 1.1622 & 4.0306 & 2.3827 & -7.3222 \end{bmatrix}$$

Table C.3. Discrete PI Controller Gain Matrices - TF/TA

$$K_1 = \begin{bmatrix} 0.1372 & 0.8360 & 15.3257 & 0.1741 & 0.8983 \\ 0.1549 & -0.8360 & 15.9544 & -0.1741 & -0.8983 \\ 0.2707 & -0.4656 & 9.5751 & 1.3828 & 0.0093 \\ 0.2608 & 0.4656 & 9.2249 & -1.3828 & -0.0093 \\ -0.0155 & 1.4562 & -0.5475 & 0.3824 & -1.1936 \end{bmatrix}$$

$$K_2 = \begin{bmatrix} 0.0411 & 0.2508 & 4.5977 & 0.0522 & 0.2695 \\ 0.0465 & -0.2508 & 4.7863 & -0.0522 & -0.2695 \\ 0.0812 & -0.1397 & 2.8725 & 0.4148 & 0.0028 \\ 0.0782 & 0.1397 & 2.7675 & -0.4148 & -0.0028 \\ -0.0046 & 0.4368 & -0.1643 & 0.1147 & -0.3581 \end{bmatrix}$$

Table C.4. Step Response PI Controller Gain Matrices - ACM Entry

$$K_1 = \begin{bmatrix} 5.4705 & 319.1986 & 145.8124 & 13.6863 & 39.6138 \\ 5.4705 & -319.1986 & 145.8124 & -13.6863 & -39.6138 \\ 7.9174 & -103.6666 & -18.4503 & 143.8869 & -7.2031 \\ 7.9174 & 103.6666 & -18.4503 & -143.8869 & 7.2031 \\ 0.0000 & 543.6125 & 0.0000 & 61.1122 & 13.4587 \end{bmatrix}$$

$$K_2 = \begin{bmatrix} 0.0028 & 8.4049 & 6.9320 & -3.8274 & 106.9155 \\ 0.0028 & -8.4049 & 6.9320 & 3.8274 & -106.9155 \\ 0.0027 & 1.3925 & 7.9268 & 1.2441 & -34.6890 \\ 0.0027 & -1.3925 & 7.9268 & -1.2441 & 34.6890 \\ 0.0000 & 24.4185 & 0.0000 & -6.5138 & 180.3718 \end{bmatrix}$$



Table C.5. Step Response FI Controller Gain Matrices - ACM Exit

$$K_1 = \begin{bmatrix} -0.0058 & 0.2178 & 0.7526 & -0.0085 & 0.0583 \\ -0.0055 & -0.2223 & 0.7138 & 0.0093 & -0.0596 \\ -0.0163 & -0.1734 & -0.6660 & 1.3210 & -0.0077 \\ -0.0147 & 0.1801 & -0.8705 & -1.3197 & 0.0095 \\ -0.0007 & 0.4651 & 0.0851 & -0.2897 & -0.1137 \end{bmatrix} * 10^3$$

$$K_2 = \begin{bmatrix} -0.8029 & 5.4103 & -94.2627 & 9.1723 & 85.0569 \\ -0.7614 & -4.9904 & -82.6466 & 13.2984 & -78.4553 \\ -1.6540 & 9.2572 & -183.2629 & 27.4612 & -59.1481 \\ -1.4359 & -8.1117 & -164.1554 & 20.5369 & 77.1570 \\ -0.0909 & 7.0755 & -17.6024 & -3.6862 & 174.8087 \end{bmatrix}$$

Table C.6. Step Response PI Controller Gain Matrices - TF/TA

$$K_1 = \begin{bmatrix} 2.7661 & 100.5031 & 108.0596 & 4.5846 & 11.7829 \\ 3.1223 & -100.5031 & 113.2086 & -4.5846 & -11.7829 \\ 5.4248 & -55.8763 & 78.4220 & 80.0561 & 3.4695 \\ -0.3102 & 175.4099 & -4.4842 & 12.0628 & 3.7161 \end{bmatrix}$$

$$K_2 = \begin{bmatrix} 0.0411 & 0.2508 & 4.5977 & 0.0522 & 0.2695 \\ 0.0465 & -0.2508 & 4.7863 & -0.0522 & -0.2695 \\ 0.0812 & -0.1397 & 2.8725 & 0.4148 & 0.0028 \\ 0.0782 & 0.1397 & 2.7675 & -0.4148 & -0.0028 \\ -0.0046 & 0.4368 & -0.1643 & 0.1147 & -0.3581 \end{bmatrix}$$

Table C.7.  $w$  plane roots for ACM Entry and TFTA for the step response method

ACM ENTRY	TFTA
$-4.70E^{-6}$	$-4.70E^{-6}$
$6.63E^{-6}$	$6.60E^{-6}$
$-2.34E^{-4}$	$-2.45E^{-4}$
$-2.86E^{-3} \pm j2.10E^{-3}$	$-3.73E^{-3} \pm j3.18E^{-3}$
$-2.2034 \pm j .7398$	$-2.3131$
$-2.8844 \pm j 1.3522$	$-2.5416$
$-1.4674 \pm j 4.8738$	$-8.1269$
$-9.9482 (5)$	$-2.8595 \pm j 8.5404$
$-1.1482 \pm j 11.652$	$-9.9482 (5)$
$-45.617 \pm j 27.997$	$-11.434$
$-55.799 \pm j 31.105$	$-16.310$
$-56.411 \pm j 31.192$	$-24.174 \pm j 44.036$
$-56.522 \pm j 31.006$	$-51.822$
$-57.916 \pm j 31.327$	$-50.148 \pm j 30.743$
	$-55.239 \pm j 29.878$
	$-54.500 \pm j 31.901$
	$-57.237 \pm j 31.264$

## Appendix D. ADAPTIVE ALGORITHM

The following source code for the adaptive algorithm is a FORTRAN subroutine obtained from Hammond (4) which has to be linked to *MATRIX<sub>X</sub>*. This algorithm will require more default memory than found in *MATRIX<sub>X</sub>*, so the stack size must be increased in the *MATRIX<sub>X</sub>* FORTRAN code. Specific instructions to increase the stack size and link FORTRAN code can be found in the *MATRIX<sub>X</sub>* users manual. Also note that the most recent versions of the IMSL Library and *MATRIX<sub>X</sub>* are used.

```
C-----
C|
C| THIS PROGRAM PROVIDES A RECURSIVE LEAST SQUARES ESTIMATION |
C| OF THE PARAMETERS FOR THE CRCA 5 X 5 A AND B COEFFICIENTS. |
C|          LAST REVISION 11 SEPTEMBER 1989                    |
C| THIS PROGRAM SHOULD BE LINKED TO VERSION 10.0 IMSL LIBRARY |
C|          AND WAS WRITTEN TO RUN ON MATRIXX VERSION 7.0.    |
C|          SEE FILE FOR.COM FOR THE APPROPRIATE COMMANDS     |
C-----
      SUBROUTINE UPDUSR (INFO,NUMBER,T,U,NU,X,XDOT,NX,Y,NY,
+          RP,IP)
      DOUBLE PRECISION T,U(*),X(*),Y(*),XDOT(*),RP(*)
      INTEGER          INFO(4), IP(*)
      CHARACTER*3 CNUM
C
      INTEGER MAXNUM
      PARAMETER (MAXNUM=1)
C
      IF (NUMBER.GT.MAXNUM) THEN
          INFO(1)=-2
          WRITE(CNUM,111) NUMBER
111      FORMAT(I3)
          CALL MATWR(' ')
          CALL MATWR
+          ('SIM_ERROR: NOT ABLE TO UPDATE USER FUNCTION'//CNUM)
          RETURN
      ENDIF
      CALL USR01 (INFO,T,U,NU,X,XDOT,NX,Y,NY,RP,IP)
      RETURN
      END
```

```

C-----
C| START OF USER SUBROUTINE FOR THE RECURSIVE LEAST SQUARES |
C| ESTIMATION AND GAIN MATRIX CALCULATIONS FOR THE ARMA |
C| MODEL REPRESENTATION |
C-----

SUBROUTINE USR01(INFO,T,U,NU,X,XDOT,NX,Y,NY,RP,IP)
DOUBLE PRECISION T,U(*),X(*),XDOT(*),Y(*),RP(*),
+ XNPLUS(100,5),GAMD1(5,5),XNPLUST(5,100),
+ XNPLUSPN(5,100),PN(100,100),GAMMA(5,5),
+ FORGET(5,5),PNXNPLUS(100,5),
+ GON(5,5),HINV(5,5),A1ARMA(5,5p1 10),
+ A2ARMA(5,5),B1ARMA(5,5),B2ARMA(5,5),
+ K1(5,5),K2(5,5),PND2(100,100),
+ THED2(5),THED4(100),
+ THETA(100),EYE5(5,5),GAMMAI(5,5),THED3(5),
+ SIGMA(5),GO(5,5),GODEN(5,5),PIT(5),
+ GODENI(5,5),PNPLUS(100,100),THETA1(100),
+ PXPLGAM(100,5),WK4REA(40),GOI(5,5)
INTEGER IP(*), INFO(4),N,IA,IDGT,IER,I,J,K,L
LOGICAL INIT,STATE,OUTPUT

INIT = INFO(2).NE.0
STATE = INFO(3).NE.0
OUTPUT= INFO(4).NE.0
IF (STATE .OR. (.NOT. OUTPUT)) THEN
GOTO 999
ENDIF

N=5 !PARAMETERS FOR IMSL LIBRARY
LDA=5 !PARAMETERS FOR IMSL LIBRARY
LDAINV=5 !PARAMETERS FOR IMSL LIBRARY

C-----
C| CHECK FOR INITIALIZATION OF THE THETA(0) AND P(0) |
C|-----

TSTART=.050 !3 PERIODS
IF (TSTART.GT.T) THEN
OPEN(UNIT=102,FILE='THETANOM.RLS',STATUS='OLD')!THETA
DO I=1,100
READ(102,*)THETA(I)
END DO
CLOSE(102)
OPEN(UNIT=103,FILE='PONOM.RLS',STATUS='OLD') !PN
DO I=1,100
DO J=1,100
READ(103,*)PN(I,J)
END DO

```

```

        END DO
        CLOSE(103)
        GOTO 600 !INSURES FULLY POPULATED XNPLUS
    ENDIF

C-----
C|          CALCULATION OF NEW PARAMETER VECTOR          |
C-----
        CALL MMULT1 (5,100,1,XNPLUST,THETA,THED2)
        DO I=1,5
            THED3(I) = U(I+10)-THED2(I)
        END DO
        CALL MMULT1 (100,5,1,PXPLGAM,THED3,THED4)
        DO J=1,100
            THETA1(J) = THETA(J) + THED4(J)
        END DO

C-----
C| UPDATE PARAMETER VECTOR FOR NEXT ITERATION          |
C-----
        DO I=1,100
            THETA(I)=THETA1(I)
        END DO

C-----
C|          THE RECURSIVE UPDATE EQUATION STARTS HERE.          |
C-----
C-----
C| UPDATE XNPLUS WITH THE OUTPUT FOR NEXT ITERATION          |
C-----
600    K=1                                !COUNTER FOR UPDATE MATRIX
        DO J=75,95,5
            DO I=1,5
                XNPLUS(J+I,K) = U(I+5)    !U(I+5)--U(T-2)
            END DO
            K=K + 1
        END DO

C-----
C|          K=1                                !COUNTER FOR UPDATE MATRIX
        DO J=50,70,5
            DO I = 1,5
                XNPLUS(J+I,K)=U(I)        !U(I)--U(T-1)
            END DO
            K=K + 1
        END DO

C-----
        K=1
        DO J=25,45,5

```

```

      DO I=1,5
        XNPLUS(J+I,K) = -U(I+15)  !UPDATES Y(T-2)
      END DO
      K=K+1
    END DO
    K=1
C-----
    DO J=0,20,5
      DO I=1,5
        XNPLUS(J+I,K)= -U(I+10)  ! UPDATES Y(T-1)
      END DO
      K=K+1
    END DO
C-----
C| CALCULATION OF P(K) * XN(K+ 1) |
C-----
      CALL MMULT (100,100,5,PN,XNPLUS,PNXNPLUS)
C-----
C|          CALCULATE XNPLUST * PN |
C-----
C-----
C| THE FOLLOWING LOOP UPDATES THE FORGETTING FACTOR MATRIX |
C-----
      DO I=1,5
        DO J=1,5
          IF(I.EQ.J)THEN
            FORGET(I,J)=U(31)
          ELSE
            FORGET(I,J)=0
          END IF
        END DO
      END DO
      DO I=1,5
        DO J=1,100
          XNPLUST(I,J) = XNPLUS(J,I)
        END DO
      END DO
      CALL MMULT (5,100,100,XNPLUST,PN,XNPLUSPN)
C-----
C|          CALCULATE X(N+1)T*PN*X(N+1) |
C-----
      CALL MMULT (5,100,5,XNPLUSPN,XNPLUS,GAMD1)
C-----
C|          CALCULATE GAMMA(N+1) |
C-----

```

```

      DO I=1,5
        DO J=1,5
          GAMMA(I,J) = FORGET(I,J) + GAMD1(I,J)
        END DO
      END DO

C-----
C|      COMPUTE GAMMA(N+1) INVERSE USING IMSL ROUTINE      |
C-----
      CALL DLINRG (N,GAMMA,LDA,GAMMAI,LDAINV)
      CALL MMULT  (100,5,5,PNXNPLUS,GAMMAI,PXPLGAM)
C-----
C|      CALCULATE PNPLUS, UPDATE OF COVARIANCE MATRIX      |
C-----
      CALL MMULT  (100,5,100,PXPLGAM,XNPLUSPN,PND2)
C=====
      DO J=1,100
        DO K=1,100
          PNPLUS(J,K)=PN(J,K)-PND2(J,K)
        END DO
      END DO

C-----
C| UPDATE COVARIANCE MATRIX AND PREPARE FOR NEXT ITERATION |
C-----
      DO I=1,100
        DO J=1,100
          PN(I,J) = PNPLUS(I,J)
        END DO
      END DO

C-----
C|
C| THIS CONCLUDES THE BASIC CALCULATION OF THE LEAST SQUARES |
C| ESTIMATE OF THE PARAMETER VECTOR THETA.  NEXT THE GAIN    |
C| MATRICES WILL BE CALCULATED                               |
C|
C-----
C-----
C|
C| CALCULATION OF THE IDENTITY MATRIX FOR 5 X 5              |
C-----
      DO I=1,5
        DO J=1,5
          IF(I.EQ.J)THEN
            EYES(I,J)=1
          ELSE
            EYES(I,J)=0
          END IF
        END DO
      END DO

```

```

        END IF
      END DO
    END DO
C-----CALCULATION OF H AND H INVERSE-----
    K=0
    DO I=1,5
      DO J=1,5
        A1ARMA(I,J)=THETA(K + J)
        A2ARMA(I,J)=THETA(25 +K + J)
        B1ARMA(I,J)=THETA(50+K+J)
        B2ARMA(I,J)=THETA(75+K+J)
        GON(I,J)  =B1ARMA(I,J) + B2ARMA(I,J)
        GODEN(I,J) =EYES(I,J) + A1ARMA(I,J) + A2ARMA(I,J)
      END DO
      K=K + 5
    END DO
C=====
    CALL DLINRG (N,B1ARMA,LDA,HINV,LDAINV)
    CALL DLINRG (N,GODEN,LDA,GODENI,LDAINV)
C-----
C|          INITIALIZE SIGMA MATRIX |
C-----
    DO I=1,5
      SIGMA(I)=U(I+20)
    END DO
C-----
C|          INITIALIZE PI MATRIX |
C-----
    DO I=1,5
      PIT(I)=U(25+I)
    END DO
C-----
C|  CALCULATION OF G(O) AND INV(GO) |
C-----
    CALL MMULT (5,5,5,GODENI,GON,GO)
    CALL DLINRG (N,GO,LDA,GOI,LDAINV)
C-----
C|  CALCULATION OF K1 AND K2 FOR GAIN |
C-----
    DO I=1,5
      DO J=1,5
        K1(I,J)= HINV(I,J)*SIGMA(J)
        K2(I,J)= GOI(I,J)*PIT(J)
      END DO
    END DO

```



```

C-----
C| THE FOLLOWING ROUTINES WILL PREPARE THE OUTPUTS OF THE USER |
C| BLOCK. Y(1) - Y(25)=K1, Y(26)-Y(50)=K2,Y(51)-Y(150)=THETA |
C|-----

```

```

      L=25
      K=0
      DO I=1,5
        DO J=1,5
          Y(J+K)=K1(I,J)
          Y(J+L)=K2(I,J)
        END DO
      K=K+5
      L=L+5
      END DO
      DO I=1,100
        Y(I+50)=THETA(I)
      END DO
999 RETURN
      END

```

```

C-----
C| SUBROUTINE MMULT FOR THE MATRIX MULTIPY-SIZE > 1 |
C-----

```

```

      SUBROUTINE MMULT (MATARW,MATACL,MATABCL,MATA,MATB,MATC)
      DOUBLE PRECISION MATC(MATARW,MATABCL),MATA(MATARW,MATACL),
+      MATB(MATACL,MATABCL)
      INTEGER MATARW,MATACL,MATABCL
      DO I=1,MATARW
        DO K=1,MATABCL
          SUM=0 !RESET PRODUCT SUM
          DO J=1,MATACL
            SUM=SUM + MATA(I,J)*MATB(J,K)
          END DO
          MATC(I,K)=SUM
        END DO
      END DO
      RETURN
      END

```

```

C-----
C| MATRIX MULTIPLY ROUTINE FOR MATRICES WITH A COLUMN |
C-----

```

```

      SUBROUTINE MMULT1 (MATARW,MATACL,MATABCL,MATA,MATB,MATC)
      DOUBLE PRECISION MATC(MATARW),MATA(MATARW,MATACL),
+      MATB(MATACL)
      INTEGER MATARW,MATACL,MATABCL
      DO I=1,MATARW

```


```
SUM=0                !RESET PRODUCT SUM
DO J=1,MATACL
  SUM = SUM + MATA(I,J)*MATB(J)
END DO
MATC(I) = SUM
END DO
RETURN
END
```

### Bibliography

1. Bokor, J. and L. Keviczky, "ARMA Canonical Forms Obtained from Constructibility Invariants," *International Journal of Control*, Vol 45, No 3, pp 861-873, 1987.
2. Bradshaw, A. and Porter, B. "Singular Perturbation Methods in the Design of Tracking Systems Incorporating Inner-Loop Compensators and Fast Sampling Error-Actuated Controllers," *International Journal of Systems Science*, Vol 12, pp 1207 - 1220. October 1981.
3. D'Azzo, J. and C. Houpis. *Linear Control Systems Analysis and Design*. Chapter 20 (Third Edition). New York: McGraw-Hill, 1981.
4. Hammond, Daryl, *Multivariable Control Law Design for the Control Reconfigurable Combat Aircraft (CRCA)*, MS Thesis, AFIT/GE/ENG/88D-14, School of Engineering, Air Force Institute of Technology (AU) Wright-Patterson AFB, Ohio, 1988.
5. Houpis, Constantine H. and Gary Lamont. *Digital Control Systems*. McGraw-Hill, 1981.
6. "MATRIX<sub>X</sub> User's Guide," Integrated Systems Inc., Palo Alto, California, 1982
7. Neumann, Kurt, *A Digital Rate Controller for the CRCA using Quantitative Feedback Theory*, MS Thesis, AFIT/GE/ENG/88D-14, School of Engineering, Air Force Institute of Technology (AU) Wright-Patterson AFB, Ohio, 1988.
8. Porter, B. and R.N. Fripp, "Design of Fail-Safe Adaptive Digital Set-Point Tracking Controllers for Multivariable Plants," *Proceeding IFAC Conference*. 1986.
9. Porter, B., and A.H. Jones. "Design of Adaptive Digital Set-Point Tracking Controllers Incorporating Recursive Step-Response Matrix Identifiers for Multivariable Plants." *Fourth IASTED International Symposium on Modelling, Identification and Control*. Grindelwald, Switzerland. 19-22 February 1985.
10. Porter, B., and A.H. Jones. "Design of Tunable Digital Set-Point Tracking Controllers for Linear Multivariable Plants Using Step-Response Matrices." *Third IASTED International Symposium on Modelling, Identification and Control*. Innsbruck, Austria. 14-17 February 1984.
11. Velez, Julio E., *Multivariable Control Law Design for the AFTI/16 With a Failed Control Surface Using a Parameter-Adaptive Controller*, MS Thesis, GE/ENG/87D-69, School of Engineering, Air Force Institute of Technology (AU) Wright-Patterson AFB, Ohio, 1987.
12. Weinstein, Warren, et. al., "Control Reconfigurable Combat Aircraft Development Phase 1 - R and D Design Evaluation," AFWAL-TR-87-3011, Wright Patterson AFB, OH, May 1987.
13. Wittenmark, Björn, and Karl J. Astrom, "Practical Issues in the Implementation of Self-Tuning Control," *Automatica*, Vol 20, No.5, 1984, pp 595-605.

### *Vita*

Captain Jamie Foelker attended the United States Air Force Academy and received a Bachelor of Science degree in Electrical Engineering in 1985. Her previous assignment was at Rome Air Development Center, Griffiss AFB, NY where she worked in speech processing. In May 1988 she was assigned to the School of Engineering, Air Force Institute of Technology.

A large rectangular area of the document has been redacted with black ink, obscuring several lines of text.

REPORT DOCUMENTATION PAGE				Form Approved OMB No. 0704-0188	
1a. REPORT SECURITY CLASSIFICATION <b>UNCLASSIFIED</b>			1b. RESTRICTIVE MARKINGS		
2a. SECURITY CLASSIFICATION AUTHORITY			3. DISTRIBUTION/AVAILABILITY OF REPORT <b>Approved for public release; distribution unlimited</b>		
2b. DECLASSIFICATION/DOWNGRADING SCHEDULE					
4. PERFORMING ORGANIZATION REPORT NUMBER(S)			5. MONITORING ORGANIZATION REPORT NUMBER(S)		
6a. NAME OF PERFORMING ORGANIZATION <b>School of Engineering</b>		6b. OFFICE SYMBOL (If applicable) <b>AFIT/EN</b>	7a. NAME OF MONITORING ORGANIZATION		
6c. ADDRESS (City, State, and ZIP Code) <b>Air Force Institute of Technology Wright-Patterson AFB OH 45433-6583</b>			7b. ADDRESS (City, State, and ZIP Code)		
8a. NAME OF FUNDING/SPONSORING ORGANIZATION <b>WRDC Flight Dynamics Lab</b>		8b. OFFICE SYMBOL (If applicable) <b>FIGL</b>	9. PROCUREMENT INSTRUMENT IDENTIFICATION NUMBER		
8c. ADDRESS (City, State, and ZIP Code) <b>Wright Patterson AFB OH 45433-6583</b>			10. SOURCE OF FUNDING NUMBERS		
			PROGRAM ELEMENT NO.	PROJECT NO.	TASK NO.
					WORK UNIT ACCESSION NO.
11. TITLE (Include Security Classification) <b>DISCRETE PROPORTIONAL PLUS INTEGRAL (PI) MULTIVARIABLE CONTROL LAWS FOR THE CONTROL RECONFIGURABLE COMBAT AIRCRAFT (CRCA)</b>					
12. PERSONAL AUTHOR(S) <b>Jamie L. Foelker, B.S., Capt, USAF</b>					
13a. TYPE OF REPORT <b>MS Thesis</b>		13b. TIME COVERED FROM _____ TO _____		14. DATE OF REPORT (Year, Month, Day) <b>1989 December</b>	
15. PAGE COUNT <b>146</b>					
16. SUPPLEMENTARY NOTATION					
17. COSATI CODES			18. SUBJECT TERMS (Continue on reverse if necessary and identify by block number)		
FIELD	GROUP	SUB-GROUP	<b>Control Theory, Flight Control Systems, Multivariable Control, Adaptive Control Systems.</b>		
19. ABSTRACT (Continue on reverse if necessary and identify by block number)					
<p>Thesis Advisor: John J. D'Azzo, PhD Professor of Electrical Engineering</p>					
20. DISTRIBUTION/AVAILABILITY OF ABSTRACT <input checked="" type="checkbox"/> UNCLASSIFIED/UNLIMITED <input type="checkbox"/> SAME AS RPT <input type="checkbox"/> DTIC USERS			21. ABSTRACT SECURITY CLASSIFICATION <b>UNCLASSIFIED</b>		
22a. NAME OF RESPONSIBLE INDIVIDUAL <b>John J. D'Azzo, PhD</b>			22b. TELEPHONE (Include Area Code) <b>(513) 255-3450</b>		22c. OFFICE SYMBOL <b>AFIT/ENG</b>

UNCLASSIFIED

2 Multivariable control laws developed by Dr. Brian Porter of the University of Salford, England are used to successfully perform maneuvering tracking tasks with the NASA/Grumman Control Reconfigurable Combat Aircraft (CRCA). Porter's method is used to design discrete Proportional plus Integral (PI) control laws. Output and selected state rate feedback are used. The results in three no failure flight conditions show robust tracking control of the CRCA for five selected maneuvers. Single failures are introduced to test the ability of the fixed-gain designs to successfully control the aircraft and perform the maneuvers. The time responses show that discrete PI control law can make the CRCA successfully perform all five maneuvers for two of the three control surface failures investigated in two of the three point designs. The step response PI control law results in stable control for only one of three failure situations. For high gains, the system transfer function becomes asymptotically diagonal (the outputs are decoupled). Based on this property, the frequency analysis is obtained for the discrete PI design using each output with respect to its associated input. Phase margins in excess of  $45^\circ$ , gain margins of greater than 6dB, and bandwidths in the range of 5-10 rad/sec are the result. The adaptive controller displays a larger than expected roll angle output in two of the maneuvers as compared to the step response PI results. An adaptive algorithm using a recursive least squares estimation is run with failure introduction occurring at one of two times in the simulation. The adaptive results also display decoupling of the outputs in the steady state.

UNCLASSIFIED